



International Agreement Report

Heat Transfer Processes During Intermediate and Large Break Loss-of-Coolant Accidents (LOCAs)

Prepared by
I. Vojtek

Reactor Safety Corporation
Gesellschaft fuer Reaktorsicherheit
Porschungsgelaende, 8046 Garching,
The Federal Republic of Germany

Office of Nuclear Regulatory Research
U.S. Nuclear Regulatory Commission
Washington, D.C. 20555

September 1986

Prepared as part of
The Agreement on Research Participation and Technical Exchange
under the International Thermal-Hydraulic Code Assessment
and Application Program (ICAP)

Published by
U.S. Nuclear Regulatory Commission

NOTICE

This report was prepared under an international cooperative agreement for the exchange of technical information. Neither the United States Government nor any agency thereof, or any of their employees, makes any warranty, expressed or implied, or assumes any legal liability or responsibility for any third party's use, or the results of such use, of any information, apparatus product or process disclosed in this report, or represents that its use by such third party would not infringe privately owned rights.

Available from

Superintendent of Documents
U.S. Government Printing Office
P.O. Box 37082
Washington, D.C. 20013-7082

and

National Technical Information Service
Springfield, VA 22161



International Agreement Report

Heat Transfer Processes During Intermediate and Large Break Loss-of-Coolant Accidents (LOCAs)

Prepared by
I. Vojtek

Reactor Safety Corporation
Gesellschaft fuer Reaktorsicherheit
Porschungsgelaende, 8046 Garching,
The Federal Republic of Germany

Office of Nuclear Regulatory Research
U.S. Nuclear Regulatory Commission
Washington, D.C. 20555

September 1986

Prepared as part of
The Agreement on Research Participation and Technical Exchange
under the International Thermal-Hydraulic Code Assessment
and Application Program (ICAP)

Published by
U.S. Nuclear Regulatory Commission

Translated by: Fischer Translation Service
1928 Catocin Terrace
Silver Spring, MD 20906

NOTICE

This report documents work performed under the sponsorship of the Kraftwerk Union in the Federal Republic of Germany. The information in this report has been provided to the USNRC under the terms of an information exchange agreement between the United States and the Federal Republic of Germany (Technical Exchange and Cooperation Arrangement Between the United States Nuclear Regulatory Commission and the Bundesminister Fuer Forschung und Technologie of the Federal Republic of Germany in the field of reactor safety research and development, April 30, 1981). The Kraftwerk Union has consented to the publication of this report as a USNRC document in order that it may receive the widest possible circulation among the reactor safety community. Neither the United States Government nor the Kraftwerk Union or any agency thereof, or any of their employees, makes any warranty, expressed or implied, or assumes any legal liability of responsibility for any third party's use, or the results of such use, of any information, apparatus, product or process disclosed in this report, or represents that its use by such third party would not infringe privately owned rights.

SUMMARY

Within the framework of this research project there were examined the heat transfer ranges, as they occur during the high pressure phase of a LOCA with intermediate and large breaks. Special attention was given to the phenomena important for the prediction of the highest clad tube temperatures of the maximum and minimum critical heat flux and to the steam-droplets cooling. The experimental results of the 25-rod bundle tests, conducted at the KWU facility in Karlstein, were used as a data-base for the verification of the assembled models and correlations. The values of the heat flux and of the heat transfer coefficients, obtained from these measurements, were used for the comparison with the calculated results and allowed the evaluation of the used correlations and models. The local values of the important thermal and fluid dynamic parameters, required for this comparison, were calculated with the aid of the computer code BRUDI-VA. In particular, the following correlations were evaluated on hand of these experimental results:

Maximum critical heat flux:

- W-3 correlation
- B-W-2 correlation
- Macbeth correlation
- Zuber-Griffith correlation
- Biasi correlation
- CISE correlation
- Slifer-GE correlation
- Smalin correlation
- Tong correlation
- Thorgenson correlation
- Monde-Katto correlation

Minimum heat flux:

- Berenson modification of the Zuber correlation

Minimum temperature difference in case of rewetting:

- Berenson correlation
- Henry correlation
- Ilceje correlation

Correlations for the calculations of the heat transfer coefficients in the sphere of steam-droplets cooling:

- modified Dougall-Rohsenow correlation
- Groeneveld-5.7 correlation
- Condie-Bengston-IV correlation
- Groeneveld-Delorme correlation
- Chen-Ozkaynak-Sunderam correlation

The verification of the correlations for the calculations of the maximum critical heat flux made apparent the limitation of the spheres of application of the individual correlations and showed, that none of these correlations can be recommended for the entire range of the test parameters for a safe prediction of the DNB moment and location. The verification of the correlations for the calculation of the heat transfer coefficients after the exceeding of the maximum critical heat flux showed, that these correlations also lead only in certain ranges of the test parameters to a good consistency between the measurement and the calculated results. The use of the chosen correlations for the calculation of the minimum temperature difference between wall and coolant and the minimum critical heat flux showed, that none of these correlations, at least in the parameter combinations that resulted from the 25-rod bundle tests, can be used for the prediction of the rewetting phenomenon.

On hand of the results of the verification of the correlations for the calculation of the heat transfer coefficients in the case of steam-droplets cooling there was developed a new "two components correlation." The application of this correlation within the entire range of the test parameters of the 25-rod bundle measurements (pressure 2 to 12 MPa, mass flow density 300 to 1400 kg/m²·s, steam quality 0.3 to 1, and wall temperature 300 to 700°C) led to a very good consistency between measurement and calculated results.

ABSTRACT

The general purpose of this project was the investigation of the heat transfer regimes during the high pressure portion of blowdown. The main attention has been focussed on the evaluation of those phenomena which are most important in reactor safety, such as maximum and minimum critical heat flux and forced convection film boiling heat transfer. The experimental results of the 25-rod bundle blowdown heat transfer tests, which were performed at the KWU heat transfer test facility in Karlstein, were used as a database for the verification of different correlations which are used or were developed for the analysis of reactor safety problems. The computer code BRUDI-VA was used for the calculation of local values of important thermohydraulic parameters in the bundle.

In particular the following correlations have been evaluated in this study:

Maximum critical heat flux:

- W-3 correlation
- B-W-2 correlation
- Macbeth correlation
- Zuber-Griffith correlation
- Biasi correlation
- CISE correlation
- Slifer-GE correlation
- Smolin correlation
- Pong correlation
- Thorgerson correlation
- Monde-Katto correlation

Minimum critical heat flux and minimum film boiling temperature:

- Berenson modification of the Zuber correlation
- Berenson correlation
- Henry correlation
- Iloeje correlation

Heat transfer coefficients in flow film boiling:

- modified Dougall-Rohsenow correlation
- Groeneveld-5.7 correlation

- Condie-Bengston-IV correlation
- Groeneveld-Delorme correlation
- Chen-Ozkaynak-Sundaram correlation.

The evaluation of correlations for the prediction of critical heat flux, film boiling heat transfer coefficients and minimum film boiling temperature showed that none of the correlations should be used over the entire range of test parameters investigated.

Using results of this investigations a new equilibrium correlation for the calculation of forced film boiling heat transfer coefficients has been developed. This correlation is shown to agree well with the experimental data over the following range of testparameter: Mass flow rate 300 to 1400 kg/m²·s, pressure 2 to 12 MPa and quality 0.3 to 1.0.

TABLE OF CONTENTS

1.	Introduction	1
2.	Foundations and definitions	2
2.1	Forced convection with water as a coolant	3
2.2	Subcooled nucleate boiling	4
2.3	Nucleate boiling	4
2.4	Transfer from nucleate boiling to film boiling, resp. steam-droplets flow	4
2.4.1	Transfer from nucleate boiling to film boiling	4
2.4.2	Transfer from nucleate boiling to steam-droplet cooling	5
2.5	Film boiling	5
2.6	Steam-droplets cooling	6
2.7	Transfer from film boiling, resp. steam-droplets cooling to nucleate boiling	6
2.8	Forced steam convection	6
3.	Experimental investigations	7
3.1	The test device	7
3.2	Instrumentation	8
3.3	Test program	9
3.3.1	DNB tests	9
3.3.2	Post DNB tests	11
4.	Calculation of the heat transfer coefficients from the test data and the evaluation of the results	12
4.1	Calculation of the heat transfer coefficients from the test data	12
4.2	Compilation of the important parameters from the test	12
5.	Calculation of the local thermal and fluid dynamic parameters	14
5.1	The computer code BRUDI-VA	14
5.1.1	Basic equations of the homogenous point of equilibrium model	14
5.1.2	Calculation of the two-phase pressure loss	15

5.1.3	Heat conduction model	16
5.1.4	Heat transfer model	16
5.2	Calculation of the chosen tests and determination of the local thermal and fluid dynamic parameters at the DNB, dry-out and RND moment	16
6.	Compilation and comparison of the correlations for the calculation of the heat transfer coefficients in the region of the forced convection with one-phase coolant	18
6.1	Forced water convection	18
6.2	Forced steam convection	19
6.3	Comparison of the correlations	20
7.	Compilation and comparison of the correlations for the calculation of the heat transfer coefficients (HTC) of the subcooled and saturated nucleate boiling	21
7.1	Calculation of the necessary temperature difference for bubbles formation with subcooled fluid	21
7.2	Calculation of the heat transfer coefficients in the region of the subcooled nucleate boiling	21
7.3	Calculation of the heat transfer coefficients in the region of nucleate boiling	22
7.4	Comparison of the correlations	23
8.	Transfer from nucleate boiling to film boiling, resp. steam-droplets cooling - (maximum critical heat flux)	25
8.1	Vessel film boiling	25
8.2	Heat transfer crisis with forced convection, high heat flux and low steam-content - (DNB)	27
8.2.1	Semi-empirical models	27
8.2.2	Empirical models	31
8.3	Heat transfer crisis with forced convection, low to intermediate heat flux, and intermediate to high steam content (dry-out)	33
8.3.1	Analytical models	33
8.3.2	Semi-empirical and empirical correlations	36
8.4	Verification of the correlations for the calculation of the maximum critical heat flux (KHB) based on the experimental results	38

8.4.1	Selection of the correlations	38
8.4.2	Evaluation of the correlations for the calculation of the maximum critical heat flux	44
9.	Heat transfer at boiling and steam-droplets cooling	45
9.1	Film boiling	45
9.1.1	Film boiling with wettable wall	45
9.1.2	Film boiling with not wettable wall	46
9.1.3	Vessel film boiling	46
9.2	Steam-droplets cooling	49
9.2.1	Equilibrium models and correlations	50
9.2.2	Non-equilibrium models	52
9.3	Comparison of each of the correlations based on the recalculation of selected 25-rod bundle tests	56
9.3.1	Recalculation of the test DNB1	57
9.3.2	Recalculation of the test DNB3	59
9.3.3	Recalculation of the test DNB9	61
9.3.4	Recalculation of the test PDNB11	63
9.4	Evaluation of the correlations for the calculation of the heat transfer coefficients in the steam-droplets cooling region	64
10.	Transfer from steam-droplets cooling or film boiling to nucleate boiling (RNB-rewetting)	65
10.1	Compilation of the experimental data from the 25-rod bundle investigation	65
10.2	Correlations for the calculation of the minimum critical heat flux and of the minimum temperature difference with rewetting	66
10.3	Investigation of the correlations based on the results of the 25-rod bundle tests	68
10.4	Evaluation of the correlations	70
11.	Development of a new correlation for the calculation of the heat transfer coefficients in the steam-droplets cooling region	71
11.1	Heat transfer between wall and steam phase	72

11.1.1	Comparison of various slippage and drift equations	73
11.2	Heat transfer between wall and droplets	76
11.2.1	Determination of the surface inherent to the heat transfer between wall and droplets	76
11.2.2	Determination of the droplet diameter	76
11.2.3	Determination of the number of droplets	78
11.3	Heat transfer between steam and droplets	79
11.4	Calculation of the individual components of the heat flux density between wall and steam-droplets flow	80
11.5	Formulation in agreement with the similarity theory of the new model for the calculation of the heat transfer coefficients with steam-droplets cooling	85
12.	Conclusions	92
13.	Bibliography	93
	Attachments 1-11	99
	Distribution	141

INDEX OF FIGURES

Figure 1: Heat transfer and flow configurations with intermediate heat flux	2
Figure 2: Heat transfer and flow configurations with high heat flux	3
Figure 3: Schematic representation of the measuring section	7
Figure 4: Heating conductor geometry and power distribution	7
Figure 5: Position of the thermocouple elements in the bundle	8
Figure 6: Typical processes of the test parameters of the DNB tests	10
Figure 7: Typical processes of the test parameters of the post-DNB tests	11
Figure 8: Correlation of the temperature difference with rewetting and of the electric power	13
Figure 9: Pressure difference along the measuring section Test DNB-2	15
Figure 10: Pressure difference along the measuring section Test DNB-9	15
Figure 11: Comparison between the measured and the calculated wall temperatures - Test DNB-9	17
Figure 12: Reynolds number multiplier F according to Chen	24
Figure 13: Suppression factor S according to Chen	24
Figure 14: Boiling curve according to Nukiyama for container boiling with 0.1 MPa	26
Figure 15: Model representation for the determination of the critical heat flux according to Tong	29
Figure 16: Model of the annular flow with entrainment and deposition	33
Figure 17: Harwell correlation for the determination of the entrainment coefficient	34
Figure 18: Harwell correlation for the determination of the deposition coefficient	35
Figure 19: Comparison of the critical heat flux correlations Test DNB3	40
Figure 20: Comparison of the critical heat flux correlations Test DNB3	41

Figure 21: Comparison of the critical heat flux correlations Test DNB9	42
Figure 22: Comparison of the critical heat flux correlations Test DNB9	43
Figure 23: Schematic representation of film boiling in vessel boiling	46
Figure 24: Model of the vessel film boiling according to Berenson	49
Figure 25: Comparison of the equilibrium correlations Test DNB1	57
Figure 26: Comparison of the non-equilibrium correlations Test DNB1	58
Figure 27: Comparison of the equilibrium correlations Test DNB3	59
Figure 28: Comparison of the non-equilibrium correlations Test DNB3	60
Figure 29: Comparison of the equilibrium correlations Test DNB9	61
Figure 30: Comparison of the non-equilibrium correlations Test DNB9	62
Figure 31: Comparison of the equilibrium correlations Test PDNB11	63
Figure 32: Measuring points $T_w - T_{sat} = f(P)$	65
Figure 33: Measuring points $T_w - T_{sat} = f(q)$	65
Figure 34: Correlation of G to $T_w - T_{sat}$	66
Figure 35: Correlation of X to $T_w - T_{sat}$	66
Figure 36: Comparisons of the correlations for the calculation of ΔT_{min}	68
Figure 37: Comparison of the minimum and actual heat flux	69
Figure 38: Model representation for the heat transfer in the steam-droplets cooling phase	71
Figure 39: Comparison of several correlations for the calculation of the heat transfer coefficient with forced steam convection	72
Figure 40: Comparison of various slippage equations	74
Figure 41: Comparison of the steam velocities calculated with and without drift	75
Figure 42: Comparison of the wall temperatures and the heat transfer coefficients calculated with and without slippage	75

Figure 43: Comparison of the correlations for the calculation of the droplet diameter	77
Figure 44: HTC between steam and droplets	79
Figure 45: Heat flux density of steam on droplets	79
Figure 46: Components of the heat flux in steam-droplets cooling	82
Figure 47: Comparison of the droplets mass flow densities	83
Figure 48: Components of the heat flux density acc. to the "two-component model"	84
Figure 49: Results from the recalculation of the test DNB1 with the application of the new correlation for the calculation of the heat transfer coefficients	88
Figure 50: Results of the recalculation of the test DNB3 with the application of the new correlation for the calculation of the heat transfer coefficients	89
Figure 51: Results from the recalculation of the test DNB9 with the application of the new correlation for the calculation of the heat transfer coefficients	90
Figure 52: Results from the recalculation of the test PDNB11 with application of the new correlation for the calculation of the heat transfer coefficients	91

INDEX OF TABLES

Table 1:	Variation of the test parameters of the DNB tests	10
Table 2:	Variation of the test parameters of the post DNB tests	11
Table 3:	Values of the Macbeth correlation coefficients for various pressure ranges	32
Table 4:	Comparison of the critical heat flux correlations	39
Table 5:	Values of the correlation coefficients for the Groeneveld correlation	52

EXPRESSIONS (Notations)

a	m	characteristic length
a		correlation constant
A		correlation constant
B		correlation constant
C		correlation constant
C _p	J/kg K	specific heat capacity
D	m	diameter, equivalent diameter
f		pressure loss factor
F	m ²	area [surface]
F		Chen factor
g	m/sec ²	acceleration due to gravity
G	kg/m ³ sec	mass flow density
h	J/kg	specific enthalpy
Δh _e *	J/kg	modified evaporation heat
Δh _e	J/kg	evaporation heat
H	m	height
<j>	m ³ /sec	volume flow
K		constant
K _{SD}		Stefan-Boltzmann constant
K _α		absorption coefficient
l	m	length
M	kg	mass
m	kg	mass
\dot{M}	kg/sec	mass flow
N		number
P	Pa (bar)	pressure
p	m	heated range
P _c	Pa (bar)	critical pressure
Q	W	heat flux
q	W/m ² (W/cm ²)	heat flux density
R	m	radius
R _{sp}	Ohm·mm ² /m	specific resistance
S		Chen suppression factor
S	m	thickness
s		slip[slippage]
t	sec	time
T	°C, K	temperature

W	kg/sec	mass flow
w	m/sec	velocity
X		steam content
X_{tt}		Martinelli-Nelson parameter
Y		Miropolskij parameter
α	W/m ² K	heat transfer coefficient
δ	m	film thickness, droplets diameter
ϵ		emission number
η	kg/m·sec	dynamic viscosity
θ	m	film thickness
λ	W/mK	heat conductivity
ψ		volumetric steam content
ρ	kg/m ³	density
τ	N/m ²	tangential stress
τ	sec	time
σ	N/m	surface stress

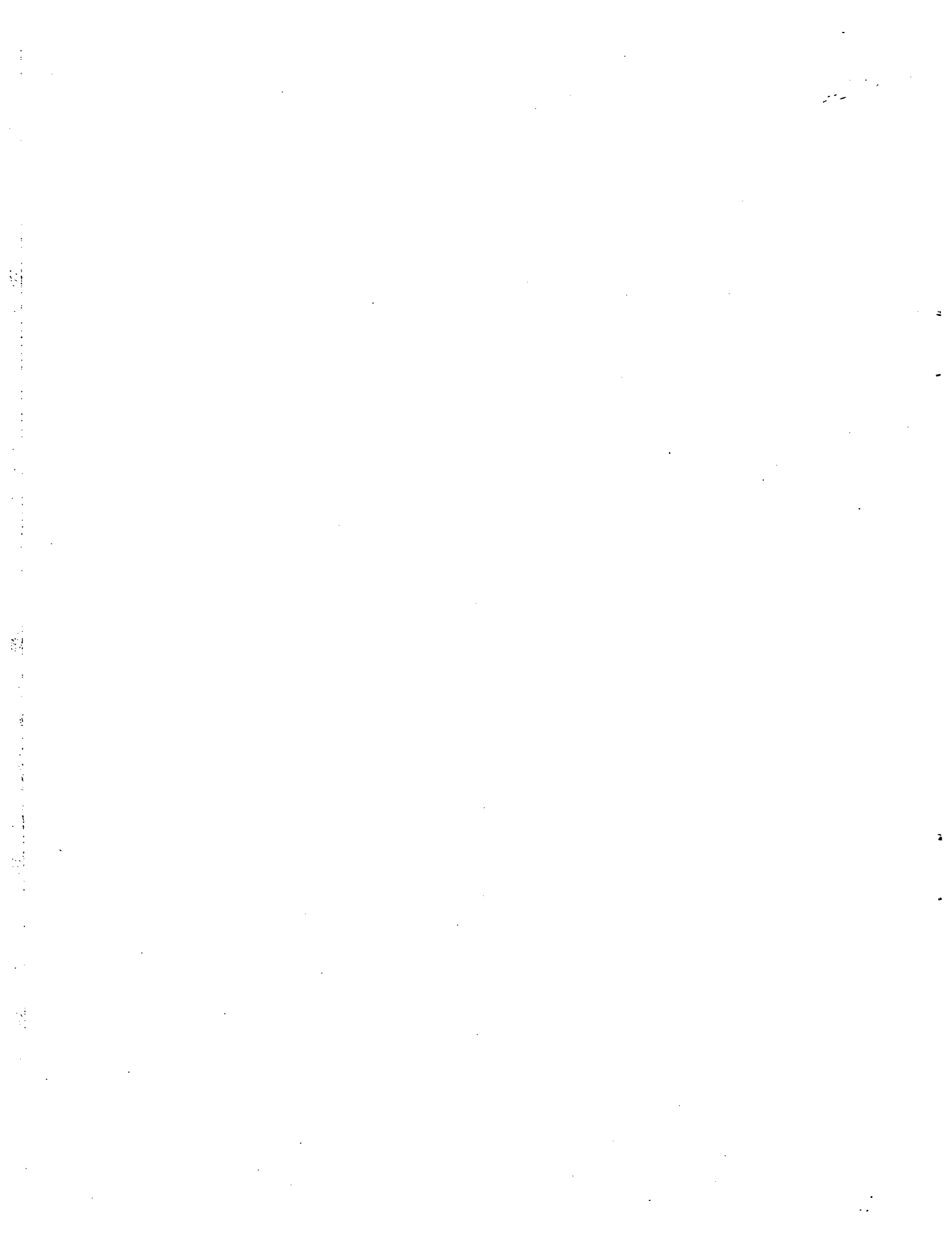
Characteristic factors

Gr	Grashoff number
Nu	Nusselt number
Pr	Prandtl number
Re	Reynolds number
We	Weber number

Subscripts (and superscripts)

A	outlet [discharge]
a	actual [real]
B	Berenson
bs	nucleate boiling
d	steam
D	deposition
DNB	Departure from nucleate boiling
Do	dry-out

E	inlet (entrainment)
e	equilibrium
e _{ff}	effective
f	fluid [liquid]
H	Henry
hom	homogenous (without slippage)
in	inlet
inj	injection
I	Iloeje
K	convection
l	local
LF	liquid film
mic	microscopical
mac	macroscopical
max	maximum
min	minimum
stat	stationary value
T	droplets
TOT	in toto
tp	two-phase
w	wall
ZP	two-phase



1. INTRODUCTION

In the safety analyses of light water reactors there are examined hypothetical LOCA cases. Depending on the size and the position of the assumed breaks, the important thermal and fluid dynamic parameters, such as pressure, mass flow and enthalpy in the primary loop, undergo more or less quick changes compared with the conditions under normal operation. The therefrom resulting reduction of the core mass flow can lead to a so-called exceeding of the maximum critical heat flux (KHB) [CHF] at the fuel rods and to a high increase of the clad tube temperatures. Thus, an accurate knowledge of the heat transfer conditions under high pressure and mass flow transients is one of the most important prerequisites for a correct prediction of the process of the clad tube temperatures in the case of LOCA. Therein, of decisive influence upon the process of the clad tube temperatures are the moment of the exceeding of the maximum critical heat flux and the magnitude of the heat transfer coefficients (WUK) in the subsequent phase of film boiling and steam-droplets cooling. For the clarification of these problems, intermittently controlled tests with a 25-rod bundle with PWR geometry were conducted in the KWU facility, within the framework of the German emergency cooling program. The task of this research project was the analytical examination of the heat transfer conditions under considerable pressure and mass flow transients and under high pressure.

2. FOUNDATIONS AND DEFINITIONS

The heat transfer conditions and the thereto belonging configurations of flow, as they occur in the case of LOCA with intermediate and large breaks in the central respectively hot channel of a pressurized water reactor core are schematically represented in Fig. 1 resp. Fig. 2. Hereafter, are discussed and explained the heat transfer and flow conditions in each of the regions.

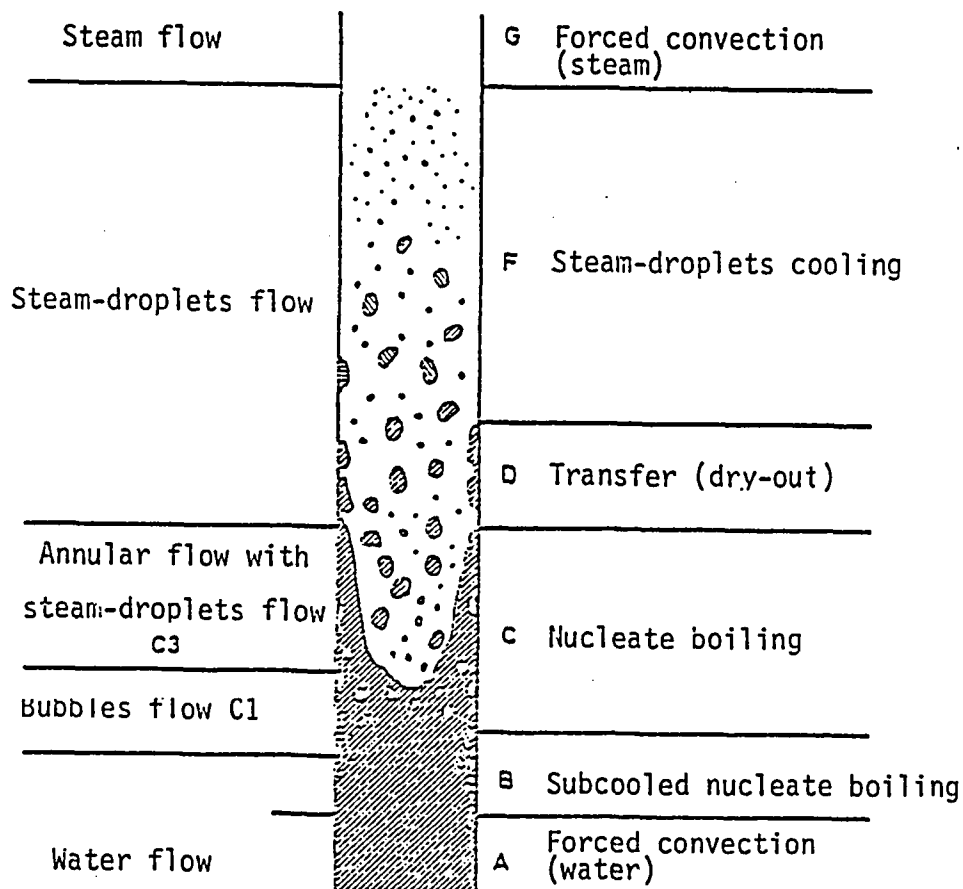


Fig. 1: Heat transfer and flow configurations with intermediate heat flux

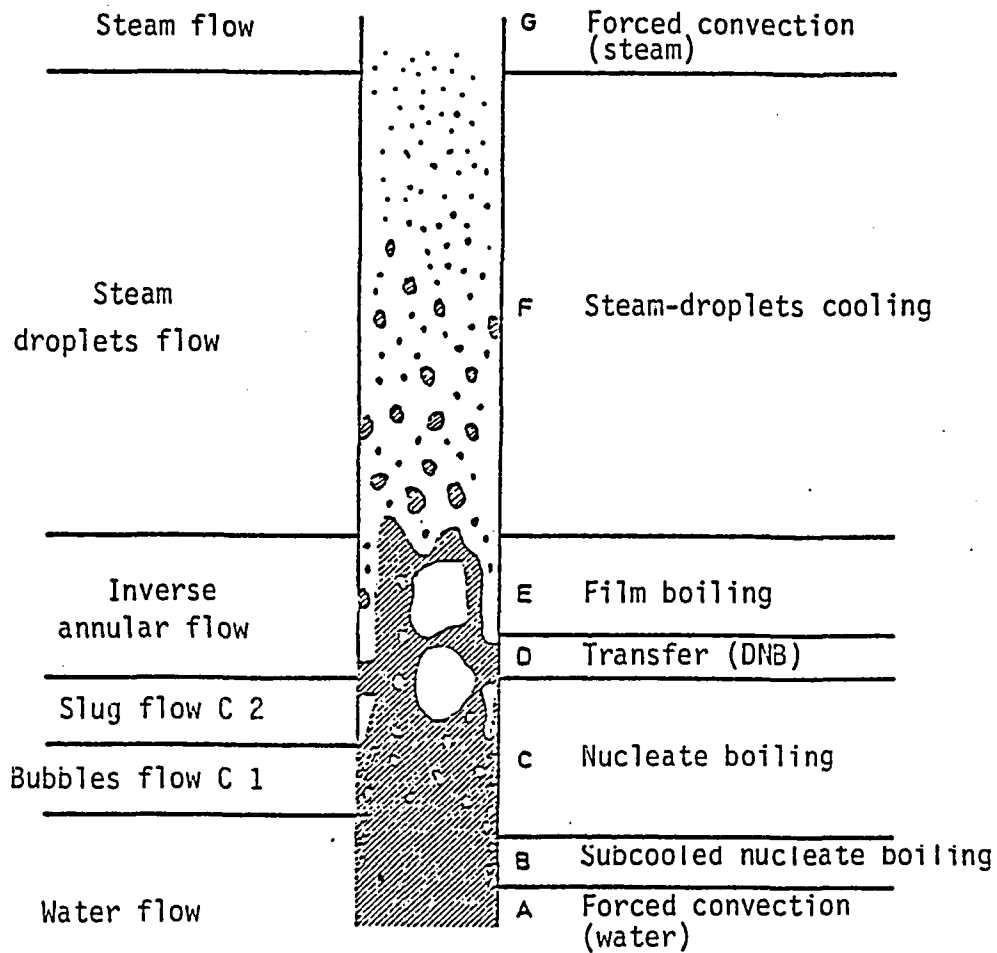


Fig. 2: Heat transfer and flow configurations with high heat flux

2.1 Forced convection with water as coolant (Region A, Fig. 1, 2)

This type of heat transfer occurs in steady-state operating conditions and in the first, subcooled phase of LOCA in the greatest part of the reactor core. The thereto belonging configuration of flow is the single-phase, fully developed, turbulent flow.

2.2 Subcooled nucleate boiling (region B, Fig. 1, 2)

The mean water temperature in this region lies only a little below the saturation temperature. Bubbles are formed on the wall if the wall temperature presents a certain increase above the saturation temperature. Due to the action of the flux, the bubbles are broken off the wall and condense in the subcooled region of the flow. Because of the movement of the bubbles in the center of the flow there occurs the destruction of the laminar boundary layer and in increased mass transfer in the layers in the proximity of the wall takes place. This leads to a significant improvement of the heat transfer between wall and coolant. Also, in this case, the flow is fully turbulent, but partially with a destroyed boundary layer.

2.3 Nucleate boiling (region C, Fig. 1, 2)

When the saturation temperature reaches over the entire flow cross-section, the bubbles that are broken off the wall spread into the flow, do not condense any longer and the average enthalpy lies now above the boundary value of $x = 0$. Due to the velocity distribution, the constantly originating bubbles on the wall are conveyed to the center of the flow, they coalesce and displace the water into the less accelerated layers near the wall. The heat transfer between wall and coolant is also very effective in this region and amounts to only a few degrees Kelvin. The configurations of flow inherent to this heat transfer can appear to be quite different and range from a bubble flow (region C1), through a slug flow (region C2, Fig. 2), to the annular flow with steam-droplets cooling in the center (region C3, Fig.).

2.4 Transfer from nucleate boiling to film boiling, resp. steam-droplets flow (the first heat transfer crisis)

2.4.1 Transfer from nucleate boiling to film boiling (region D, Fig. 2)

The transfer from nucleate boiling to the film boiling is characterized by a high heat flux density and a low steam content. When the steam production

at nuclear boiling reaches a determined limit because of the high heat flux density, the water is displaced from the wall and the heat is transferred to the water only through the conduction in the thin steam layer. The sudden reduction of the heat transfer coefficient (WUK) brings about a steep increase of the wall temperature. This type of transfer from nuclear boiling to film boiling is hence called "Departure from Nucleate Boiling - DNB." Characteristic for this heat transfer crisis is the change of configuration of flow of bubbles and slug flow to the inverse annular flow (region D, Fig. 1, 2).

2.4.2 Transfer from nucleate boiling to steam-droplets cooling (region D, Fig. 1)

As shown in Fig. 1, in this transfer there exist completely different conditions in the flow channel as in the above described transfer from nucleate boiling to film boiling. In this case, the heated wall is covered only with a thin film of water from which are broken off individual droplets because of the great velocity difference between steam nucleus and water film. Thus, in the center there is created a steam-droplets flow, also called mist flow: Due to the constant evaporating of the water film, it becomes always thinner downward the flow until it fully evaporates at the end of this region. After the drying of the water film, the heat transfer coefficient (WUK) does suddenly decrease also in this case, and the wall temperature increases rapidly. This transfer from nucleate boiling to the steam-droplets cooling is called "dry-out" in the literature and also henceforth. The configuration of flow changes from an annular flow to steam-droplets cooling.

2.5 Film boiling (region E, Fig. 2)

Film boiling is a heat transfer process which can chiefly occur at boiling in the pool with a heated wall. In the case of a formed flow, the pure film boiling could be observed locally limited only with a high heat flux density. During a transient process with quickly dropping pressure, this heat transfer range is also limited in time.

2.6 Steam-droplets cooling (region F, Fig. 1, 2)

The heat transfer conditions and the magnitude of the heat transfer coefficient (WUK) in this region are of decisive influence on the process of the clad tube temperatures after an exceeding of the maximum critical heat flux. The analytical examination of the heat transfer in a steam-droplets flow (liquid deficient region) was one of the main tasks of this research project and it is dealt with in details in Chapters 9 and 11.

2.7 Transfer from film boiling, resp. steam-droplets cooling, to nucleate boiling (the second heat transfer crisis)

In the new intermittent examinations with reactor LOCA-like conditions, there was not only observed the first heat transfer crisis (DNB, dry-out) but also the second one, the transfer from steam-droplets cooling or film boiling to nucleate boiling. This process - described as "Return to Nucleate Boiling (RNB)" in the literature - is thoroughly investigated in Chapter 10.

2.8 Forced steam convection (region G, Fig. 1, 2)

If even the last droplets evaporate in the center of the flow because of the constant addition of heat and the pressure relief, the steam is superheated with a constant addition of heat. The inherent configuration of flow in this region is, in most of the cases, the fully developed turbulent steam flux.

3. EXPERIMENTAL INVESTIGATIONS

The experimental investigation of the intermittent heat transfer conditions during reactor LOCA-like transients was conducted in the KWU facility within the framework of the research project RS-37C, sponsored by the BMFT (Federal Minister for Technology). The purpose of the controlled 25-rod bundle tests was the experimental determination of the heat transfer coefficient (WUK) in the region of the film boiling and of the steam-droplets cooling, and the investigation of various parameters on the magnitude of the maximum critical heat flux.

3.1 The test device

Figure 3 shows a schematic representation of the testing device.

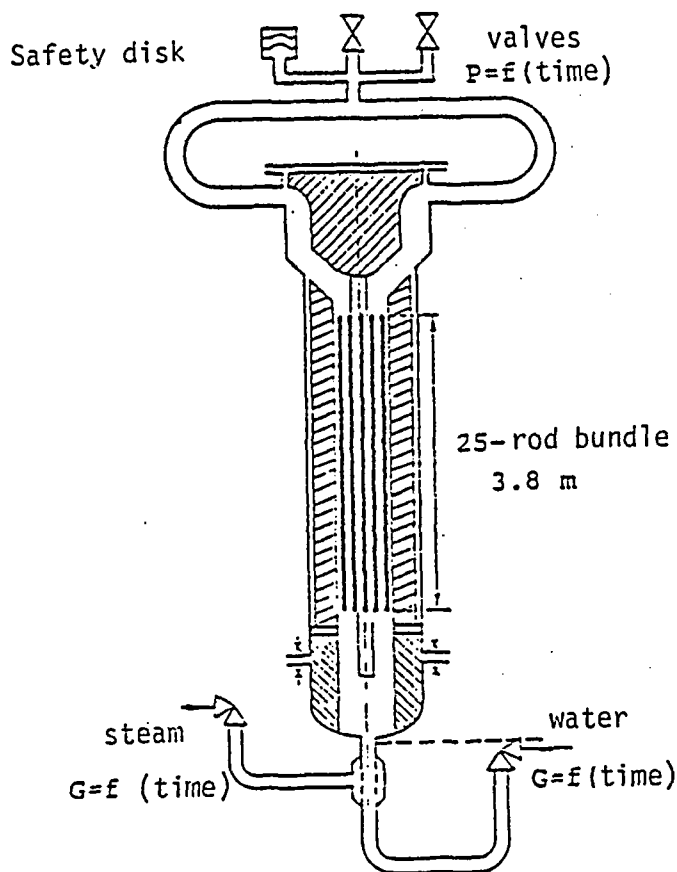


Fig. 3: Schematic representation of the measuring section

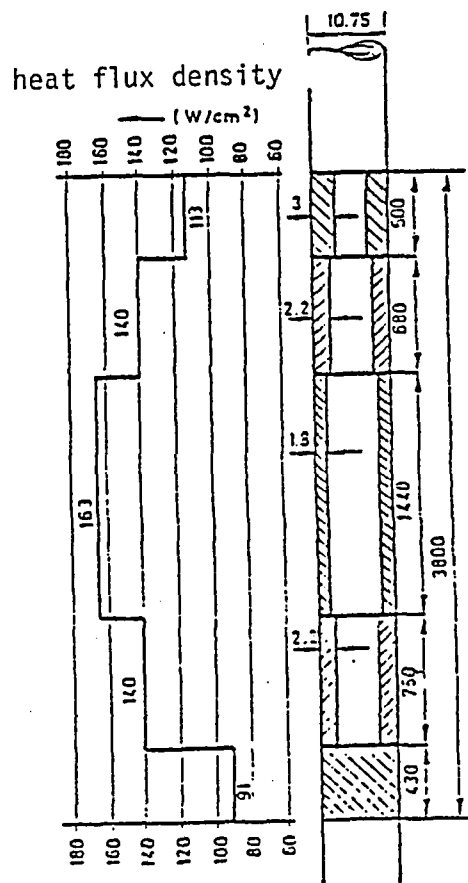


Fig. 4: Heating conductor geometry and power distribution

The most important element of the testing device is the measuring section with the electrically heated 25-rod bundle. The axial power distribution of the five-stage, direct-heated heating conductor is shown in Fig. 4. The measuring section is designed for a maximum pressure of 16 MPa. The inlet mass flow and the inlet enthalpy were controlled by means of the valves in the main steam pipe and in the water pipe. At the outlet of the measuring section are installed two quick-controllable valves and a safety disk, with the aid of which the desired pressure distribution is reproduced. The desired heating capacity, adjustable in time, of maximum 5 MW was generated in the thereto belonging direct current plant. A detailed description of the testing device is contained in /1 and 2/.

3.2 Instrumentation

The following parameters were measured in each conducted test.

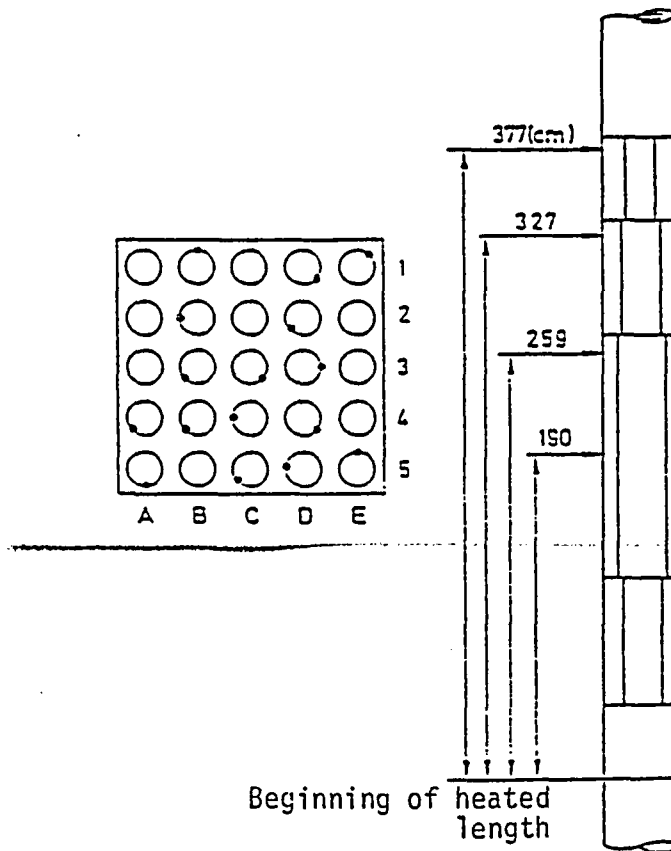


Fig. 5: Position of the thermocouple elements in the bundle

- absolute pressure at the measuring section inlet and outlet
- pressure difference between inlet and outlet
- coolant temperature at the inlet and outlet
- water and steam mass flows in the inlet pipes
- electrical current and voltage
- 8 temperatures in the measuring section wall
- 80 heating conductor wall temperatures at several positions in the rod (Fig. 5).

3.3 Test program

Due to reasons of technical testing nature, the tests were divided into two testing groups, the so-called "DNB tests" and the so-called "post-DNB tests."

3.3.1 DNB tests

The main purpose of the DNB tests was that of furnishing information about the influence of the various test parameters upon the DNB delay times and upon the value of the heat transfer coefficient (WUK) immediately after the occurrence of the DNB. The test runs, compiled in Table 1, were set up in connection with the LOCAS between the reactor pressure vessel and the steam generator. In view of the importance of the hot channel for the safe technical investigation, all of the DNB test runs were conducted with a heating capacity similar to that of the hot channel. But since all 25 rods had to be equally heated in order to be able to reproduce also the other thermal and fluid dynamic conditions that appear in the hot channel of a pressurized water reactor, the following parameter variations had to be carried out:

- a) Bundle inlet enthalpy and initial mass flow as in the reactor, the outlet enthalpy higher (DNB1, DNB2, DNB3)
- b) Bundle outlet enthalpy and initial mass flow as in the reactor, the inlet enthalpy lower (DNB4, DNB5, DNB6)
- c) Rod inlet and outlet enthalpy as in the reactor, the mass flow higher (DNB7, DNB8, DNB9).

In the post-DNB phase, the inlet mass flow was reduced for each of the three types a), b) resp. c) to three different levels ($G/G_{STAT} = 0.45$; $G/G_{STAT} = 0.3$; and $G/G_{STAT} = 0.2$). In order to investigate the influence of the pressure drop after the beginning of the blowdown upon the DNB delay times, two test runs were conducted with a lower pressure drop time of 0.7 (DNB10) resp. 1.2 s (DNB11). The typical time behaviors of the pressure, of the heating capacity and of the inlet mass flow are represented in Fig. 5.

Table 1: Variation of the test parameters of the DNB tests

Test	Initial mass flow density kg/m ² ·s	Mass flow density in the post DNB region kg/m ² ·s	Inlet enthalpy kJ/kg
DNB-1	3300.	1419.	1284.
DNB-2	3300.	957.	1284.
DNB-3	3300.	660.	1284.
DNB-4	3300.	1450.	1233.
DNB-5	3300.	990.	1233.
DNB-6	3300.	660.	1233.
DNB-7	3828.	1378.	1284.
DNB-8	3828.	957.	1284.
DNB-9	3828.	689.	1284.
DNB-10	3300.	660.	1233.
DNB-11	3300.	600.	1233.

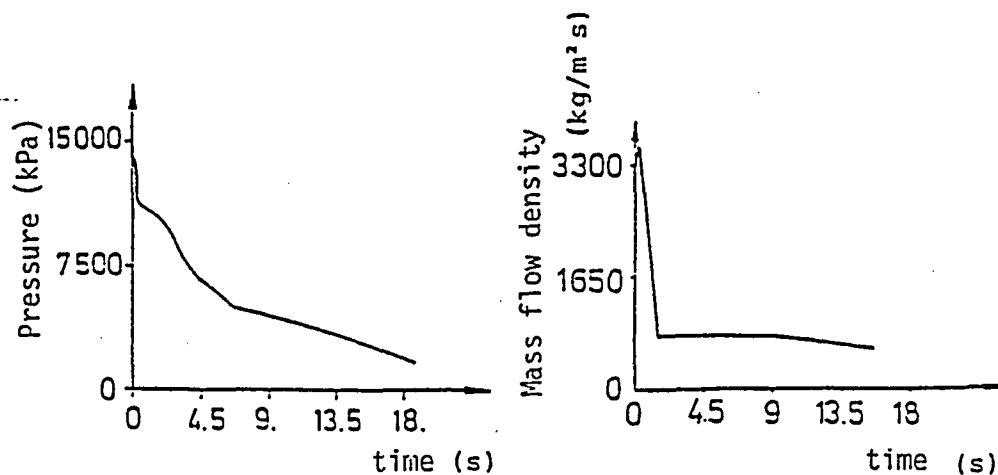


Fig. 6: Typical processes of the test parameters of the DNB tests

3.3.2 Post DNB tests

The purpose of these tests was the experimental determination of the heat exchange coefficient in the region of the steam-droplets cooling with different mass flows and pressure transients. The test runs, compiled in Table 2, were set up in connection with the accident conditions with various leak cross-sections (0.25F to 2F). The inlet mass flow of this test series, maintain constant during a test run, was varied between the values $G/G_{STAT} = 0.4$ and $G/G_{STAT} = 0.03$. The blowdown time, determining the pressure gradient during a test, amounted to 15, 25, 50 resp. 150 s. The bundle inlet enthalpy remains constant during a test and was varied between $1.086 \cdot 10^3$ and $1.55 \cdot 10^5$ kJ/kg. Figure 7 shows typical time processes of the two controlled test parameters.

Table 2: Variation of the test parameters of the post DNB tests

Test	Inlet enthalpy kJ/kg	Mass flow density kg/m ² s	Maximum heat flux density W/cm ²	Pressure relief period s
PD 1	1247.	1254.	162.	21.
PD 3	1086.	248.	113.	23.7.
PD 5	1238.	858.	121.	29.
PD 7	1086.	248.	113.	29.
PD 8	1519.	157.	74.	35.
PD 9	1519.	165.	78.	29.
PD 10	1466.	91.	74.	32.5
PD 11	1295.	319.	112.	51.
PD 14	1461.	91.	74.	150.

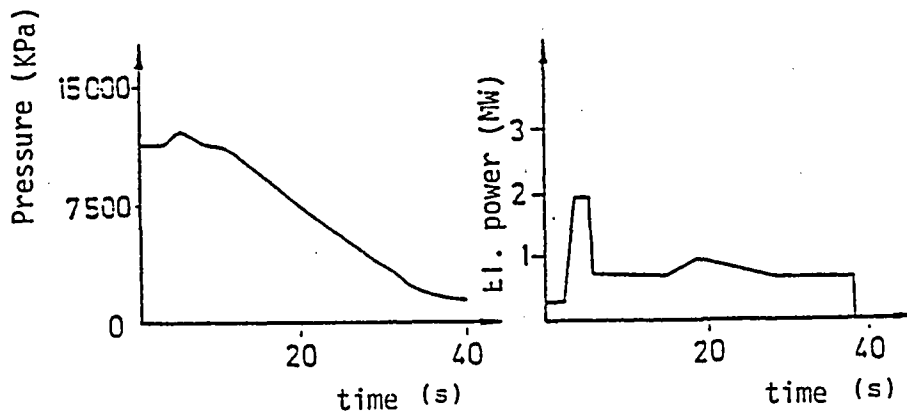


Fig. 7: Typical processes of the test parameters of the post DNB tests

4. CALCULATION OF THE HEAT TRANSFER COEFFICIENTS FROM THE TEST DATA AND THE EVALUATION OF THE RESULTS

4.1 Calculation of the heat transfer coefficients from the test data

The task of the KWU Co. in Erlangen was the determination of the heat transfer coefficients from the measured time processes of the heating conductor wall temperature, the heating capacity and the pressure at the outlet. More detailed information about the inverse heat conduction program, used for the calculation of the heat transfer coefficients, and several examples of the results are contained in /3/.

4.2 Compilation of the important parameters obtained from the test

From the tracings of the test results there were taken the required parameters and made possible for the direct access of a sorting program in the form of data records. The following data records were established:

a) Test data of the DNB, resp. dry-out moment

For the rods B2, D3, D4, D2, D3, and D4 the below data were established from the tracings of the 11 DNB tests and the 21 post DNB tests:

- height of the measuring point
- DNB, resp. dry-out moment
- electrical power
- heat flux
- pressure

These values were established for the first and, as the case may be, also for the second DNB, resp. dry-out, moment.

b) Test data for the RNB moment

For the rods B2, B3, B4, C3, C4, D2, D3, and D4 the following values were determined for the tests in which occurred RNB, and incorporated into the RNB data records:

- height of the measuring point
- RNB moment
- wall temperature
- saturation temperature
- pressure

- electrical power
- heat flux immediately prior to RNB
- heat transfer coefficient

The data from these data records can be interpolated and expressed at will in respect to each other.

By using a special plotting program there can be represented the dependence of any pairs of values from these data records in the form of printer plots. As example, there is shown in Fig. 8 the correlation of the temperature difference between wall and saturation temperature and the electric power. These data records were subsequently expanded with the mathematically ascertained values of the mass flow and the steam content at the DNB, dry-out and RND moment.

This data collection contains at present 624 parameter combinations for DNB, resp. dry-out, conditions and more than 400 parameter combinations for the conditions with RNB.

The description of the individual programs and of the input data is contained in /4/.

DT = F(GE) FOR ALL TESTS (2.5 to 3.27 M)

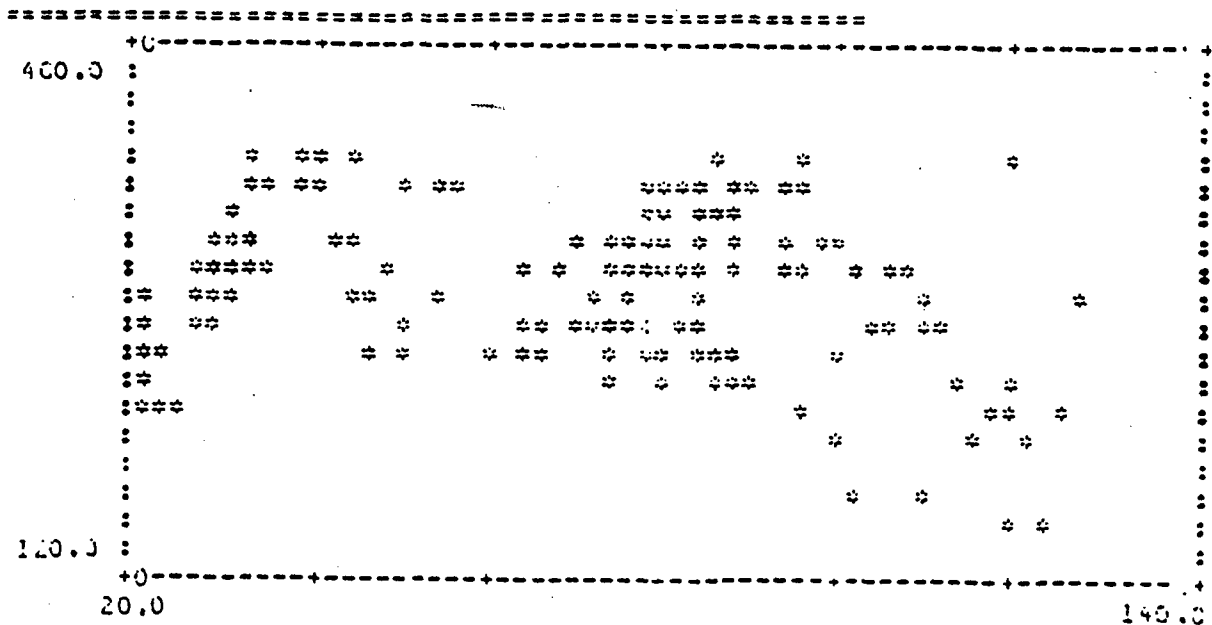


Fig. 8: Correlation of the temperature difference with rewetting and of the electric power

5. CALCULATION OF THE LOCAL THERMAL AND FLUID DYNAMIC PARAMETERS

The local values of the thermal and fluid dynamic parameters required for the evaluation, not measured in the experimental investigation, were calculated in the supplementary analysis of the tests with the aid of the computer code BRUDI-VA.

5.1 The computer code BRUDI-VA

The computer code is a substantially modified version of the blowdown code BRUCH-D /5, 6/ and was developed for the evaluation of the 25-rod bundle tests. This computer program is based on a so-called homogenous point of equilibrium model.

5.1.1 Basic equations of the homogenous point of equilibrium model

Starting from the one-dimensional formulation of the conservation theorems for mass and energy and the equation of condition, the following differential set of equations can be differentiated for the homogenous point of equilibrium model

$$\dot{M} = G_E - G_A \quad (1)$$

$$\dot{P} = [-\dot{M}(h + \frac{v}{\epsilon_h}) - (G \cdot h)_A + (G \cdot h)_E + Q] / [M(\frac{\epsilon_p}{\epsilon_h} + v)] \quad (2)$$

$$\text{with } \epsilon_p = (\frac{\partial v}{\partial p})_h \text{ and } \epsilon_h = (\frac{\partial v}{\partial h})_p$$

$$(\frac{\partial}{\partial t} (\rho/2 w^2 \cdot F), \frac{\partial}{\partial z} (\rho/2 w^3), \frac{\partial}{\partial t} F \text{ and } g \cdot \rho \cdot w \cdot \sin \phi \cdot F \text{ are disregarded})$$

Through the integration of the theorem of conservation of momentum between the points i and $i+1$ of the flow path with constant time, the equation for \dot{G} is derived

$$\dot{G} = \left(\int_i^{i+1} \cdot \frac{dz}{F} \right)^{-1} [P_i - P_{i+1} - g \cdot \rho (H_{i+1} - H_i) - K \cdot G \cdot |G|] \quad (4)$$

(with omission of $\frac{\rho}{2} (w_{i+1}^2 - w_i^2)$).

The still unknown values of K , resp. Q , are determined with the aid of correlations for the calculation of the two-phase pressure loss, respectively with the aid of a heat conduction and heat transfer model.

5.1.2. Calculation of the two-phase pressure loss

For the calculation of the pressure loss coefficient in the region of the two-phase flow there was used the Martinelli model. The comparison between the measured and the calculated pressure difference between measuring section inlet and outlet (Figures 9 and 10) shows a good consistency between measurement and calculation.

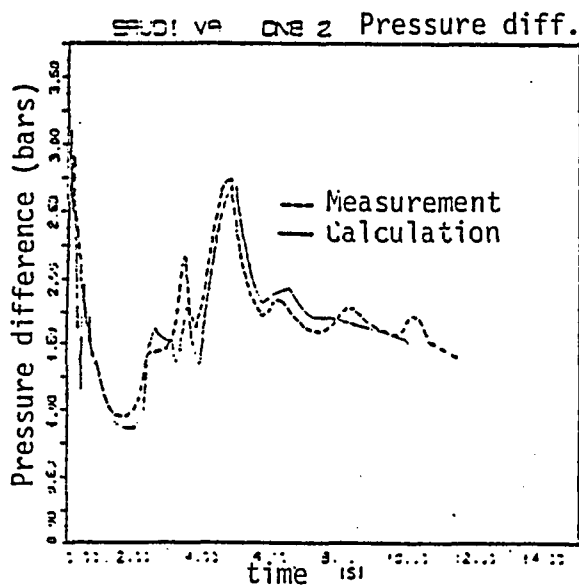


Fig. 9: Pressure difference along the measuring section Test DNB-2

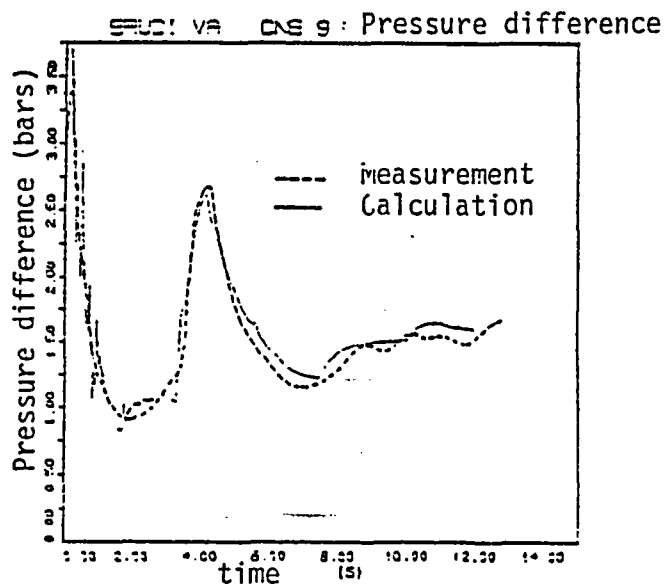


Fig. 10: Pressure difference along the measuring section Test DNB-9

5.1.3 Heat conduction model

The fuel rod model implemented in the computer code BRUCH-D did not allow the simulation of the heat production by means of electric current in the heat conductor wall. Therefore, for the evaluation of the 25-rod bundle tests there was developed a heat conductor model. The following hypotheses were taken for the specifications of the model describing the intermittent heat conduction:

- The axial heat conduction was neglected,
- The heat is conducted only on the external wall,
- The heat is produced only in the heat conductor wall and calculated with the aid of the Lenz-Joule law from the current and the specific resistance,
- The temperature dependence of the values of ρ , C_p , γ and R_{sp} was taken into consideration.
- The wall thickness remains constant within a heat conductor segment.

The heat conductor model was technically designed for the program in such a manner, that the number of the radial layers for each of the heat conductor segments can be chosen at will.

5.1.4 Heat transfer model

The examination of the heat transfer conditions in the high pressure phase during LOCA was the task of this research project and it is dealt with in details in the below chapters.

5.2 Calculation of the chosen tests and determination of the local thermal and fluid dynamic parameters at the DNB, dry-out and RND moment

The purpose of the calculation of the chosen experiments was the determination of the local values of the mass flow and of the steam content in the bundle from the boundary conditions that had been measured or had been determined from the measurements. The following parameters were given as boundary conditions for the individual computer runs:

- Geometry and pressure loss coefficients
- Inlet mass weight rate of flow
- Inlet enthalpy
- Pressure at the measuring section outlet
- Heat flux

The calculated values of the mass flow and steam content at the DNB, resp. dry-out, moment are contained in Attachment 1. In Attachment 2 are compiled the important parameters at the RNB moment.

These computer runs were concomitantly used for the verification of the heat conductor model and of the Martinell-Nelson model for the calculation of the two-phase pressure loss.

The slight deviations between the measured and the calculated temperature are caused by the necessary flattening of the heat flux curves (Fig. 11). The consistency of the time slopes of the pressure difference along the measuring section can be described as good (Fig. 9 and 10). A detailed information about the calculation of the 25-rod bundle tests is contained in /7/ and /8/.

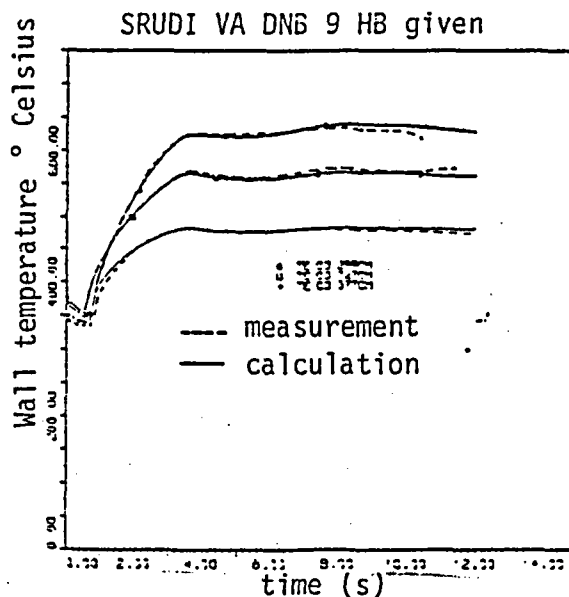


Fig. 11: Comparison between the measured and the calculated wall temperatures - test DNB-9

6. COMPILATION AND COMPARISON OF THE CORRELATIONS FOR THE CALCULATION OF THE HEAT TRANSFER COEFFICIENTS IN THE REGION OF THE FORCED CONVECTION WITH ONE-PHASE COOLANT

6.1 Forced water convection

For the calculation of the heat transfer coefficients (WUK) with fully developed turbulent flow there were chosen two correlations, well established on hand of test results:

a) Dittus-Boelter correlation /9/

$$\alpha = 0.023 \cdot \frac{\lambda_f}{D} \cdot Re_f^{0.8} \cdot Pr_f^{0.4} \quad (5)$$

$$\text{with } Re_f = \frac{G \cdot D}{\eta_f} \text{ and } Pr_f = \frac{\eta_f \cdot C_p}{\lambda_f}$$

The physical characteristics are calculated with the mean temperature between wall and coolant.

$$\text{Region of validity: } 5000 \leq Re \leq 7 \cdot 10^5 \\ 0.7 \leq Pr \leq 100$$

b) Sieder-Tate correlation /10/

$$\alpha = 0.023 \cdot \frac{\lambda_f}{D} \cdot Re_f^{0.8} \cdot Pr_f^{0.33} \cdot \left(\frac{\eta_f}{\eta_f^*} \right)^{0.14} \quad (6)$$

The reference temperature for the physical characteristics is the water temperature η^* is calculated with the wall temperature [sic].

$$\text{Region of validity: } 2300 \leq Re \leq 10^6 \\ 0.6 \leq Pr \sim 70$$

For the calculation of the heat transfer coefficients (WUK) with laminar flow there was used the Sieder-Tate correlation

- Sieder-Tate correlation for laminar flow /10/

$$\alpha = 1.86 \cdot \frac{\lambda_f}{D} \cdot (Re \cdot Pr \cdot \frac{D}{l})^{0.33} \cdot (\frac{\eta_f}{\eta_f^*})^{0.14} \quad (7)$$

The physical characteristics are calculated with the coolant temperature.
For η_f^* is used the wall temperature.

Region of validity: $Re \leq 2300$
 $Pr \sim 1$

6.2 Forced steam convection

For the calculation of the heat transfer coefficients with turbulent flow there were chosen the following correlations:

- Dittus-Boelter equation /9/

$$\alpha = 0.023 \cdot \frac{\lambda_d}{D} \cdot Re_d^{0.8} \cdot Pr_d^{0.4} \quad (8)$$

with $Re_d = \frac{G \cdot D}{\eta_d}$ and $Pr_d = \frac{\eta_d \cdot Cp_d}{\lambda_d}$

The physical characteristics are calculated with the mean temperature between wall and coolant.

Region of validity: $5000 \leq Re \leq 7 \cdot 10^5$
 $0.7 \leq Pr \leq 100$

- McEligot correlation /11/

$$\alpha = 0.021 \cdot \frac{\lambda_d}{D} \cdot Re_d^{0.8} \cdot Pr_d^{0.4} \cdot (\frac{T_d}{T_w})^{0.5} \quad (9)$$

The physical characteristics are calculated with the mean temperature between wall and steam.

Region of validity:

$$1450 \leq Re \leq 4.5 \cdot 10^4$$

The heat transfer coefficients in the region of the laminar steam flow were calculated with the aid of the Hausen correlation.

- Hausen correlation for laminar steam flow/12/

$$\alpha = 3.66 \cdot \frac{\lambda_d}{D} \cdot \left(\frac{T_d}{T_w} \right)^{0.25} \quad (10)$$

λ_d is calculated with the mean temperature between wall and steam.

Region of validity:

$$Re \leq 2300$$

6.3 Comparison of the correlations

The values of the heat transfer coefficients, as calculated with these correlations for typical parameter combinations in loss-of-coolant accidents, are shown in Attachment 3 and compared with each other. An examination of these correlations within a wider parameter scope is contained in /13/.

7. COMPILATION AND COMPARISON OF THE CORRELATIONS FOR THE CALCULATION OF THE HEAT TRANSFER COEFFICIENTS (WUK) OF THE SUBCOOLED AND SATURATED NUCLEATE BOILING

7.1 Calculation of the necessary temperature difference for bubbles formation with subcooled fluid

For the calculation of the temperature difference between the wall and saturation temperatures, necessary for the formation of bubbles, there were chosen two empirical equations.

- Jens-Lottes equation /14/

$$\Delta T_{bs} = 7.9 \cdot (q \cdot 10^{-4})^{0.25} \cdot e^A \quad (11)$$

$$A = - \frac{P}{6.205 \cdot 10^6}$$

Region of validity:

$$\begin{aligned} P &\leq 14 \text{ MPa} \\ q &\leq 11 \cdot 10^6 \text{ W/m}^2 \\ G &\leq 10000 \text{ kg/m}^2 \cdot \text{s} \end{aligned}$$

- Thom equation /15/

$$\Delta T_{bs} = 2.25 \cdot (q \cdot 10^{-4})^{0.5} \cdot e^A \quad (12)$$

$$A = \frac{P}{8.687 \cdot 10^6}$$

Region of validity:

$$\begin{aligned} 5 \text{ MPa} &\leq P \leq 14 \text{ MPa} \\ q &\leq 160 \cdot 10^4 \text{ W/m}^2 \\ 1000 &\leq G \leq 3800 \text{ kg/m}^2 \cdot \text{s} \end{aligned}$$

7.2 Calculation of the heat transfer coefficients in the region of the subcooled nucleate boiling

For the calculation of the heat flux there was used the modified Chen correlation.

- Modified Chen correlation /16/

$$q = \alpha_{\text{mac}} (T_w - T_f) + \alpha_{\text{mic}} (T_w - T_{\text{sat}}) \quad (13)$$

$$\text{with } \alpha_{\text{mac}} = 0.023 \cdot \frac{\lambda_f}{D} \cdot \text{Re}_f^{0.8} \cdot \text{Pr}_f^{0.4} \quad (14)$$

$$\text{and } \alpha_{\text{mic}} = 0.00122 \cdot \left(\frac{A}{B} \right) \cdot \Delta T^{0.24} \cdot \Delta P^{0.75} \cdot S \quad (15)$$

$$\text{wherein } A = \lambda_f^{0.79} \cdot \text{Cp}_f^{0.45} \cdot \rho_f^{0.49}$$

$$B = \sigma^{0.5} \cdot \eta_f^{0.29} \cdot \Delta h_e^{0.24} \cdot \rho_d^{0.24}$$

$$\text{and } S = \left(\frac{\Delta T_{\text{eff}}}{\Delta T} \right)^{0.99} - \text{suppression factor (see Chapter 7.3)}$$

This correlation was verified by Butterworth based on experiments with water and butyl alcohol and it led to a good consistency between the calculated and the measured values. However, the exact region of validity was not given in /16/.

7.3 Calculation of the heat transfer coefficients (WUK) in the region of nucleate boiling

For the calculation of the heat transfer coefficients (WUK) during nucleate boiling there were used the Chen and Schrock-Grossmann correlations.

a) Chen correlation /17/

$$\alpha = \alpha_{\text{mic}} + \alpha_{\text{mac}} \quad (16)$$

$$\alpha_{\text{mac}} = 0.023 \cdot \frac{\lambda_f}{D} \cdot \text{Re}_f^{0.8} \cdot \text{Pr}_f^{0.4} \cdot F \quad (17)$$

$$\text{with } F = \left(\frac{\text{Re}_{zP}}{\text{Re}_f} \right)^{0.8}$$

$$\alpha_{\text{mic}} = 0.00122 \cdot \left(\frac{A}{B} \right) \cdot \Delta T^{0.24} \cdot \Delta P^{0.75} \cdot S \quad (18)$$

$$A = \lambda_f^{0.79} \cdot C p_f^{0.45} \cdot \rho_f^{0.49}$$

$$B = \sigma^{0.5} \cdot \eta_f^{0.29} \cdot \Delta h_e^{0.24} \cdot \rho_d^{0.24}$$

The curves of F and S are shown in Fig. 12 resp. Fig. 13.

Region of validity:

$$0 < x < 0.7$$

$$70 < G < 8000 \text{ kg/m}^2 \cdot \text{s}$$

$$40 < q < 2.40 \text{ W/cm}^2$$

b) Schrock-Grossmann correlation /18/

$$\alpha = 2.5 \cdot \left(\frac{1}{x_{tt}} \right)^{0.75} \cdot \alpha_o \quad (19)$$

$$\alpha_o = 0.023 \cdot \frac{\lambda_f}{D} \cdot \left[\frac{D \cdot G}{\eta_f} \cdot (1-x) \right]^{0.8} \cdot Pr_f^{0.4} \quad (20)$$

$$\frac{1}{x_{tt}} = \left(\frac{x}{1-x} \right)^{0.9} \cdot \left(\frac{\rho_f}{\rho_d} \right)^{0.5} \cdot \left(\frac{\eta_d}{\eta_f} \right)^{0.1} \quad (21)$$

Region of validity: $x > 0.02$

7.4 Comparison of the correlations

The values of ΔT_{BS} and of the heat transfer coefficients for some typical parameter combinations are contained in Attachment 4.

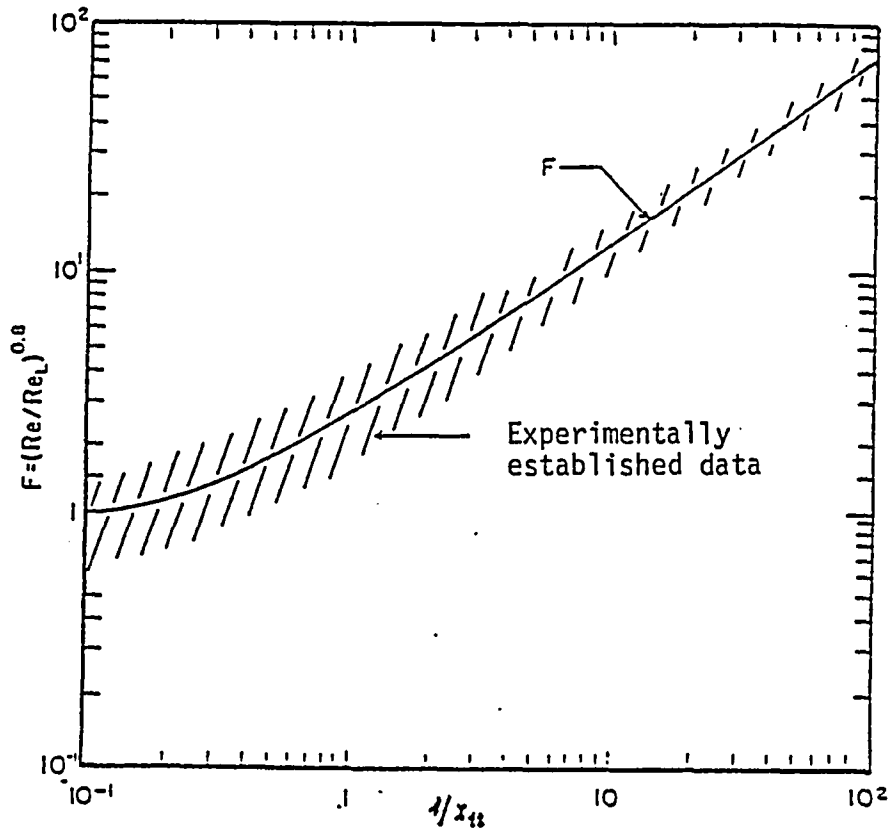


Fig. 12: Reynold's number multiplier F according to Chen

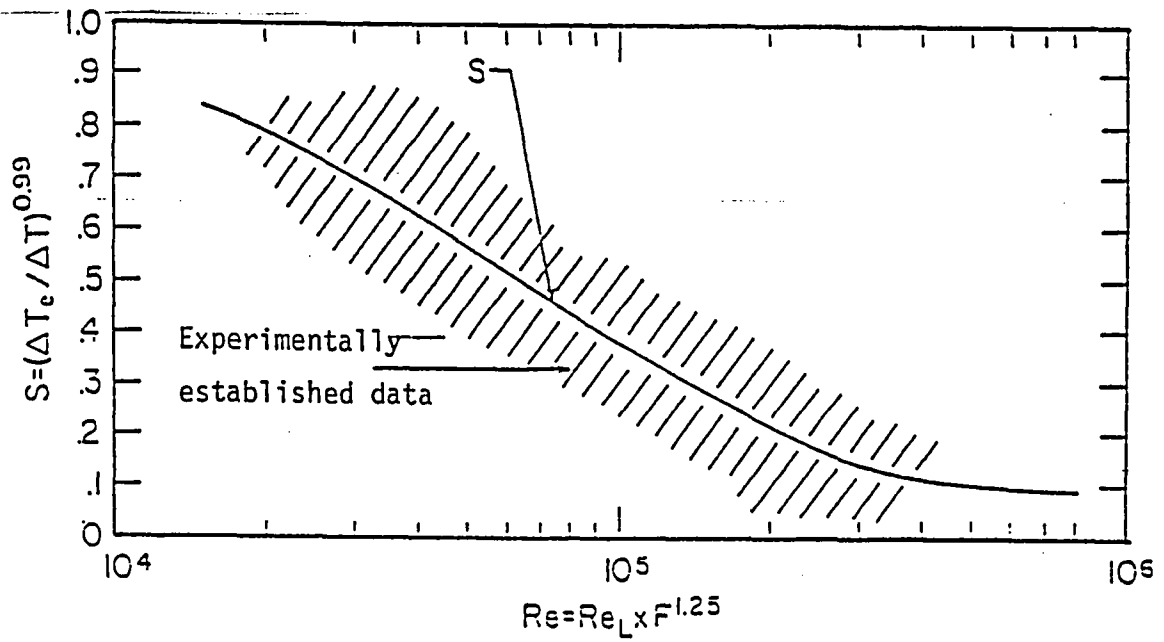


Fig. 13: Suppression factor S according to Chen

8. TRANSFER FROM NUCLEATE BOILING TO FILM BOILING, RESP. STEAM-DROPLETS COOLING - (MAXIMUM CRITICAL HEAT FLUX)

The two fundamental physical appearances of the first heat transfer crisis were already dealt with in Chapter 2. Here, there shall be examined the individual physical models and correlations for the calculation of the critical heat flux.

8.1 Vessel film boiling

The phenomenon of the critical heat flux easily examined during boiling in heated vessels. A closed process of the dependence between heat flux and temperature difference ($T_{\text{wall}} - T_{\text{sat}}$) was first represented by Nukiyama /19/ in the manner of a so-called boiling-curve (Fig. 14). Due to the rise of the heat transfer coefficients in the region of the nucleate boiling the slope of the boiling-curve becomes gradually steeper up to point B. When the heat flux reaches the value of point B, there is formed a steam film between the wall and the fluid, the heat elimination from the wall is limited now by the low heat conductivity of the steam, and the temperature difference increases suddenly (B-C jump of the boiling-curve).

The hypothesis of the fluid dynamic origin of the heat transfer crisis was first formulated by Kutateladze /20/. From the separated impulse and continuity equations for water and steam there were established the following dimensionless groups, describing the conditions during the first heat transfer crisis:

$$\frac{w_f^2}{g \cdot l}, \quad \frac{\Delta P}{\rho_f \cdot w_f^2}; \quad \frac{w_f \cdot \tau}{l}, \quad \frac{w_d \cdot \tau}{l}; \quad \frac{\rho_f \cdot w_f^2}{\rho_d \cdot w_d^2}; \quad \frac{w_d^2 \cdot \rho_d}{g \cdot l (\rho_f - \rho_d)}; \quad \frac{\sigma}{(\rho_f - \rho_d) l^2}$$

With the assumption, that with free convection the first five groups can be disregarded, there was deduced the following equation in agreement with the Rayleigh theory of stability for the maximum steam volume flow from the heated surface:

$$(j_d)_{\text{max}} = \frac{q_{\text{max}}}{\rho_d \cdot \Delta h_e} = K \cdot \left[\frac{\sigma \cdot g (\rho_f - \rho_d)}{\rho_d^2} \right]^{0.25} \quad (22)$$

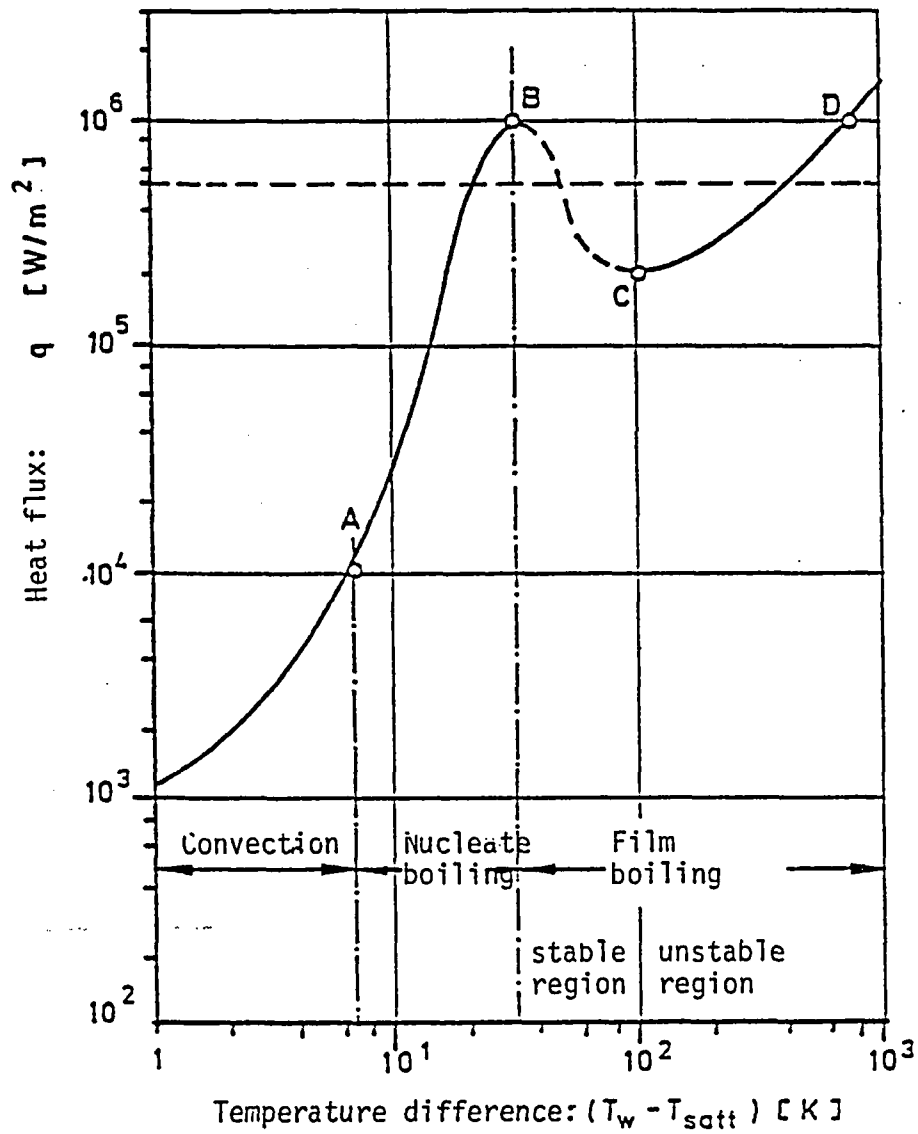


Fig 14: Boiling-curve according to Nukiyama for container boiling with 0.1 MPa

The value of K was analytically determined by Zuber

$$K = \sqrt{\frac{\pi}{128}}$$

so that the equation for the maximum critical heat flux reads:

$$q_{\max} = 0.1567 \cdot \Delta h_e \cdot \rho_d^2 [\sigma \cdot g \cdot (\rho_f - \rho_d)]^{0.25} \quad (23)$$

Similar equations were established at a later date by other authors, as for example by Zuber /21/ and Chang, Snyder /22/.

8.2 Heat transfer crisis with forced convection, high heat flux and low steam content - (DNB)

8.2.1 Semi-empirical model

Essentially, two different models were developed for the description of the physical processes during the transfer between nucleate boiling and film boiling. For the first and more simple model one starts with the premise, that the isolating steam layer is located directly between the wall and the fluid. Based on the result of an experimental investigation, Kutateladze and Leontev /23/ developed an equation for the calculation of the separation of the boundary layer in fluid flow with lateral injection of air into the flow channel.

$$\rho_{inj} V_{inj} = 2 \cdot f_f \cdot w_f \cdot \rho_f \quad (24)$$

Tong /24/ modified this equation for the conditions under DNB

$$\rho_g \cdot V_{bl} = \frac{q}{\Delta h_e} = C \cdot f_{tp} \cdot \rho_f \cdot w_f \quad (25)$$

He further used the correlation of Maines /25/ for a calculation of f_{tp} with low steam content

$$f_{tp} = Re^{-0.6} \quad (25)$$

established, based on test results, the correlation constant C as function of steam content:

$$C = 1.76 - 7.43x + 12.22 \cdot x^2 \quad (27)$$

Tong equation for the calculation of the critical heat flux (KHB):

$$q_{\max} = (1.76 - 7.43x + 12.22x^2) \cdot \Delta h_e \cdot \left(\frac{\eta_f}{D}\right)^{0.6} w_f^{0.4} \cdot \rho_f^{0.4} \quad (28)$$

Starting from the Reynolds analogy, Thorgerson et al /26/ developed another equation for the calculation of the critical heat flux (KHB):

$$St = \frac{f}{2}, \quad St = \frac{\alpha}{\rho_f \cdot w_f \cdot Cp_f}$$

therefrom results:

$$\alpha = \frac{q}{\Delta T} = \frac{f}{2} \cdot \rho_f \cdot w_f \cdot Cp_f \quad (29)$$

and for the DNB conditions:

$$q_{\max} = \frac{f_{\text{DNB}}}{2} \cdot \rho_f \cdot w_f \cdot Cp_f \cdot (T_w - T_{\text{sat}}) \quad (30)$$

For the calculation of f_{DNB} there was used the equation (31):

$$f_{\text{DNB}} = 7.413 \cdot Re^{0.545} \quad (31)$$

Monde, Katto /27/ and Katto, Ishii /28/ started from the dimensional analysis for the development of their own correlations and they established for the volume-related steam velocity the following dimensionless groups:

$$\frac{q_{\max}}{\rho_d \cdot \Delta h_e \cdot w} = f \left(\frac{\rho_f}{\rho_d}; \frac{\eta_f}{\eta_d}; \frac{\sigma}{\rho_f \cdot w^2 \cdot l}; \frac{\eta_f}{\rho_f \cdot w \cdot l}; \frac{g(\rho_f - \rho_d)l}{\rho_f \cdot w^2} \right) \quad (32)$$

It was assumed that the influence of viscosity and buoyancy can be disregarded during the first-heat-transfer-crisis-in-the-flowed-through-channel, -so-that the equation (32) reads:

$$\frac{q_{\max}}{\rho_d \cdot \Delta h_e \cdot w} = f \left(\frac{\rho_f}{\rho_d}; \frac{\sigma}{\rho_f \cdot w^2 \cdot l} \right) \quad (33)$$

Through the adaption of the individual exponents and of the correlation constant to each of the used test results, there were established the following correlations:

Monde-Katto correlation /27/

$$q_{\max} = 0.0745 \cdot w \cdot \rho_d \cdot \Delta h_e \cdot \left(\frac{\rho_f}{\rho_d} \right)^{0.725} \cdot \left(\frac{\sigma}{\rho_f \cdot w^2 \cdot l} \right)^{1/3} \quad (34)$$

Katto-Ishii correlation /28/

$$q_{\max} = 0.0164 \cdot w \cdot \rho_d \cdot \Delta h_e \cdot \left(\frac{\rho_f}{\rho_d} \right)^{0.867} \cdot \left(\frac{\sigma}{\rho_f \cdot w^2 \cdot l} \right)^{1/3} \quad (35)$$

These correlations were chosen from the plethora of similar equations and used for the calculation of the critical heat flux (KHB). The figures in Attachment 5 show the comparison of the processes of q_{\max} for some typical parameter combinations.

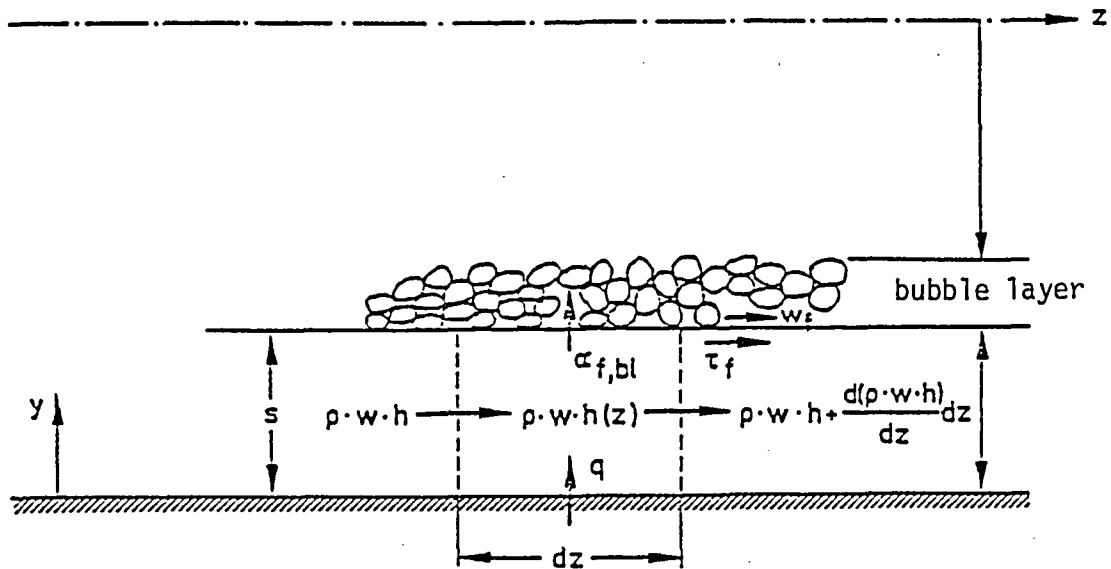


Fig. 15: Model representation for the determination of the critical heat flux according to Tong

The second model developed by Tong starts from the premise that the isolating steam layer is not located directly between wall and fluid but rather, as shown in Fig. 15, that there is a thin layer of water between wall and the bubbles. The presence of this layer of water was observed during the photographic examination with freon of the flow conditions at DNB /29/. The energy equation for the layer of water between the wall and the bubbles was established by Tong as follows /30/:

$$\frac{d}{dz} (\rho_f \cdot w_f \cdot p \cdot s \cdot h_f) + \frac{\alpha_{f,bl} \cdot p}{Cp_f} - q \cdot p = 0 \quad (36)$$

with s = thickness of layer of water
 $\alpha_{f,bl}$ = heat transfer coefficient (WUK) between layer of water and bubbles
 p = heated range

Under the assumption that $p_f \cdot w_f \cdot s$ remains constant along the flow path, the equation (36) can be simplified as follows:

$$\frac{d}{dz} (h_f - h_{f,sat}) + C(h_f - h_{f,sat}) = C \cdot \frac{Cp_f \cdot q}{\alpha_{f,bl}} \quad (37)$$

$$\text{with } C = \frac{\alpha_{f,bl}}{\rho_f \cdot w_f \cdot s \cdot Cp_f} \quad (38)$$

Since the individual parameters in the equation (38) are partially unknown, an empirical equation was established for C , based on measured results

$$C = 0.44 \cdot \frac{A}{B} \cdot \text{inch}^{-1} \quad (39)$$

$$\text{with } A = (1 - x_{DNB})^{7.9} \quad \text{and } B = (G \cdot 10^{-6})^{1.72}$$

The practical application of this model is however very difficult because of the very narrow region of validity for C and because of the complicated conversion to conditions with variable heat flux.

8.2.2 Empirical correlations

In a manner similar to the one for the preceding case, a series of empirical correlations was published for the calculation of the maximum critical heat flow (KHB). Already in the year 1964, in the treatise of Milioti /31/ there were compiled 59 correlations for the calculation of the critical heat flux, which were developed in connection with the reactor safety analysis. The deviations of the values of the maximum critical heat flux, calculated with each of the correlations, were denoted in this treatise as very large. Instead of this group of correlations there were chosen three equations, most used in the reactor safety analysis:

a) W-3 correlation /32/

$$\begin{aligned}
 q_{\max} = & 3.15459 \cdot 10^6 \cdot \\
 & \cdot \{(2.022 - 0.0004302 \cdot P) \cdot (0.1722 - 0.0000984 \cdot \\
 & \cdot P) \cdot \exp[(18.177 - 0.004129 \cdot P) \cdot x]\} \cdot \\
 & \cdot [(0.1484 - 1.596 \cdot x + 0.1729 \cdot x \cdot |x|) \cdot \quad (40) \\
 & \cdot G \cdot 10^{-6} + 1.037] \cdot [1.157 - 0.869 \cdot x] \cdot \\
 & \cdot [0.2664 + 0.8357 \cdot \exp(-3.151 \cdot D)] \cdot \\
 & \cdot [0.8258 + 0.000794 \cdot (h_l - h_{in})]
 \end{aligned}$$

Region of validity

$$\begin{aligned}
 7 \leq P \leq 16 \text{ MPa} \\
 1360 \leq G \leq 6800 \text{ kg/m}^2 \cdot \text{s} \\
 -0.15 \leq x \leq 0.15 \\
 5 \cdot 10^{-3} \leq D \leq 17.5 \cdot 10^{-3} \text{ m} \\
 0.25 \leq L \leq 3.6 \text{ m}
 \end{aligned}$$

Observation: This equation is applicable only in the case of homogenous power distribution.

b) B-W-2 correlation /33/

$$\begin{aligned}
 q_{\max} = & \frac{1.15509 - 0.40703 \cdot D}{12.71 \cdot [3.0545 \cdot G \cdot 10^{-6}]^A} \cdot \quad (41) \\
 & \cdot \{3.702 \cdot 10^7 \cdot [0.59137 \cdot G \cdot 10^{-6}]^B - 0.15208 \cdot x \cdot \Delta h_e \cdot G\}
 \end{aligned}$$

$$A = 0.71186 + 0.20729 \cdot 10^{-3} \cdot (P-2000)$$

$$B = 0.834 + 0.68479 \cdot 10^{-3} \cdot (P-2000)$$

Region of validity: $14 \leq P \leq 16$ MPa
 $1020 \leq G \leq 5430$ kg/m²·s

c) Macbeth correlation /16/

$$q_{\max} = 10^6 \cdot \frac{A+C \cdot D \cdot (G \cdot 10^{-6}) \cdot 0.25 \cdot (h_z - h_E)}{1+C \cdot I} \quad (42)$$

$$\text{with } A = y_0 \cdot D^{y_1} (G \cdot 10^{-6})^{y_2}$$

$$B = y_3 \cdot D^{y_4} (G \cdot 10^{-6})^{y_5}$$

The values of $y_0, y_1, y_2, y_3, y_4,$ and y_5 for various pressures are contained in Table 3.

Table 3: Values of the Macbeth correlation coefficients for various pressure ranges

Pressure psia	y_0	y_1	y_2	y_3	y_4	y_5	R.M.S. error %	No. of data points
15	1.12	-0.211	0.324	0.0010	-1.4	-1.05	13.8	88
220 (nom)	1.77	-0.353	-0.250	0.0166	-1.4	-0.937	4.7	237
530 (nom)	1.57	-0.366	-0.329	0.0127	-1.4	-0.737	5.7	170
1000	1.06	-0.487	-0.179	0.0055	-1.4	-0.555	7.4	405
1570 (nom)	0.720	-0.527	0.024	0.0121	-1.4	-0.096	3.4	133
2000	0.627	-0.268	0.192	0.0093	-1.4	-0.343	9.0	362
2700 (nom)	0.0124	-1.45	0.439	0.0097	-1.4	-0.529	4.7	37

Observation: The parameters in the equations (40), (41) and (42) are to be given in British units.

The values of the critical heat fluxes, calculated with these three correlations, for the same parameter combinations as in Chapter 8.2.1., are shown in Attachment 5.

8.3 Heat transfer crisis with forced convection, low to intermediate heat flux, and intermediate to high steam content (dry-out)

8.3.1 Analytical models

The known model designs for the calculation of the dry-out of the water film in dependence of the supplied energy, total mass flow and system pressure do mostly originate from a mass balance for the film flowing along the wall. The change of the liquid mass flowing in the film has to be attributed to the evaporation, to the breaking-off of droplets (entrainment) and to the originating renewed deposition of the droplets caused by the turbulent radial velocity component (Fig. 16).

The mass balance equation for the water film with an annular flow in the flowed-through-pipe was first established by Leslie and Kirby /34/ as follows:

$$\frac{\partial w_{LF}}{\partial z} = \pi \cdot D (G_D - G_E - \frac{q}{\Delta h_e} - \rho_f \cdot \frac{\partial \delta}{\partial t}) \quad (43)$$

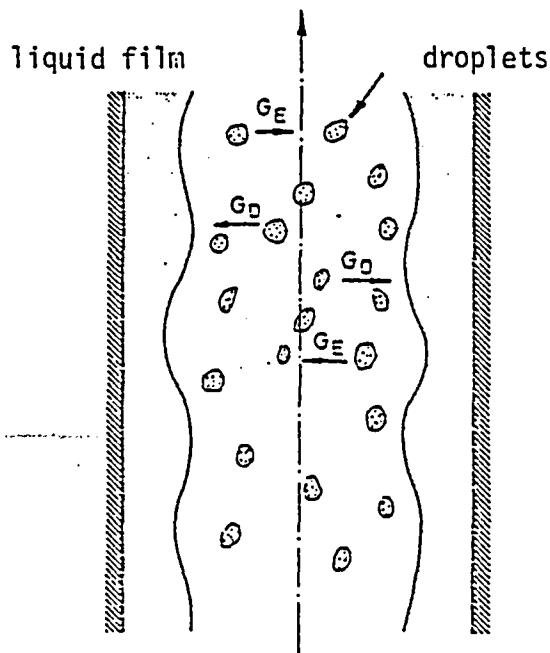


Fig. 16: Model of the annular flow with entrainment and deposition

the mass balance for the separated fluid:

$$\frac{\partial W_E}{\partial z} = \pi \cdot D(G_E - G_D) - \frac{\pi \cdot D^2}{4} \cdot \frac{\partial C}{\partial t} \quad (44)$$

with C as droplet concentration in the steam flow.

The deposition of droplets in the liquid film was described with the aid of a mass transfer coefficient K

$$G_D = K \cdot C \quad (45)$$

and

$$G_E = K \cdot C_E \quad (46)$$

Under the assumption that C_E is a function of $\tau \cdot \delta / \sigma$ and that K is a function of α , the correlations shown in Figures 17 resp. 18 were established for these two unknown quantities. For the determination of the local pressure loss (necessary for the calculation of τ) there was used the equation (47).

$$\frac{4\delta}{D} = \left[\frac{(dP/dz)_{LF}}{(dP/dz)} \right]^{0.5} \quad (47)$$

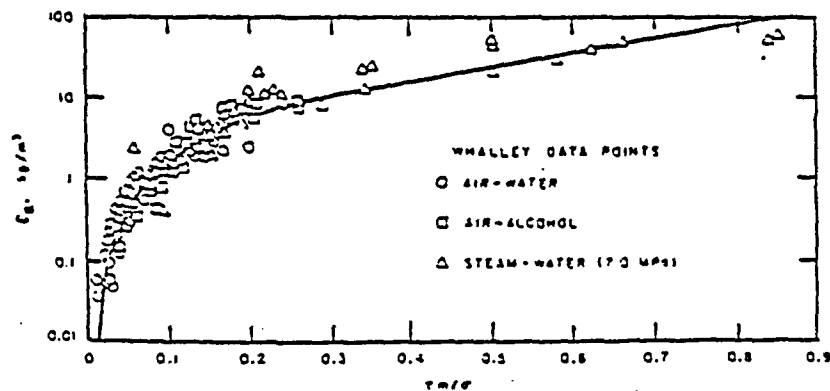


Fig. 17: Harwell correlation for the determination of the entrainment coefficient.

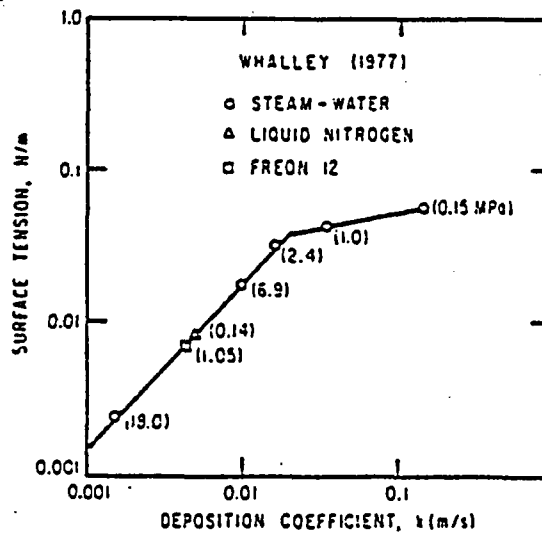


Fig. 18: Harwell correlation for the determination of the deposition coefficient

For BWR conditions, Belda /35/ developed a model for the calculation of the film thickness in dependence of time. For the determination of the film thickness in the case of a BWR LOCA one started from the conservation theorems for mass and energy, whereby the mass flows, given by film and droplets, were described by simple statements. The obtained differential equation for the film thickness in dependence of time was solved numerically and the dry-out moment was determined with film thickness = zero.

An equation for the calculation of the dry-out moment was developed by Mayinger and Belda /36/:

$$t_{DO} = \frac{\rho_f}{(\partial \rho_f / \partial P) \cdot (\partial P / \partial t)} \cdot \ln \left(\frac{A}{B} \right) \quad (48)$$

$$A = - \frac{a}{\pi \cdot D \cdot l \cdot \Delta h_e} - \delta_o \cdot \frac{\partial \rho_f}{\partial P} \cdot \frac{\partial P}{\partial t} + \frac{C \cdot D}{4 \cdot l \cdot \rho_f} \left[\int (1-\psi) \frac{\partial P}{\partial z} dt \right] t_{DO}$$

$$B = - \frac{a}{\rho_f \cdot D \cdot l \cdot \Delta h_e} + \frac{C \cdot D}{4 \cdot l \cdot \rho_f} \left[\int (1-\psi) \frac{\partial P}{\partial z} dt \right] \cdot t_{DO}$$

wherein δ_0 is the film thickness in the stationary initial state and the constant C was determined by the adaption to the test results.

$C = 0.15$ for freon 12 and $C = 0.6$ for water.

8.3.2 Semi-empirical and empirical correlations

a) Hsu-Beckner correlation /37/

Hsu and Beckner developed a correlation for the calculation of the maximum critical heat flux (KHB) in transient processes. This correlation is, according to the assertions by the authors, valid for a wide sphere of the determining parameters and can be used for both types of the first heat transfer crisis DNB and dry-out.

$$\frac{q_{\max} - q_{w,d}}{q_{w-3} - q_{w,d}} = 1.33 \cdot (0.96 - \psi)^{0.5} \quad (49)$$

wherein q_{w-3} is the heat flux with steam content $x = 0$, calculated with the aid of the W-3 correlation, and $q_{w,d}$ represents the heat flux density between wall and steam, calculated with the aid of the Dittus-Boelter correlation for heat transfer coefficient.

b) Zuber-Griffin correlation /38/

This correlation represents a modified form of the Kutateladze-Zuber correlation for the calculation of the critical heat flux (KHB) during nucleate boiling and it was developed for the range of the low mass flows.

$$q_{\max} = q_{\max, \text{Zuber}} \cdot (1 - \psi) \quad (50)$$

c) Slifer-GE correlation /39/

This correlation has a very simple form and it was divided into two regions of validity through the modification of the correlation coefficient.

$$q_{\max} = 3.155 \cdot 10^6 (0.8-x) \text{ for } G \geq 680 \text{ kg/m}^2 \cdot \text{s}$$

and

$$q_{\max} = 3.155 \cdot 10^6 (0.84-x) \text{ for } G \leq 680 \text{ kg/m}^2 \cdot \text{s}$$

(51)

d) Smolin correlation /40/

Also this correlation has a simple form and according to the assertions of the authors a relatively wide region of validity.

$$q_{\max} = 6.5 \cdot 10^5 \cdot [G^{0.2} \cdot (1-x)]^{1.2} \cdot (1.3 - 4.28 \cdot 10^{-8} \cdot P) \quad (52)$$

Region of validity:

$$380 \leq G \leq 4930 \text{ kg/m}^2 \cdot \text{s}$$

$$2.94 \leq P \leq 13.7 \text{ MPa}$$

$$-0.18 \leq x \leq 0.6$$

e) Biasi correlation /41/

$$q_{\max} = \frac{2.75 \cdot 10^4}{(100D)^n \cdot G^{0.167}} \cdot \left(\frac{1.47 \cdot A}{G^{0.167}} - x \right) \quad (53)$$

for low steam contents ($x < 0.3$) and

$$q_{\max} = \frac{1.51 \cdot 10^4 \cdot B}{(100D)^n \cdot G^{0.6}} \cdot (1-x) \quad (54)$$

for higher steam contents and $G < 300 \text{ kg/m}^2 \cdot \text{s}$

wherein

$$n = 0.4 \text{ for } D \geq 0.01 \text{ m}$$

$$n = 0.6 \text{ for } D < 0.01 \text{ m}$$

$$A = 0.7249 + 0.99 \cdot P \cdot \exp(-0.32P)$$

$$B = -1.159 + 1.49 \cdot P \cdot \exp(-0.19P) + \frac{8.99 \cdot P}{1+10P^2}$$

f) CISE correlation /42/

$$q_{\max} = \frac{1.258 \cdot \Delta h_e}{D^{0.4} \cdot A} \cdot (B-x) \quad (55)$$

$$A = \left(\frac{1}{P_r} - 1 \right) \text{ und } B = (1 - P_r) / (G \cdot 10^3)^{0.333}$$

wherein $P_r = \frac{P}{P_c}$ and $P_c = 22.1 \text{ MPa}$ - critical pressure

In Attachment 5 are shown the values of q_{\max} for chosen parameter combinations, calculated with the equations (49), (50), (51), (52), (53), and (55).

8.4 Verification of the correlations for the calculation of the maximum critical heat flux (KHB) based on the experimental results

8.4.1 Selection of the correlations

For the verification based on the results from the 25-rod bundle tests there were chosen the following correlations:

- Tong equation (28)
- Thorgerson equation (30)
- Monde-Katto equation (34)
- W-3 equation (40)
- B-W-2 equation (41)
- Macbeth equation (42)
- Silber-GE equation (51)
- Smolin equation (52)
- Zuber-Griffin equation (50)
- Biasi equation (53)
- CISE equation (55)

The chosen tests from the DNB and post-DNB test groups were recalculated with the computer code BRUDI-VA, whereby the maximum critical heat flux (KHB) was determined with the aid of each of the correlations in parallel with the calculation. If, in accordance with the corresponding correlation, the value of the critical heat flux was below the value of the local heat flux, there was effected the transfer from nucleate bubbling to the correlation for the calculation of the heat transfer coefficients in the post-DNB resp. post-dry-out regions. The moments of this transfer, as determined in the recalculation of several tests with each of the correlations, are compiled in Table 4 and compared with the test results.

Table 4: Comparison of the critical heat flux (KHF) correlations

TEST	TE Height (cm)	DNB - time delay (s)									
		Measur.	Mod. Zuber	W-3	Sli-fer	Smo-lin	B-W-2	Mac-beth	Biasi	Tong	Thor-geron
DNB-1	135	No DNB	2.6	-	-	-	-	-	-	-	-
	190	No DNB	0.7	0.65	-	-	0.7	1.2	-	0.92	0.4
	259	0.7	0.6	0.45	-	-	0.52	0.8	0.9	0.75	0.4
	327	0.4	0.5	0.2	1.1	1.1	0.4	0.6	0.6	0.8	0.4
	377	0.7	0.5	0.1	1.15	1.15	0.3	0.68	0.6	-	0.4
DNB-3	135	No DNB	0.8	0.7	1.5	1.5	0.7	1.0	1.4	-	0.38
	190	No DNB	0.65	0.5	1.2	1.2	0.65	0.84	1.0	0.64	0.38
	259	0.45	0.5	0.35	1.0	1.0	0.4	0.7	0.7	0.57	0.3
	327	0.2	0.4	0.15	0.85	0.85	0.25	0.55	0.46	0.63	0.3
	377	0.5	0.4	0.1	0.8	0.8	0.2	0.62	0.5	-	0.3
DNB-7	135	No DNB	2.3	-	-	-	-	-	-	-	-
	190	No DNB	0.8	0.65	-	-	0.8	1.4	-	-	0.6
	259	0.7	0.65	0.5	-	-	0.7	0.9	0.9	0.8	0.5
	327	0.5	0.55	0.35	1.5	-	0.4	0.65	0.65	0.8	0.4
	377	0.7	0.6	0.4	1.45	1.45	0.4	0.75	0.65	-	0.4
DNB-8	135	No DNB	1.1	0.65	-	-	-	-	-	-	-
	190	No DNB	0.8	0.6	-	-	0.82	0.93	1.2	0.85	0.8
	259	0.6	0.65	0.45	1.2	1.2	0.6	0.85	0.85	0.7	0.5
	327	0.5	0.55	0.4	0.95	0.95	0.45	0.75	0.7	0.75	0.4
	377	0.6	0.6	0.4	1.0	1.0	0.4	0.8	0.6	-	0.4
DNB-9	135	No DNB	0.9	0.85	-	-	-	-	-	-	-
	190	No DNB	0.75	0.65	1.3	1.3	0.75	0.9	1.2	0.8	0.8
	259	0.7	0.65	0.5	1.1	1.1	0.6	0.8	0.85	0.7	0.5
	327	0.5	0.55	0.4	1.0	1.0	0.5	0.75	0.7	0.78	0.4
	377	0.6	0.6	0.45	1.0	1.0	0.5	0.8	0.65	-	0.4
DNB-11	135	No DNB	2.0	-	-	-	-	-	-	-	-
	190	No DNB	1.5	1.6	3.2	3.2	1.7	1.9	1.8	1.5	1.5
	259	1.2	1.25	1.25	1.45	1.45	1.35	1.5	1.5	1.4	1.3
	327	0.9	1.2	1.2	1.75	1.75	1.3	1.45	1.5	1.5	1.2
	377	1.0	1.2	1.2	1.7	1.7	1.3	1.5	1.4	-	1.2

The Figures 19 to 22 show the processes of the critical heat flux, calculated with the chosen correlations, in the initial stage of two different DNB-tests. By way of comparison, in these figures are also plotted the processes of the heat flux as determined from measurement.

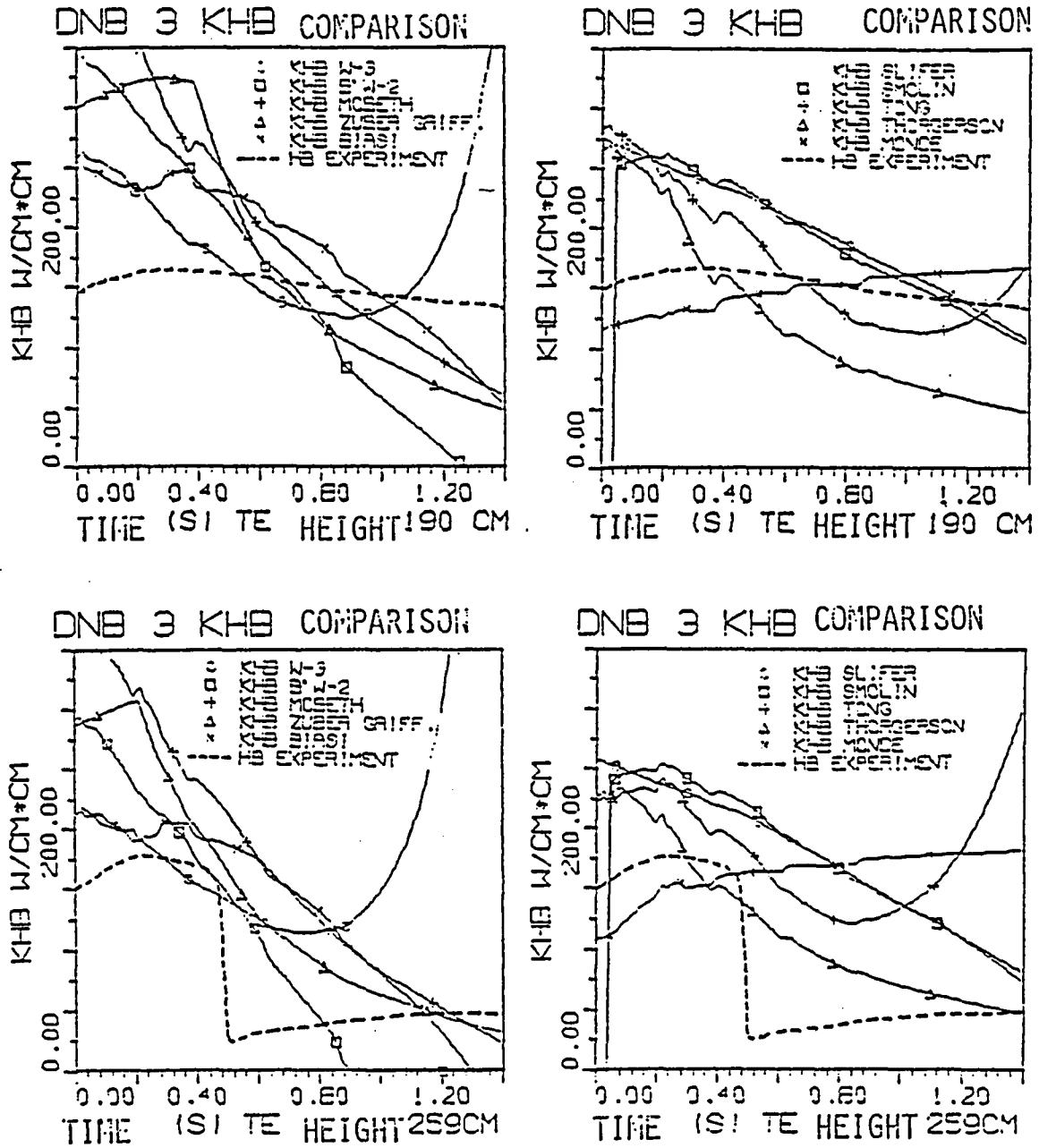


Fig. 19: Comparison of the critical heat flux (KHB) correlations - Test DNB3

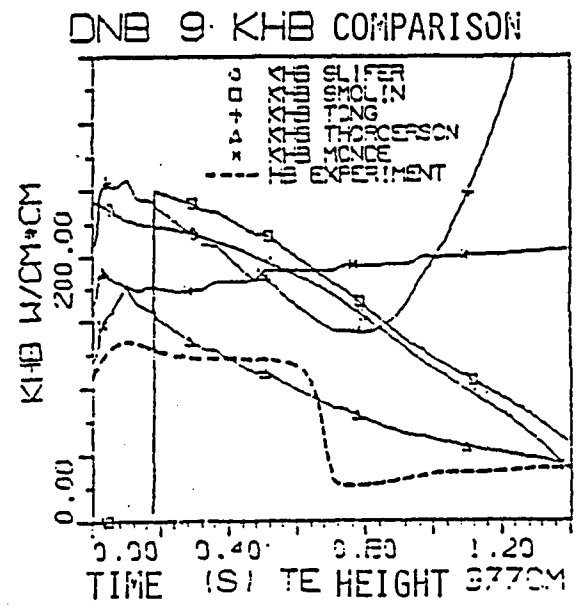
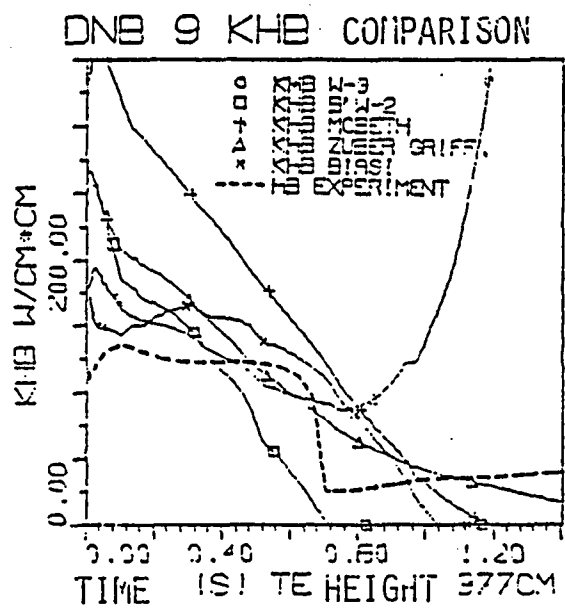
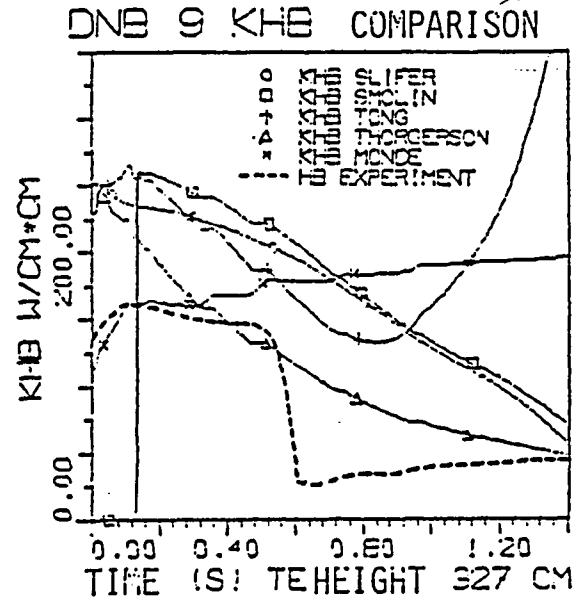
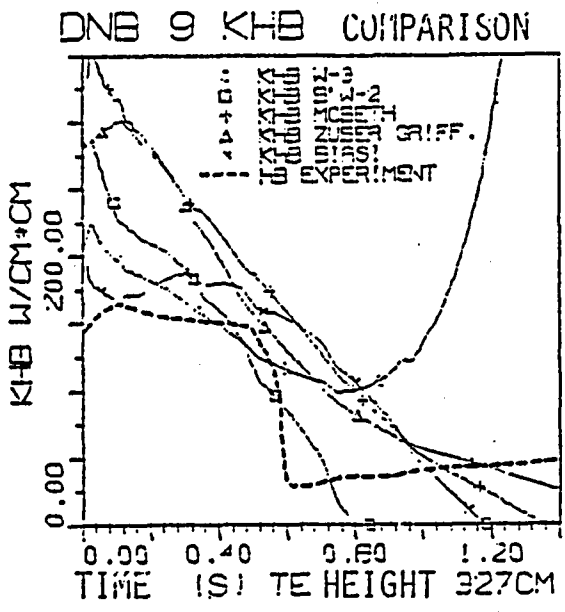


Fig. 22: Comparison of the critical heat flux (KHB) correlations - Test DNB9

8.4.2 Evaluation of the correlations for the calculation of the maximum critical heat flux

The results of the verification of the chosen correlations for the calculation of the maximum critical heat flux, compiled in this Chapter, show that none of the used correlations can calculate with sufficient accuracy for this phenomenon the critical heat flux in the abovementioned sphere of the test parameters of the 25-rod bundle tests. The graphic comparison of the processes of the critical heat flux under the same conditions in the measuring section, calculated with these correlations, shows how the values of the critical heat flux can differ. From the tabular comparison of the DNB delay times, calculated with each of the correlations, it results, that most of the equations calculated the moment of DNB too late and also an exceeding of the critical heat flux at axial positions in the bundle, whereas in the experiment the critical heat flux was not exceeded. As only realistic and, in the sense of the reactor safety analysis, conservative correlation proved to be, and this only after leaving the given region of validity, the W-3 equation. For the prediction of the dry-out moment with intermediate heat flux, based on this examination, there can be recommended the correlations by Slifer, Smolin and Biasi.

9. HEAT TRANSFER AT FILM BOILING AND STEAM-DROPLETS COOLING

This region of the heat transfer was, not only because of the importance in the reactor loss of coolant accident analysis, the center of many experimental and theoretical investigations. In this chapter is explained the phenomenology of each of the partial regions of the two-phase heat transfer after the exceeding of the maximum critical heat flux and some correlations are presented for the calculation of the heat transfer coefficients in this region. Subsequently, these correlations are used for the verification of selected tests of the research project RS 37C and the results will be compared with the test results.

9.1 Film boiling

As already mention in Chapter 2, in the case of film boiling it deals with a form of heat transfer which occurs in the high pressure phase of a LOCA with a rapid depressurization only very limited in function of time and place.

The transfer of the inverse annular flow, the flow form typical for this heat transfer mechanism, to the steam-droplets flow is additionally accelerated in a PWR bundle, in contrast to the flowed-through pipe, due to the effect of spacers and of the transverse exchange.

9.1.1 Film boiling with wettable wall

The accurate calculation of the heat eliminated from the wall in this area is very difficult because of the unstable thermal and fluid dynamic processes. The thin steam film, enveloping the wall, can be pierced by the waves at the core water flow. The liquid reaches the still wettable wall and it is again forced away from the wall by the very high evaporation. The wall temperature has however dropped because of the very effective nucleate boiling. This process can repeat itself several times.

Since the heat flux density in the case of an inverse annular flow has to be generally very high, the wall temperature increases very sharply

(up to 300 K per second) after the formation of the insulating steam film and the wetting temperature is rapidly exceeded. Therefore, the area of film boiling with wettable wall is only of subordinate importance for the calculation of the clad tube temperature processes and for the calculation of the heat transfer coefficients (WUK) there can be used by approximation the correlations described under 9.1.3.

9.1.2 Film boiling with not wettable wall

In case the wall temperature lies above the temperature of application, the liquid does always remain separated from the wall by a steam film (Leidenfrost phenomenon). The heat removal from the wall can be determined in this case with the aid of the correlations for the calculation of the heat transfer coefficients (WUK) with forced steam convection (equations (8), (9) Chapter 6.2) or with the correlations for the calculation of the heat transfer coefficients (WUK) with vessel film boiling.

9.1.3 Vessel film boiling

The conditions during film boiling in the heated vessel are schematically represented in Figure 23.

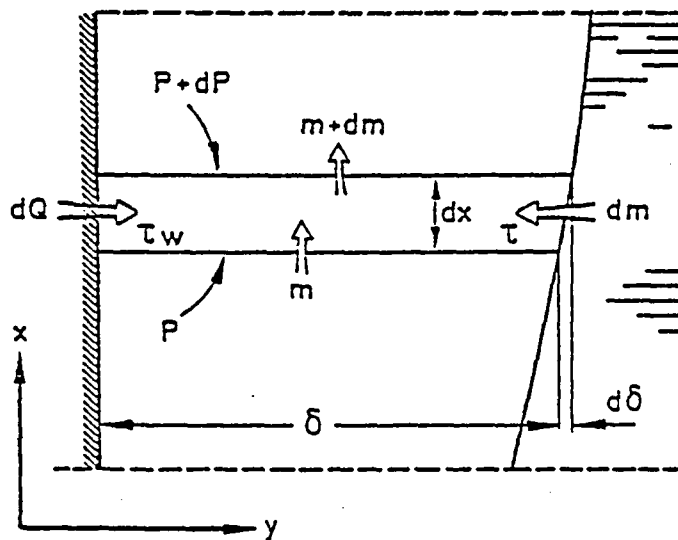


Fig. 23: Schematic representation of film boiling in vessel boiling

One of the first models of the film boiling mechanism with free convection was established by Awberry /43/. The heat that was conveyed to the water phase was calculated in this model as the sum of the heat fluxes which are conveyed to the water through the steam film because of conduction and radiation, less the heat required for the additional evaporation. According to his conception, the heat flux was then determined at the wall through the free convection in the water phase, so that for the Nusselt number there can be used the following equation:

$$Nu_f = K \cdot (Gr_f, Pr_f)^n \quad (56)$$

(n = 1/3 for horizontal plate)

All values in the equation were calculated with the mean temperature between saturation temperature (water surface) and the mean water temperature. For the calculation of the heat flux density there was derived the following equation:

$$q = \alpha(T_{sat} - T_f) = K \cdot (T_{sat} - T_f)^{4/3} [(\lambda_f^2 \cdot \rho_f^2 \cdot g \cdot \beta_f \cdot C_{p_f}) / \eta_f]^{1/3} \quad (57)$$

The correlation constant was determined through the adaption to experimental data:

$$K = 0.0015$$

Bromley /44/ postulated, in a manner similar to Awberry, that the heat from the wall is conveyed to the liquid through heat conduction and heat radiation. The heat conduction share was adequately treated pursuant to the film condensation theory of Nusselt, so that heat transfer coefficient (WUK) was defined as relation between the heat conductivity and the steam film thickness.

$$\delta = \{K \cdot \lambda_d (T_w - T_{sat}) \cdot \eta_d \cdot l / [\rho_d (\rho_f - \rho_d) \cdot g \cdot \Delta h_e^*]\}^{1/4} \quad (58)$$

$$\text{with } \Delta h_e^* = \Delta h_e [1 + 0.4 C_p (T_w - T_{sat}) / \Delta h_e] \quad (59)$$

thus, the correction for the heat transfer coefficient with laminar film boiling reads:

$$\alpha_K = \frac{\lambda_d}{\delta} = K \{[\lambda_d^3 \cdot g \cdot \rho_d (\rho_f - \rho_d) \cdot \Delta h_e^*] / [\eta_d (T_w - T_{sat}) \cdot l]\}^{1/4} \quad (60)$$

The mean value of the correlation constant was given by Bromley as $K = 0.62$. In cylinder geometry, r is replaced with D .

The heat transfer coefficient for the calculation of the radiation share was calculated according to Bromley from the following equation:

$$\alpha_{st} = \{K_{SB} / [(1/\epsilon) + (1/K_a) - 1]\} \cdot [(T_w^4 - T_{sat}^4) / (T_w - T_{sat})] \quad (61)$$

Hsu and Westwater /45/ did take into consideration the influence of the turbulence in the upper region of the steam film and developed for the convective heat transfer coefficient the equation:

$$\alpha_K = 0.002 \cdot (Re_d)^{0.6} / \{\eta_d^2 / [\lambda_d^3 \cdot \rho_d \cdot (\rho_f - \rho_d) \cdot g]\}^{1/3} \quad (62)$$

with $Re_d = \frac{4 W_d}{\pi \cdot D \cdot \eta_d}$

wherein W_d is the steam mass flow at the end of the film boiling region.

Berenson /46/ used for the determination of the characteristic geometric parameter (r resp. D in equation (60)) the Taylor-Helmholtz instability theory and established for the calculation of the convective heat transfer coefficient the following equation:

$$\alpha_K = K \cdot \{[\lambda_d^3 \cdot g \cdot \rho_d \cdot (\rho_f - \rho_d) \cdot \Delta h_e^*] / [\eta_d (T_w - T_{sat}) \cdot a]\}^{1/4} \quad (63)$$

with $a = \{\sigma / [g(\rho_f - \rho_d)]\}^{1/2} \quad (64)$

and the correlation constant $K = 0.425$.

The physical model, based on which is the reasoning of Berenson, is schematically represented in Fig. 24.

The values of the heat transfer coefficients, as they were calculated with the correlations of Bromley and Berenson, are shown in Attachment 6.

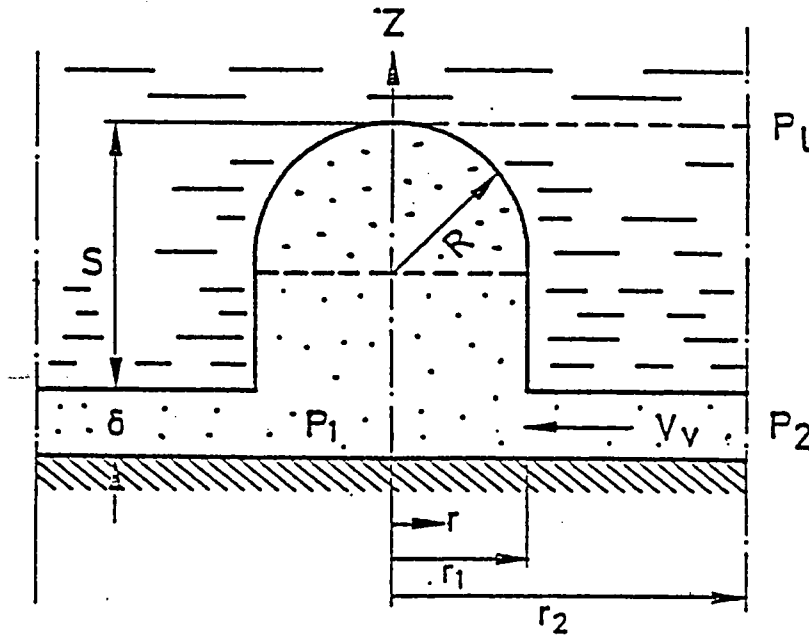


Fig. 24: Model of the vessel film boiling according to Berenson

9.2 Steam-droplets cooling

During the last few years, there were developed many more or less empirical correlations for the calculation of the heat transfer coefficients in the region of the steam-droplets cooling. Generally, these correlations can be divided into two groups:

- semi-empirical (phenomenological) models
- empirical correlations.

The empirical correlations are valid mostly only in a determined region of the parameters, without differentiating if in this region it deals with different physical processes. On the other hand, in the development of the phenomenological models it was endeavored to take into consideration the mechanism of the physical processes. The resolution of the overall

process into individual steps, led however in the majority of the cases to the need for the determination of parameters, which cannot be unobjectionably determined through measuring techniques and, thus, have to be finally established empirically.

In connection with the development of the so-called progressive computer programs hereafter will be subdivided the existing models into so-called equilibrium models, which are established on the assumption of the thermodynamic equilibrium, and the so-called nonequilibrium models, in which the thermodynamic non-equilibrium was taken into consideration.

9.2.1 Equilibrium models and correlations

Into this category fall most of the empirical correlations. They are based on the statement derived from the similarity principle for the on-phase forced convection.

$$Nu = K \cdot Re^n \cdot Pr^m \quad (65)$$

In order to take into account the varied nature of the two-phase flow, there was expanded either only the Reynolds number or the entire right side of the equation (65).

Dougall-Rohsenow and, simultaneously, Miropolskij introduced the Reynolds number modified for the two-phase flow.

$$Re_{ZP} = Re \cdot \frac{x}{\psi} \quad (66)$$

wherein the steam volume share ψ was defined as follows:

$$\psi = x / [x + s \cdot (1-x) \cdot \rho_d / \rho_f] \quad (67)$$

If the same velocity is postulated for water and steam, one obtains for the Re_{ZP} :

$$Re_{ZP} = \frac{G \cdot D}{\eta_d} [x + (1-x) \cdot \rho_d / \rho_f] \quad (68)$$

Dougall and Rohsenow /47/ inserted then this Reynolds number into the Dittus-Boelter equation-(8) for forced convection and obtained:

$$Nu_d = 0.023 \cdot Re_{ZP}^{0.8} \cdot Pr_d^{0.4} \quad (69)$$

wherein all the values of the steam were calculated with the saturation temperature. The influence of the certainly higher temperature in the boundary layer upon the magnitude of the Prandtl number was later on considered through the expansion of the right side of this equation with the correction term $(T_f/T_w)^{0.5}$, so that the modified Dougall-Rohsenow equation reads:

$$Nu_d = 0.023 \cdot Re_{ZP}^{0.8} \cdot Pr_d^{0.4} \cdot (T_f/T_w)^{0.5} \quad (70)$$

The wall and water temperature has to be inserted in this equation in degree Kelvin.

Miropolskij /48/ expanded besides the Reynolds number the right side of the equation (65) with the so-called two-phase multiplier Y

$$Y = 1 - 0.1 [(\rho_f/\rho_d) - 1]^{0.4} \cdot (1 - \psi)^{0.4} \quad (71)$$

so that his equation assumes the following form:

$$Nu = 0.023 \cdot Re_{ZP}^{0.8} \cdot Pr_d^{0.4} \cdot Y \quad (72)$$

The values for the Nusselt and the Reynolds numbers were relative to the saturation temperature, and that of the Prandtl number to the wall temperature.

Groeneveld /49/ presented in this treatise the general form of his equation for the calculation of the heat transfer coefficients (WUK) in the region of the steam-droplets cooling:

$$Nu = K \cdot Re_{ZP}^a \cdot Pr_d^b \cdot Y^c \cdot q^e \quad (73)$$

The correlation constant and the exponents were determined with the aid of various experimental data and they are contained in Table 5.

The values of the Nusselt and Reynolds numbers and of the two-phase multiplier are calculated with the saturation temperature, that of the Prandtl number with the wall temperature.

Table 5: Values of the correlation coefficients for the Groeneveld correlation

Geometry	a	b	c	d	e	No. of points	R.m.s. error(%)	Equation no.
Tubes	1.85×10^{-4}	1.00	1.57	-1.12	0.131	438	10.1	18
	1.09×10^{-3}	0.989	1.41	-1.15	0	438	11.5	19
Annuli	1.30×10^{-2}	0.664	1.68	-1.12	0.133	266	6.1	20
	5.20×10^{-2}	0.688	1.26	-1.06	0	266	6.9	21
Tubes and annuli	7.75×10^{-4}	0.902	1.47	-1.54	0.112	704	11.6	22
	3.27×10^{-3}	0.901	1.32	-1.50	0	704	12.4	23

A summary of the empirical correlations for the calculation of the heat transfer coefficients after the exceeding of the maximum critical heat flux was established by Groeneveld /50/ and it contains 24 different equations.

Conde and Bengston /51/ used the regression analysis for the evaluation of the experimental data contained in the NRC data bank and they determined the following equation for the calculation of the heat transfer coefficients (WUK):

$$\alpha = 0.05345 \cdot \{(\lambda_d^a \cdot Pr_d^b \cdot Re^c) / [D^d \cdot (x+1)^e]\} \quad (74)$$

$$\text{with } Re = \frac{D \cdot G}{\eta_d} \quad \text{und} \quad a = 0.4593; \quad b = 2.2598;$$

$$c = [0.6249 + 0.2043 \cdot \ln(x+1)]; \quad d = 0.8059 \quad \text{and} \quad e = 2.0514.$$

$$\begin{aligned} \text{Region of validity} \quad & 0.42 \leq P \leq 22.15 \text{ MPa} \\ & 40.1 \leq b \leq 3939 \text{ kg/m}^2 \cdot \text{s} \\ & x < 1 \end{aligned}$$

The values of the heat transfer coefficients for typical parameter combinations, calculated with the equations (69), (70), (72), (73), and (74), are shown in Attachment 6 and compared with each other.

9.2.2 Non-equilibrium models

The fact, that the steam and water phase in the region of the steam-droplets cooling can be in thermodynamic non-equilibrium, was determined already in

1961 during the experimental investigation by Parker and Grosh /52/. The presence of water droplets was observed during this investigation although the equilibrium steam contents lay far above the value of $x = 1$. One of the first so-called "Two-step" heat transfer models for the steam-droplets cooling was developed by Laverty and Rohsenow /53/. The first step in this model - the heat transfer from the wall to steam - serves mainly for the superheating of the steam, which is then cooled in the second step through the evaporation of the droplets. This viewpoint of the heat transfer between wall and the steam-droplets cooling was used as the basis for most of the subsequently developed models.

Forslund and Rohsenow /54/ expanded the "two-step" heat transfer model and attempted to determine quantitatively the heat transfer between wall and the droplets near the wall. The heat transfer coefficient between wall and droplets was determined with the aid of the Baumeister correlation /55/

$$\alpha_{w,T} = K_1 \cdot [(\lambda_f^3 \cdot \rho_d \cdot \rho_f \cdot g \cdot \Delta h_e^*) / B]^{0.25} \quad (75)$$

$$\text{with } B = \eta_d \cdot (T_w - T_{sat}) \cdot [(\pi \cdot \delta_T^3) / 6]^{1/3}$$

$$\text{and } \Delta h_e^* = \Delta h_e \cdot [1 + 0.35 \cdot C_{p_d} \cdot (T_w - T_{sat}) / \Delta h_e]^{-3} \quad (76)$$

The number of droplets in the proximity of the wall was calculated with the following equation:

$$N_{T,w} = K_2 \cdot N_T^{2/3} \quad (77)$$

wherein N_T is the droplets density per volume unit and was calculated as follows:

$$N_T = G \cdot [1 - x_a] / [(\rho_f \cdot w_f \cdot \pi \cdot \delta_T^3) / 6] \quad (78)$$

The local droplets diameter δ_T , still unknown in the equations (75) and (78), was calculated with the aid of the energy balance for one droplet and the initial droplets diameter, determined from some measurements.

The equation for the calculation of the heat flux density between all and droplet reads:

$$q_{w,T} = \alpha_{w,T} \cdot (\pi \cdot 8 \frac{2}{4}) \cdot N_{T,w} \cdot (T_w - T_{sat}) \quad (79)$$

Hynek, Rohsenow and Bergles /56/ determined the values of the correlation constant for various liquids

Nitrogen	$K_1 \cdot K_2 = 0.2$
Water	$K_1 \cdot K_2 \geq 1.$
Methane	$K_1 \cdot K_2 = 2.$
Propane	$K_1 \cdot K_2 = 1. \div 2.$

In lieu of the non-equilibrium models in this treatise were examined the correlation systems of Groeneveld-Delorme and Chen-Ozkaynak-Sundaram.

a) Groeneveld-Delorme model /57/

The Groeneveld-Delorme method is based on the following important assumptions:

- The wall temperature is higher than the Leyden frost temperature
- The heat removal from the wall through the flow can be disregarded
- The velocity difference between steam and water phase can be disregarded
- The entire heat removal from the wall can be calculated with the aid of a correlation for the calculation of the heat transfer coefficient (WUK) with forced convection of steam with the application of the steam velocity.

For the calculation of the heat transfer density between wall and steam there was used the Hadaller correlation /58/:

$$q_T / (T_w - T_d) = \alpha_d = \frac{\lambda_d}{D} \cdot 0.008348 \cdot Re_d^{0.8774} \cdot Pr_d^{0.6112} \quad (80)$$

The actual steam content x_a was determined from the energy balance:

$$x_a = x_e \cdot \Delta h_e / (h_d - h_f) \quad (81)$$

For the determination of the steam temperature and, thus, also of the "actual" steam enthalpy there was established an empirical equation:

$$(h_{da} - h_d) / \Delta h_e = \exp [-\tan \phi] \quad (82)$$

with the rather complicated function:

$$\phi = a \cdot Pr^b \cdot Re_{hom}^c \cdot [q \cdot D \cdot Cp_d / \lambda_d \cdot \Delta h_e]^d \cdot \sum_{i=0}^{i=2} f_i(x_e)^i \quad (83)$$

$$\text{with } Re_{hom} = G \cdot D \cdot x_e / \eta_d \cdot \psi_{hom}$$

$$\text{and } \psi_{hom} = x_e / [x_e + (\rho_d / \rho_f) (1 - x_e)]$$

The values of the correlation constant and of the exponents were given as follows:

$$a = 0.13864; \quad b = 0.2031; \quad c = 0.20006; \quad d = 0.09232;$$

$$f_0 = 1.3072; \quad f_1 = 1.0833; \quad f_2 = 0.8455$$

Region of validity	$0.71 \leq P \leq 21.47 \text{ MPa}$
	$130 \leq G \leq 5100 \text{ kg/m}^2 \cdot \text{s}$
	$-0.12 \leq x_e \leq 1.6$
	$0.005 \leq D \leq 0.02 \text{ m}$

b) Chen-Ozkaynak-Sundaram model /59/

Chen et al developed for this model a new equation, based on the Reynolds analogy, for the calculation of the convective heat transfer between wall and steam:

Starting with the statement for the Stanton number:

$$St = f/2 \quad (84)$$

the following equation was developed for the steam convection in the steam-droplets cooling region:

$$St = \alpha_{w,d} / (\rho \cdot w \cdot Cp)_d \quad (85)$$

After the introduction of $G_d = G \cdot x_a$ and the expansion of the statement also for $Pr \neq 1$ (Colburn modification of the Reynolds analogy) the equation for the convective share of the heat flux reads:

$$Q_{w,d} = G_d \cdot c_{p_d} \cdot Pr_d^{-2/3} (T_w - T_d) \cdot f/2 \quad (86)$$

For the calculation of f there was used the approximate correlation of Beattie /60/:

$$f = 0.037 \cdot Re^{-0.17} \quad (87)$$

with the following definition of the Reynolds number:

$$Re = (D \cdot \rho_d \cdot \langle j \rangle) / \eta_d; \langle j \rangle = (G_d / \rho_d) + (G_f / \rho_f)$$

For the calculation of the relation x_a/x_e there was developed a correlation with the use of several experimental results:

$$x_a/x_e = 1 - B(P) \cdot T_D \quad (88)$$

$$\text{with } B(P) = 0.26 / [1.15 - (P/P_c)^{0.65}] \quad (89)$$

$$\text{and } T_D = (T_d - T_{sat}) / (T_w - T_d) \quad (90)$$

The heat transfer through radiation was also disregarded in this model.

Region of validity

$$P \leq 19.5 \text{ MPa}$$

$$16.6 \leq G \leq 3011 \text{ kg/m}^2 \cdot \text{s}$$

$$0.5 \leq x_e \leq 1.728$$

9.3 Comparison of each of the correlations based on the recalculation of selected 25-rod bundle tests

For the investigation of the equilibrium and non-equilibrium correlations the tests DNB1, DNB3 and DNB9 were selected from the "DNB test series" and the test PDNB11 was selected from the "Post DNB test series."

9.3.1 Recalculation of the test DNB1

The curves of the important test parameters, of the local values of the mass flow calculated with the computer code BRUDI-VA, and of the steam contents, and a complete set of the calculated results in comparison with the test are compiled in Attachment 7.

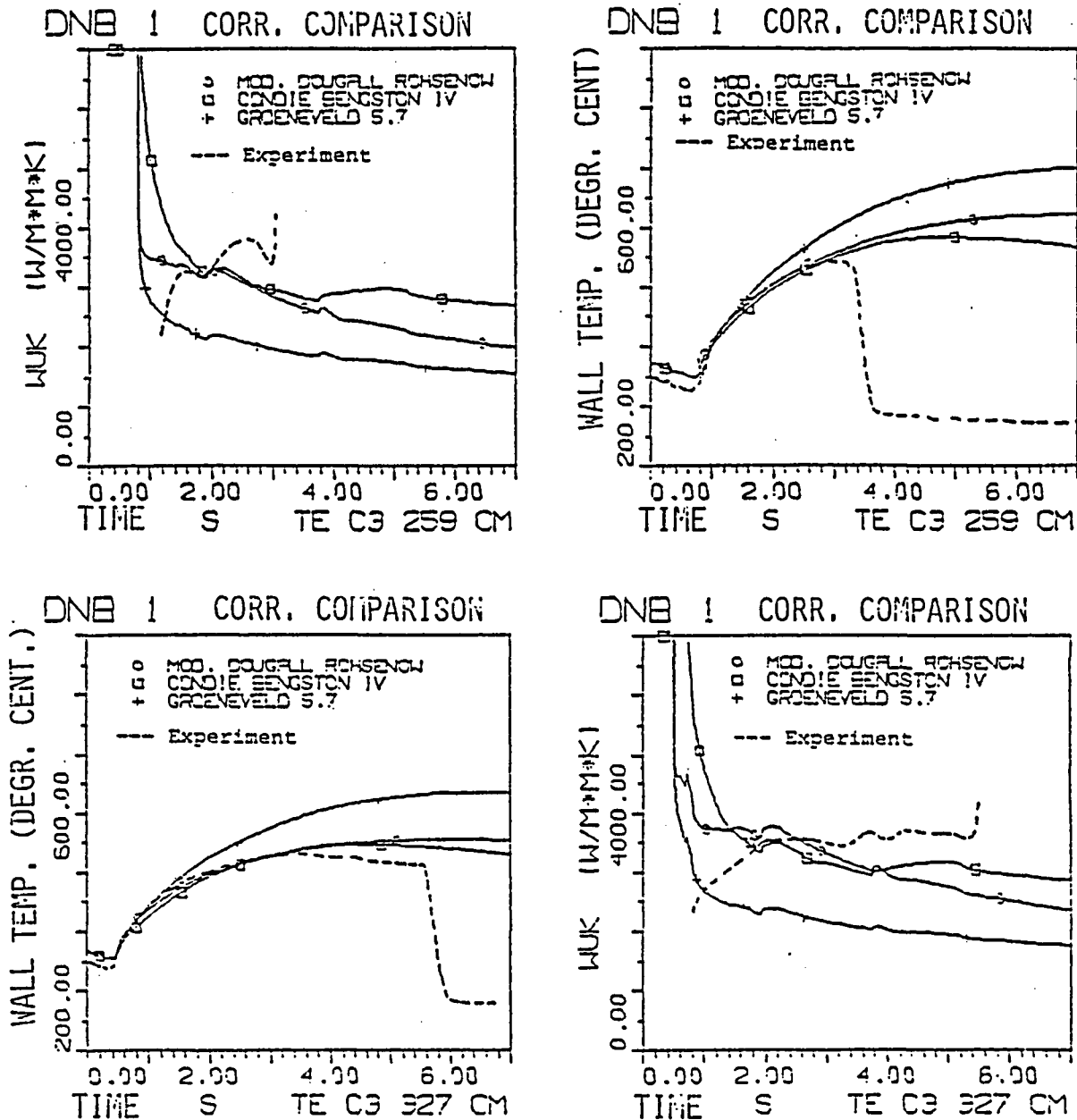


Fig. 25: Comparison of the equilibrium correlations - Test DNB1

The values of the wall temperatures and of the heat transfer coefficients, as they were calculated with the equilibrium correlations at two different axial positions in the bundle, are compared in Fig. 25 to each other and with the values determined from the test.

The comparison of the values of the wall temperature, calculated with the non-equilibrium correlations, of the heat flux, of the steam temperature, and of the actual steam content is shown in Fig. 26.

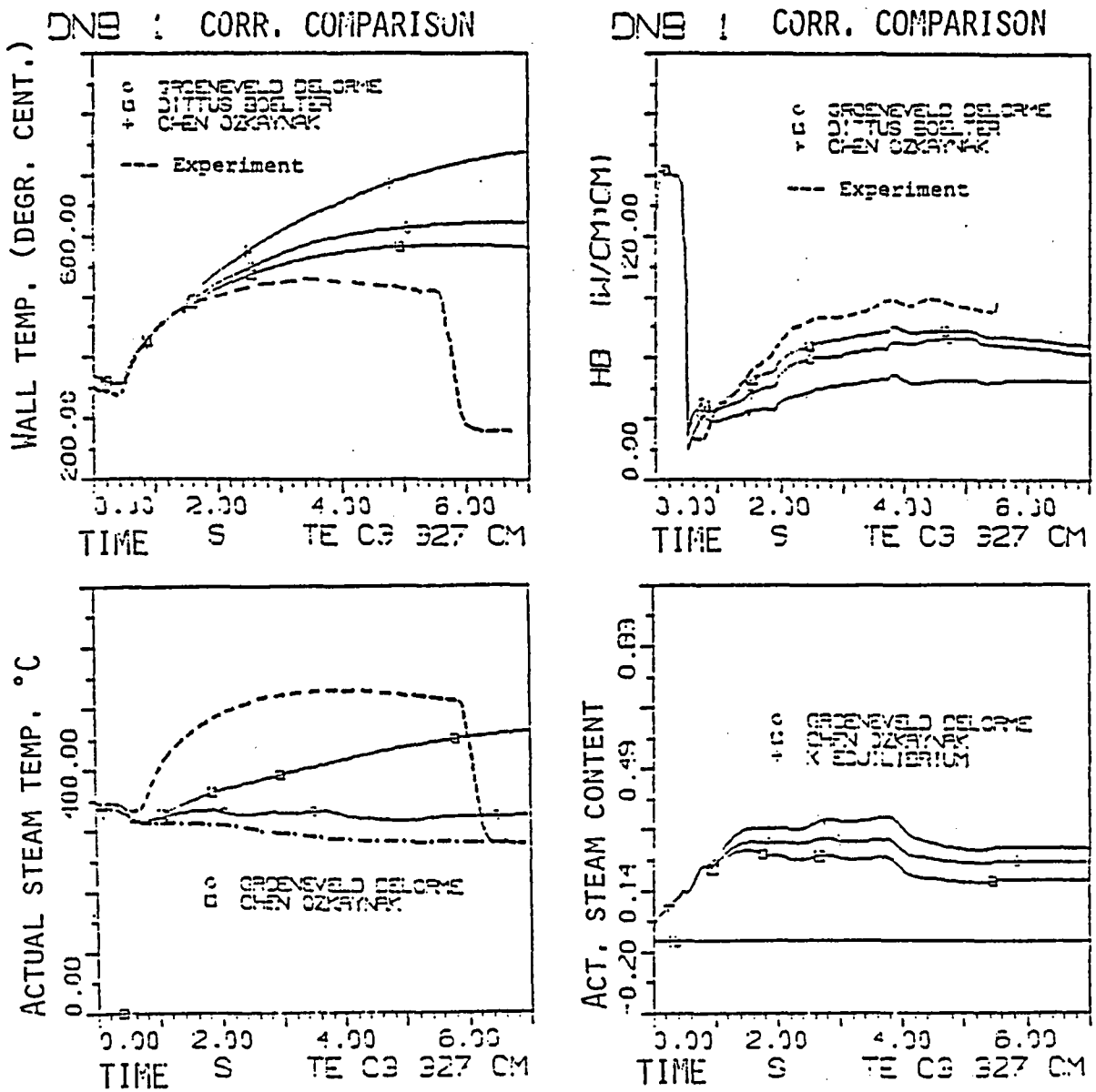


Fig. 26: Comparison of the non-equilibrium correlations - Test DNB1

9.3.2 Recalculation of Test DNB3

The curves of the important test parameters, of the local values of the mass flow, calculated with the computer code BRUDI-VA, and of the steam content, and a complete set of the calculated results in comparison with the test are compiled in Attachment 8.

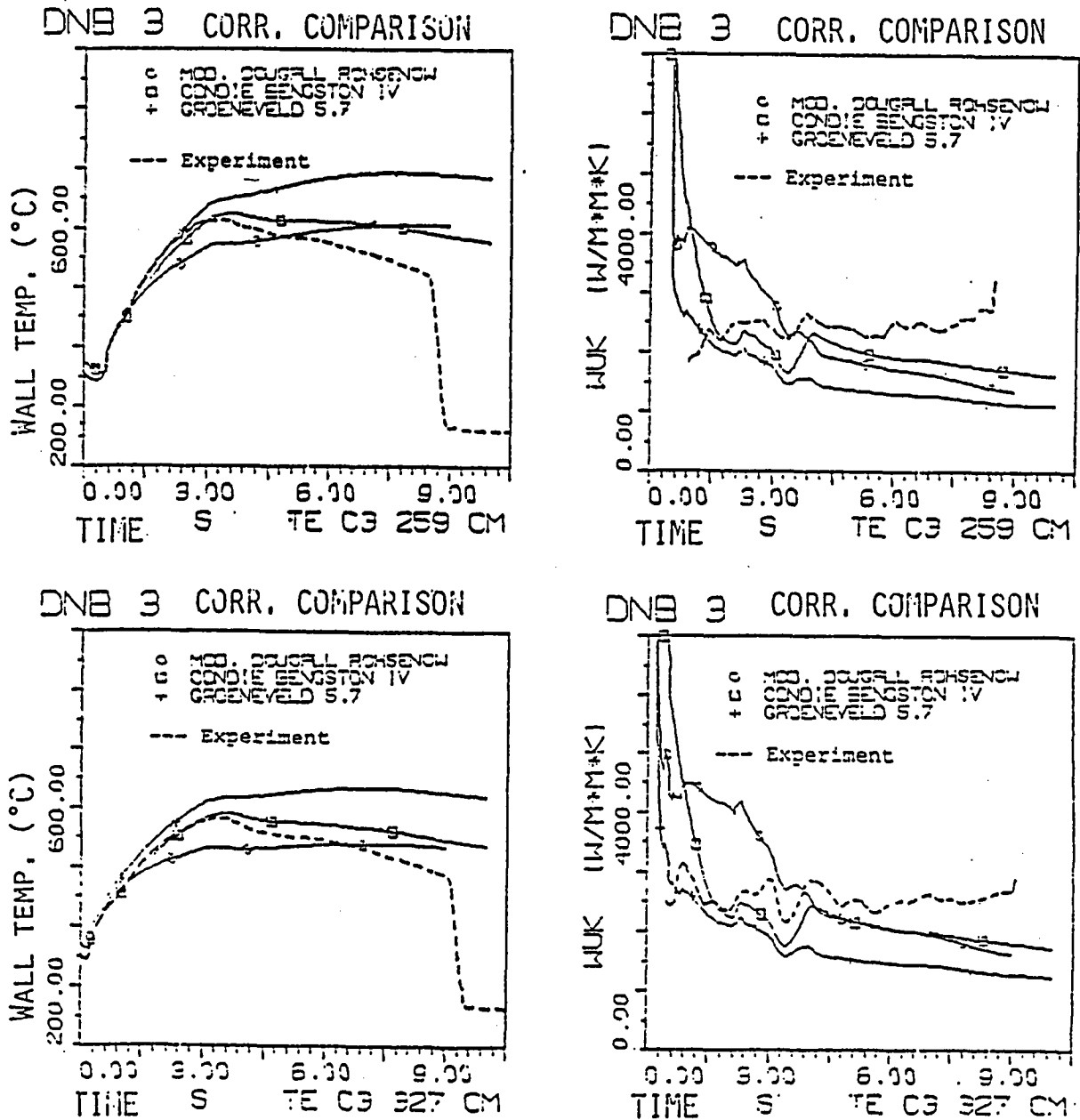


Fig. 27: Comparison of the equilibrium correlations - Test DNB3

The values of the wall temperatures and of the heat transfer coefficients, as they were calculated with the equilibrium correlations at two different axial positions in the bundle, are compared in Fig. 27 to each other and with the values determined from the test.

The comparison of the values of the wall temperature, calculated with the non-equilibrium correlations, of the heat flux, of the steam temperature, and of the actual steam content is shown in Fig. 28.

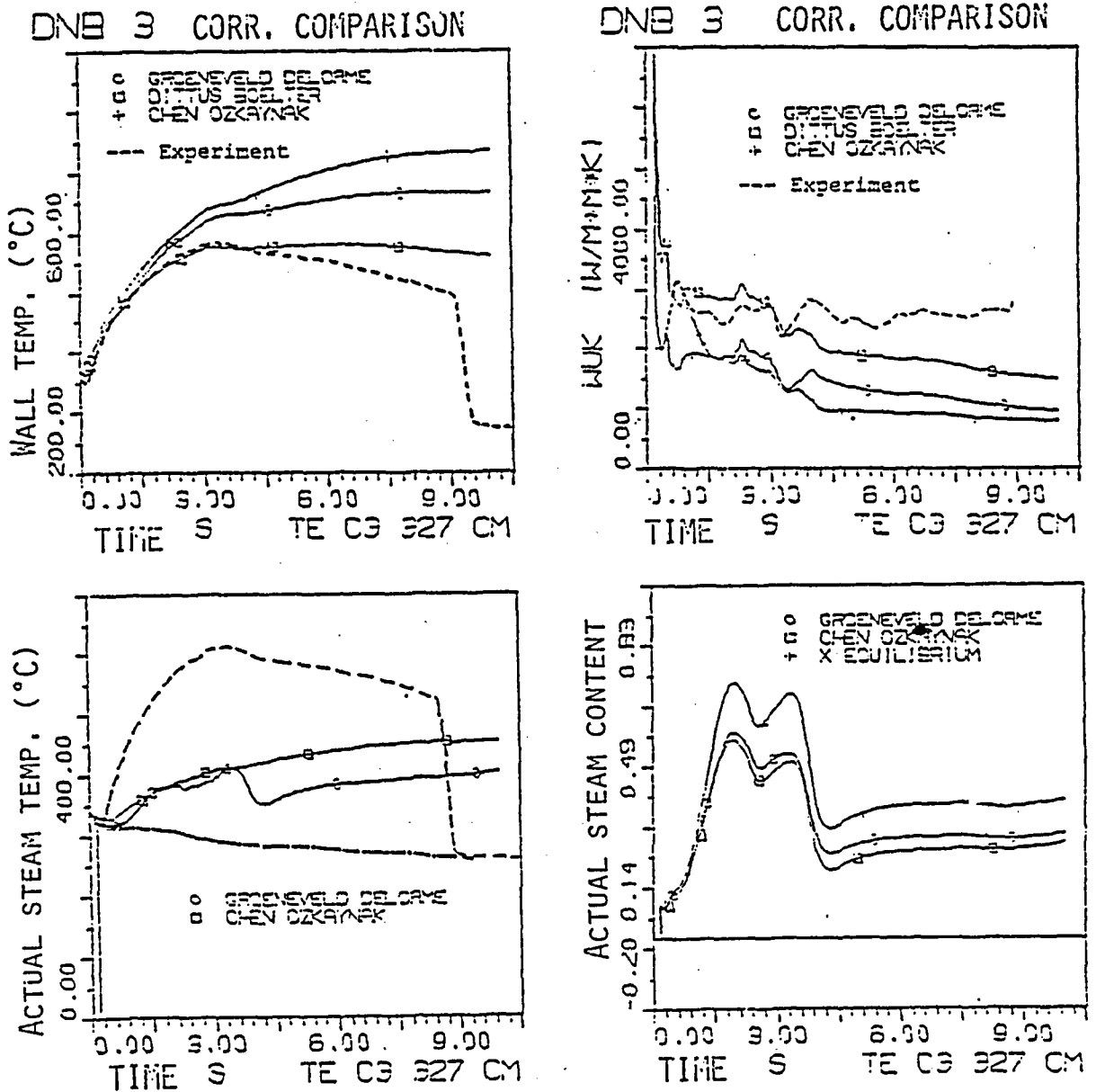


Fig. 28: Comparison of the non-equilibrium correlations - Test DNB3

9.3.3 Recalculation of the Test DNB9

The curves of the important test parameters, of the local values of the mass flow, calculated with the computer code BRUDI-VA, and of the steam content, and a complete set of the calculated results in comparison with the test are compiled in Attachment 9.

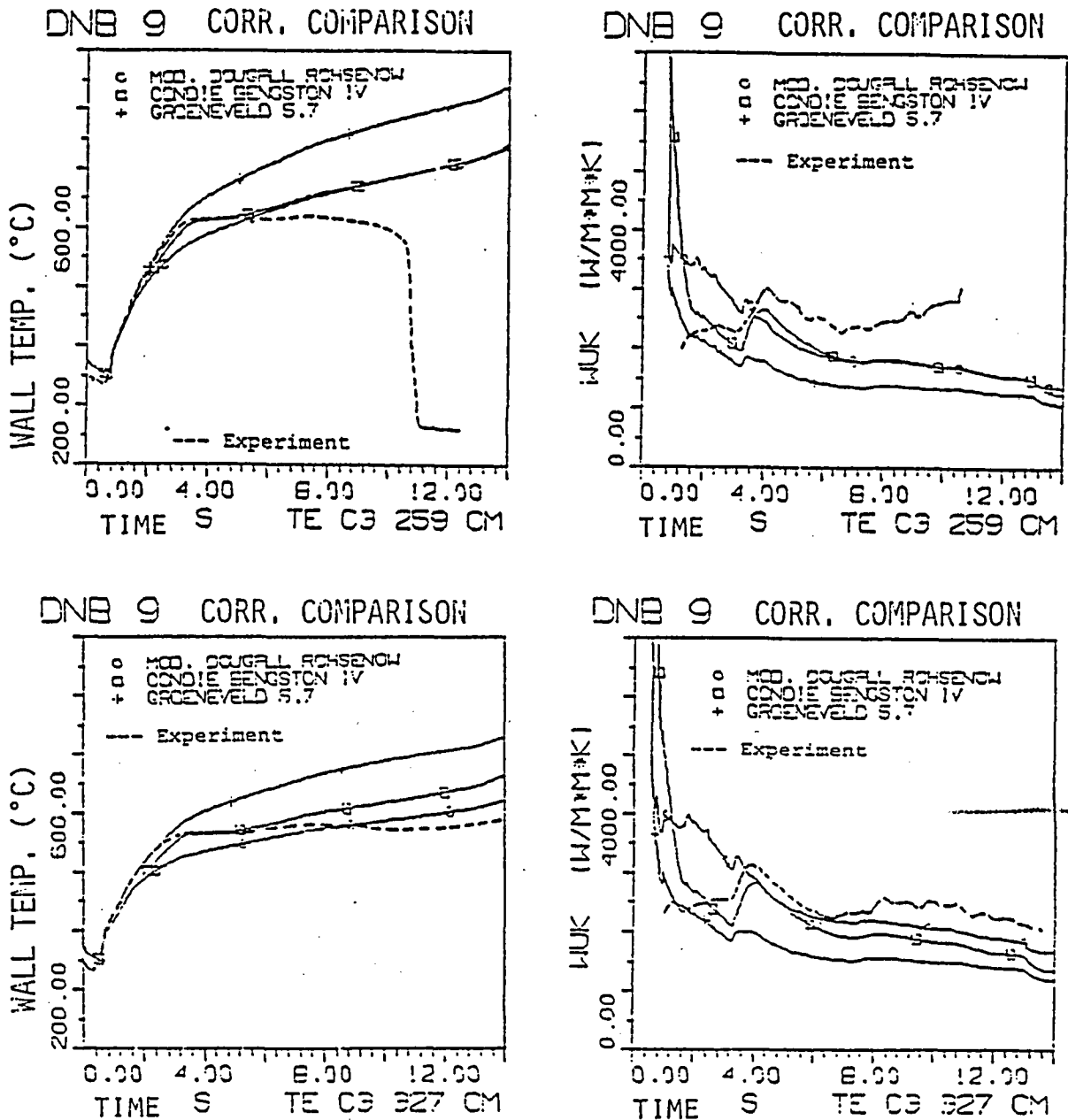


Fig. 29: Comparison of the equilibrium correlations - Test DNB9

The values of the wall temperatures and of the heat transfer coefficients, as they were calculated with the equilibrium correlations at two different axial positions in the bundle, are compared in Fig. 29 to each other and with the values determined from the test.

The comparison of the values of the wall temperature, calculated with the non-equilibrium correlations, of the heat flux, of the steam temperature, and of the actual steam content is shown in Fig. 30.

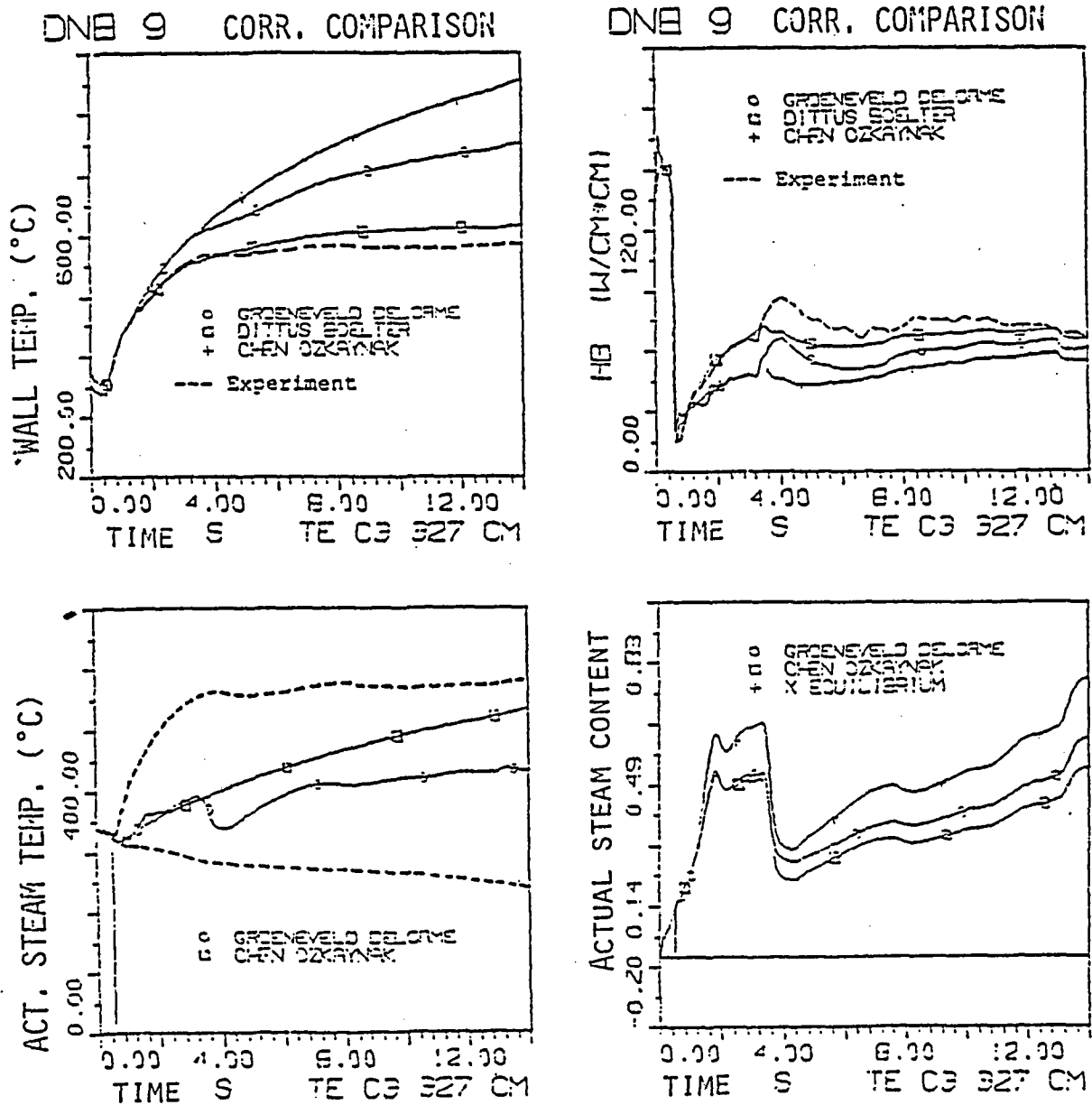
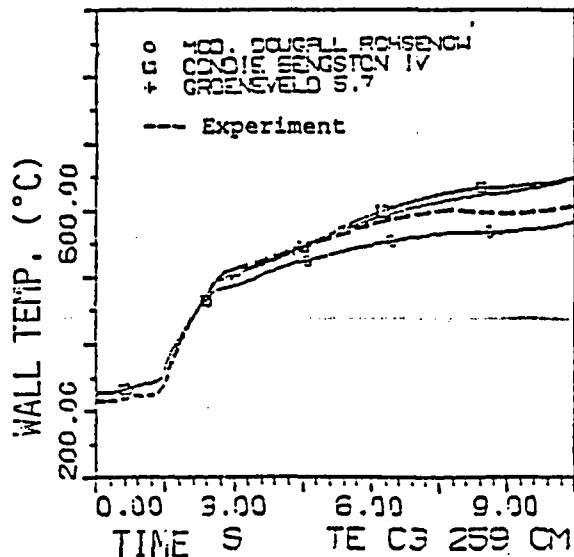


Fig. 30: Comparison of the non-equilibrium correlations - Test DNB9

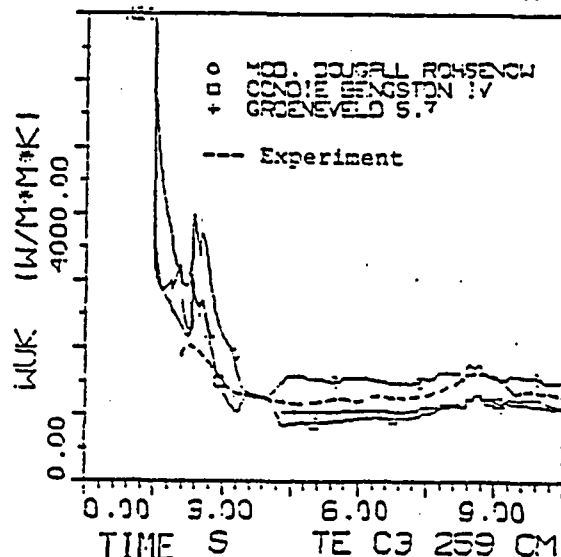
9.3.4 Recalculation of the Test PDNB11

The curves of the important test parameters, of the local values of the mass flow, calculated with the computer code BRUDI-VA, and of the steam content, and a complete set of of the calculated results in comparison with the test are compiled in Attachment 10.

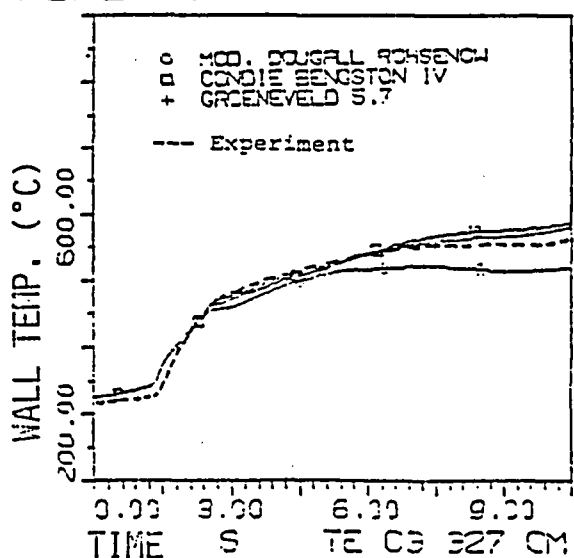
PDNB 1! CORR. COMPARISON



PDNB 1! CORR. COMPARISON



PDNB 1! CORR. COMPARISON



PDNB 1! CORR. COMPARISON

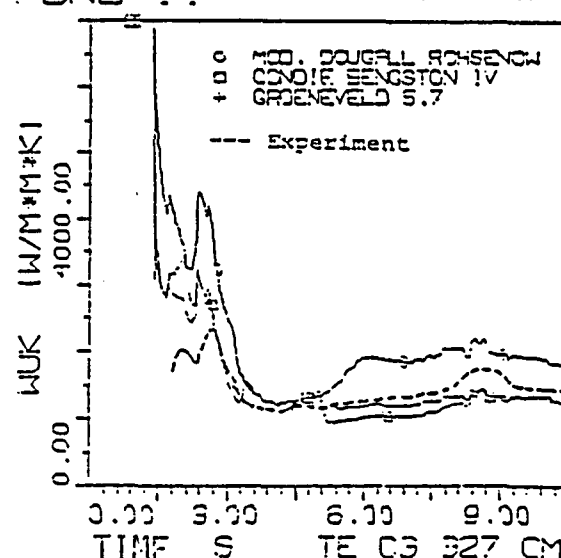


Fig. 31: Comparison of the equilibrium correlations - Test PDNB11

The values of the wall temperatures and of the heat transfer coefficients, as they were calculated with the equilibrium correlations at two different axial positions in the bundle, are compared in Fig. 31 to each other and with the values determined from the test.

9.4 Evaluation of the correlations for the calculation of the heat transfer coefficients in the steam-droplets cooling region

The recalculation of the selected tests with the utilization of the various correlations for the calculation of the heat transfer coefficients in the region after the exceeding of the critical heat flux showed, that none of the selected correlations can be recommended for the entire scope of the test parameters. In the recalculation of the tests with intermediate to high steam content ($0.5 < \chi < 0.9$) and with intermediate mass flow density (1300 to 1800 kg/m²·s) there could be obtained a good agreement between calculated and test results if the modified correlation of Dougall-Rohsenow was used for the calculation of the heat transfer coefficients. In the recalculation of the tests with a lower mass flow density ($G < 1000$ kg/m²·s) the curves of the measured wall temperatures were better reproduced with aid of the Condie-Bengston equation and partially also with that of Groeneveld. The application of the newer non-equilibrium correlations showed to be rather complicated and did not lead to a better agreement between the calculated and the test results.

10. TRANSFER FROM STEAM-DROPLETS COOLING OR FILM BOILING TO NUCLEATE BOILING (RNB-REWETTING)

10.1 Compilation of the experimental data from the 25-rod bundle investigation

As already mentioned in Chapter 4.2, the following parameters were compiled for the specific RNB moment in the RNB data set.

- RNB moment
- Wall temperature
- Saturation temperature
- Pressure
- Electric power
- Heat flux immediately prior to RNB
- Heat transfer coefficient

In the recalculation of the test there were determined the pertinent values of the mass flow and of the steam content and they were inserted into the data set. The Figures 32 to 35 show the dependence of the temperature difference of pressure, heat flux, mass flow, and steam content.

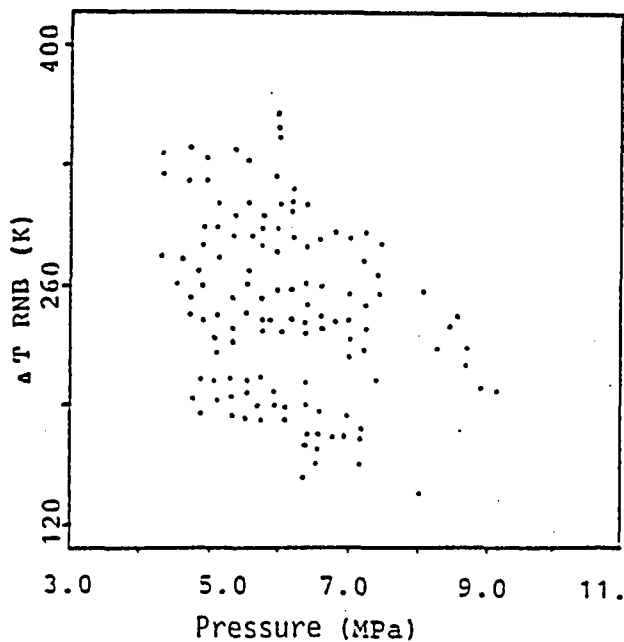


Fig. 32: measuring points

$$T_w - T_{sat} = f(P)$$

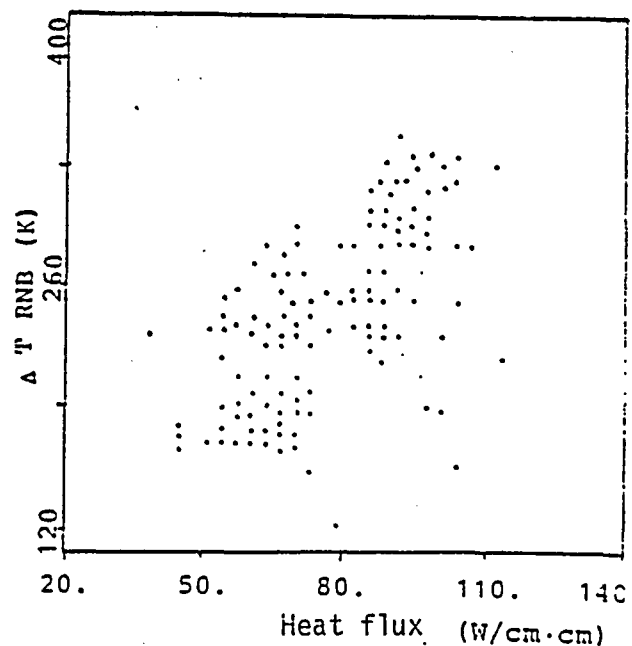


Fig. 33: measuring points

$$T_w - T_{sat} = f(q)$$

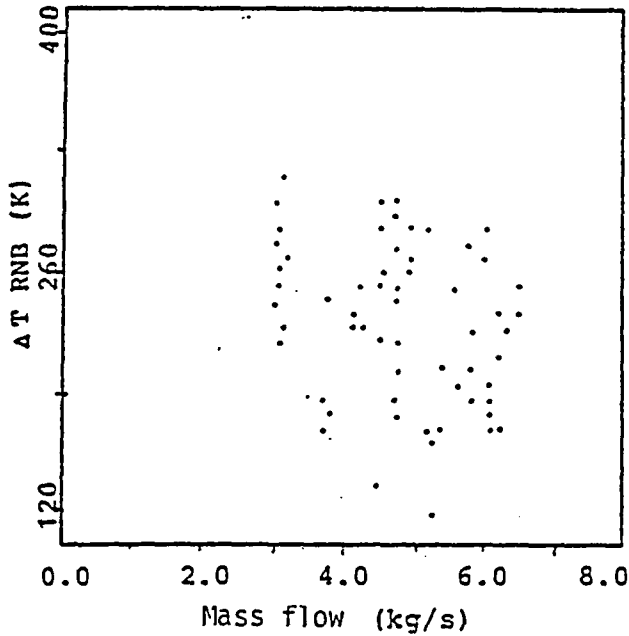


Fig. 34: Correlation of G to $T_w - T_{sat}$

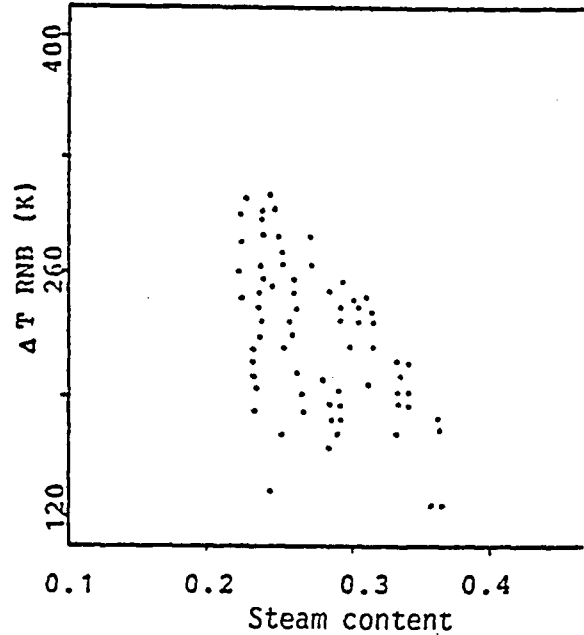


Fig. 35: Correlation of X to $T_w - T_{sat}$

10.2 Correlations for the calculation of the minimum critical heat flux and of the minimum temperature difference with rewetting

The transfer from steam-droplets cooling or film boiling back to the nucleate boiling in the high pressure phase of a LOCA was thoroughly investigated only after both nuclear LOFT tests (L2-2 and L2-3) had been conducted. For the calculation of the minimum critical heat flux or of the minimum temperature difference with rewetting, in these investigations were mostly used the correlations of Berenson, Henry and Iloeje.

Berenson /61/ used his correlation for the determination of the heat transfer coefficient in the proximity of the minimum of the Nukiyama boiling curve (Fig. 14).

$$\alpha_{mn} = \alpha_K = \left\{ \left[\lambda_D^3 \cdot g \cdot \rho_D \cdot (\rho_f - \rho_D) \cdot \Delta h_e^* \right] / \left[\eta_D (T_w - T_{sat}) \cdot a \right] \right\}^{1/4} \quad (91)$$

$$\text{with } a = \left\{ \sigma / \left[g(\rho_f - \rho_D) \right] \right\}^{1/2}$$

The Zuber correlation for the calculation of the maximum critical heat flux was modified by Berenson and adapted to the conditions with rewetting.

$$q_{\min} = 0.09 \cdot \rho_d \cdot \Delta h_e \cdot [g \cdot \sigma \cdot (\rho_f - \rho_d) / (\rho_f - \rho_d)^2]^{1/4} \quad (92)$$

The equation for the calculation of the minimum temperature difference with rewetting was obtained by dividing the equations (87) and (86):

$$\Delta T_{\min, B} = 0.127 \cdot (\rho_d \cdot \Delta h_e) / \lambda_d \cdot [g(\rho_f - \rho_d) / (\rho_f - \rho_d)]^{2/3} \cdot [\sigma / (g \cdot (\rho_f - \rho_d))]^{1/2} \cdot [\eta_d / (\rho_f - \rho_d)]^{1/3} \quad (93)$$

The minimum temperature difference resulting from this equation was used as the basis for the development of further empirical correlations.

Henry /82/ investigated, among others, the influence of the relative values upon the magnitude of the minimum temperature difference and he established the following equation:

$$[(T_{\min, H} - T_{\min, B}) / (T_{\min, B} - T_f)] = 0.42 \cdot [A]^{0.6} \quad (94)$$

$$\text{wherein } A = [\sqrt{\lambda_f \cdot \rho_f \cdot C_{p_f}} / \sqrt{\lambda_w \cdot \rho_w \cdot C_{p_w}}] \cdot [\Delta h_e / \Delta T_{\min, B}]$$

$$\text{and } T_{\min, B} = \Delta T_{\min, B} + T_{\text{sat}}$$

Iloje et al /63/ developed an empirical correlation, in which the influence of mass flow and steam content is taken into consideration and he determined the correlation coefficients based on own tests.

$$\Delta T_{\min, l} = 0.29 \cdot \Delta T_{\min, B} (1 - 0.295 \cdot x^{2.45}) [1 + (G \cdot 10^{-4})^{0.49}] \quad (95)$$

The tests with an internally flowed-through tube were conducted within the following range of the test parameters:

$$68 \leq G \leq 340 \text{ kg/m}^2 \cdot \text{s}$$

$$0.3 \leq x \leq 1$$

$$P = 6.9 \text{ MPa}$$

$$D = 0.0124 \text{ - internally flowed-through}$$

10.3 Investigation of the correlations based on the results of the 25-rod bundle tests

During the recalculation of the tests DNB3 and DNB9, the values of the minimum temperature difference and of the minimum critical heat flux were calculated with the aid of the correlations (93), (84), (95), and (92).

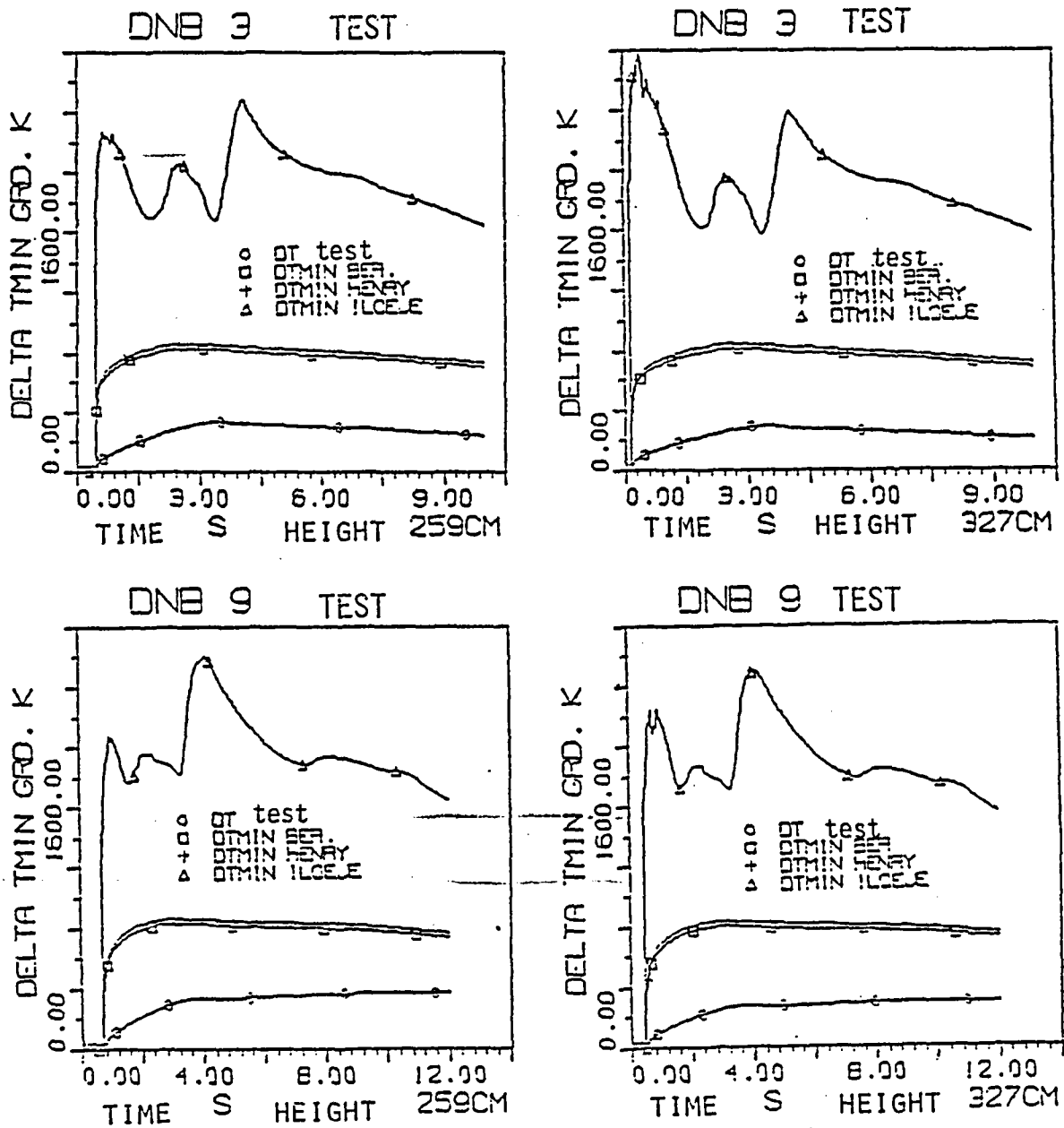


Fig. 36: Comparisons of the correlations for the calculation of ΔT_{min}

In Fig. 36 are compared the values of the ΔT_{\min} with the temperature difference between wall and saturation temperature, determined from the test. Fig. 37 shows the comparison of the local heat flux with the values of q_{\min} which were calculated with the Berenson correlation (92).

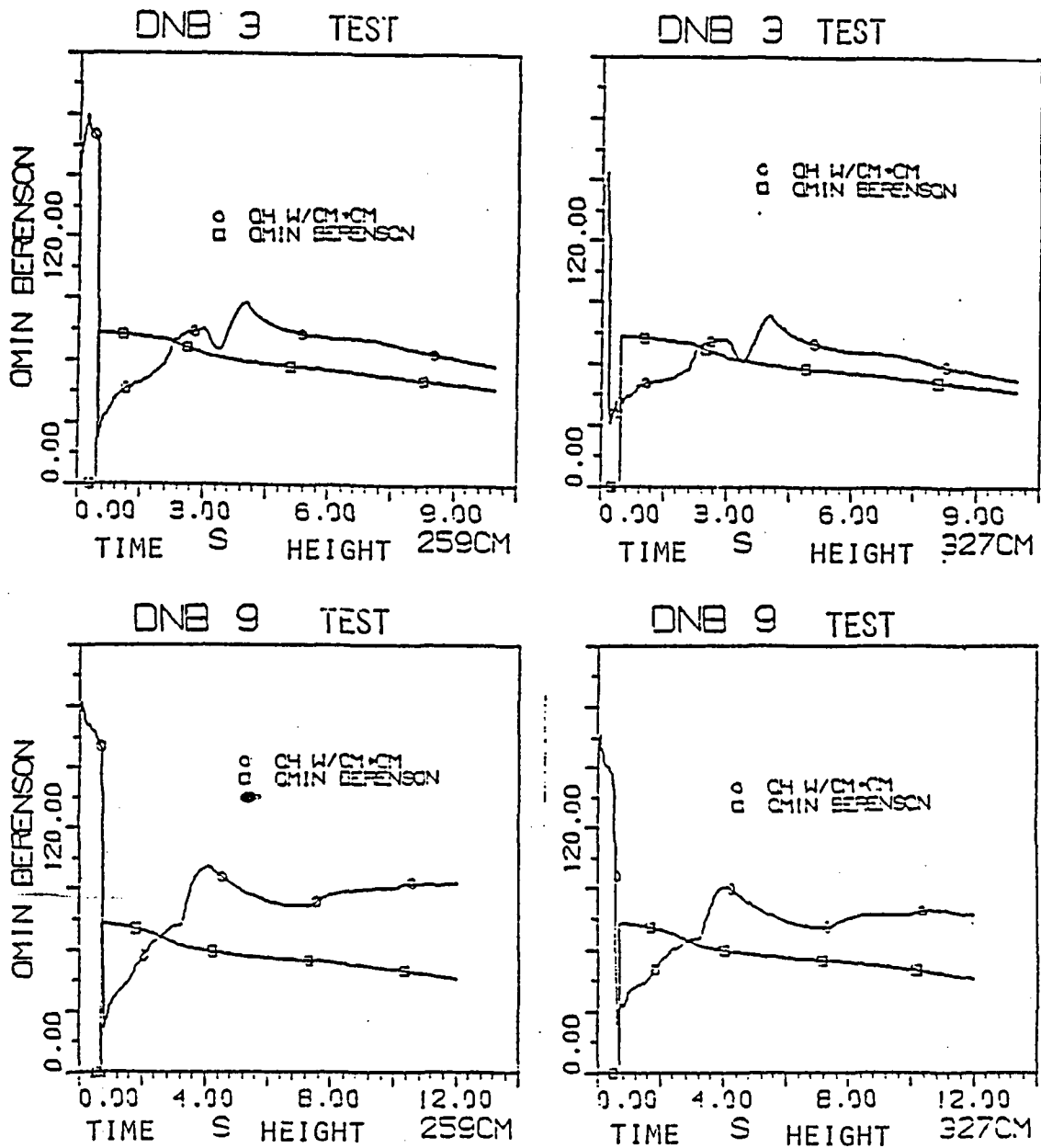


Fig. 37: Comparison of the minimum and actual heat flux

10.4 Evaluation of the correlations

From the comparison of the minimum temperature difference, calculated with the aid of correlations, with the test results it follows that all three correlations rendered too high values of ΔT_{\min} . The Berenson correlation for the calculation of the minimum critical heat flux (KHB) [CHF] is mass flow and steam content independent and, thus, inadequate for the application to the conditions in a flowed-through coolant channel.

Further, it has to be established that precisely for the parameters that are typical for the high pressure phase of a LOCA there exist only a few published test results. The experimental results, determined within the framework of the 25-rod bundle tests, are thus very valuable and they can be used for the verification of the correlations and models.

11. DEVELOPMENT OF A NEW CORRELATION FOR THE CALCULATION OF THE HEAT TRANSFER COEFFICIENTS IN THE STEAM-DROPLETS COOLING REGIME

The comparison of the calculated and test results in Chapter 9 showed, that none of the used correlations for the heat transfer coefficients in the steam-droplets cooling phase can be recommended without limitations to be applied to all of the test parameters. The individual correlations, that were developed and verified based in the majority of the cases on deadbeat investigations, covering only a certain phase of the important parameters, did show significant deviations from the test results ascertained from the 25-rod bundle tests. Also the use of later models, in which the thermodynamic non-equilibrium between the two phases was taken into consideration and which separated the heat transfer mechanism into individual steps, did not lead to an approximation of the calculated time behaviors of the wall temperature to the test results. Therefore, each of the heat transfer processes during steam-droplets cooling was thoroughly investigated.

Figure 36 shows the heat transfer mechanism in the steam-droplets cooling phase.

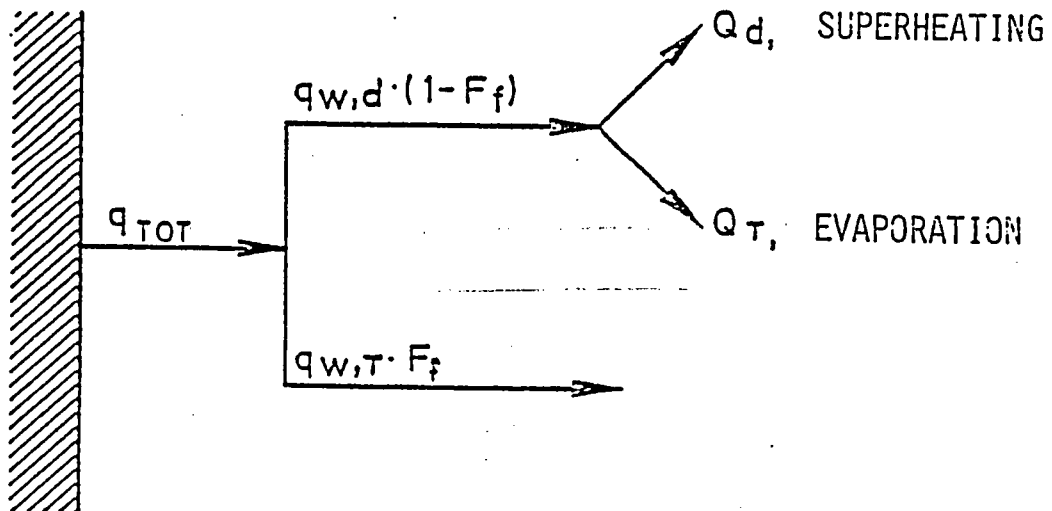


Fig. 38: Model representation for the heat transfer in the steam-droplets cooling phase

According to this consideration, the entire heat flux density is made up of two components:

$$q_{TOT} = q_{w,d}(1-F_f) + q_{w,T} \cdot F_f \quad (96)$$

wherein $q_{w,d}$ - is the amount of heat per surface unit of the heated wall, eliminated by the steam phase (convection and radiation)

and $q_{w,T}$ - is the amount of heat per surface unit of the heated wall, eliminated by the water phase (convection, conduction, radiation).

11.1 Heat transfer between wall and steam phase

For the calculation of the heat transfer coefficients between wall and the steam phase there were used not only the correlations given in Chapter 6 (equations 8 and 9) but also the Hadaller correlation (equation 80) and the Chen equation (equation 80) derived from the Reynolds-Colburn analogy.

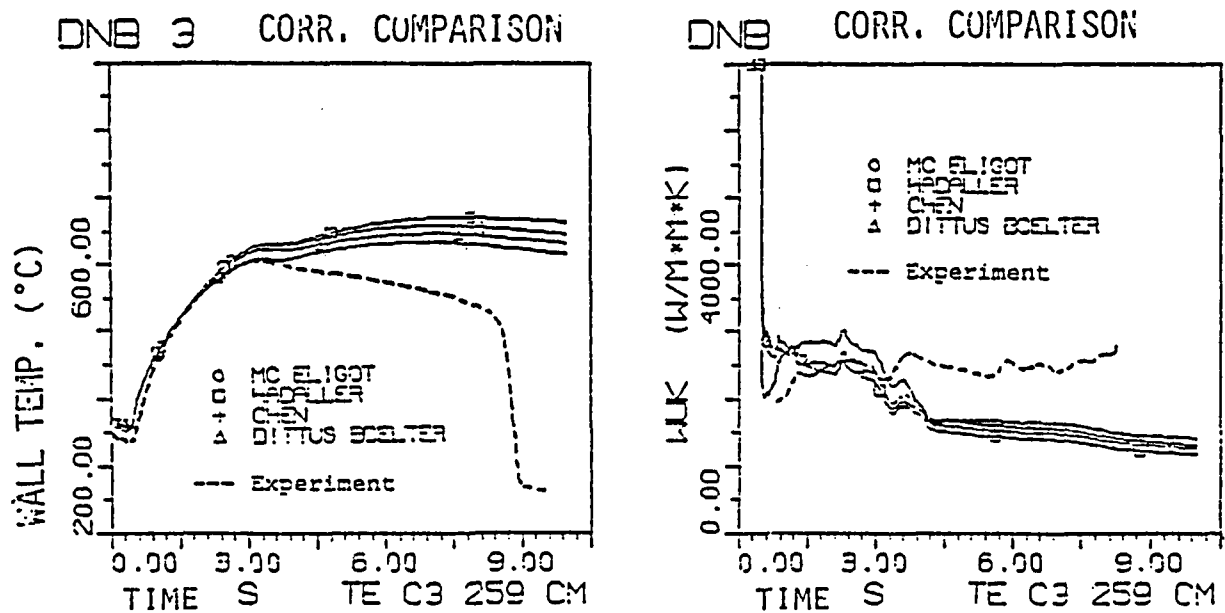


Fig. 39: Comparison of several correlations for the calculation of the heat transfer coefficients with forced steam convection.

The processes of the wall temperatures and of the heat transfer coefficients, calculated with these correlations, as they were determined in the recalculation of the DNB3 test, are shown in Figure 39 and they are compared with the experimentally established values of the entire heat flux density.

For the calculations of the Reynolds number in the correlations, there was firstly taken the homogenous steam velocity and the density of the steam. The heat flux density was calculated in this case with the entire temperature difference between the wall and the saturation temperatures. As shown by the results, the heat eliminated from the wall by the pure steam convection is too low. If it is postulated that between the droplets present in the steam flux and the wall there does not take place a direct heat transfer, and the heat is eliminated from the wall solely by the steam convection, the steam velocity has to be considerably higher as the one calculated with the homogenous statement. In other words, there has to exist a considerable slippage between steam and droplet.

Therefore, the known equations for the calculation of the slippage and the drift correlations were set up and used for the determination of the steam velocity.

1.1.1 Comparison of various slippage and drift equations

For the calculation of the slippage there were used the following correlations:

a) Ahmad correlation /64/:

$$S_A = (\rho/\rho_d)^{0.205} \cdot \left(\frac{G \cdot D}{\eta} \right)^{-0.016} \quad (97)$$

b) Groeneveld modification of the Ahmad equation /65/:

$$S_{DO} = 0.5 \cdot (S_A - 1) + 1 \quad (98)$$

c) Hein correlation /66/:

$$S_H = 1 + 4 \cdot e^{-7.5x} \quad (99)$$

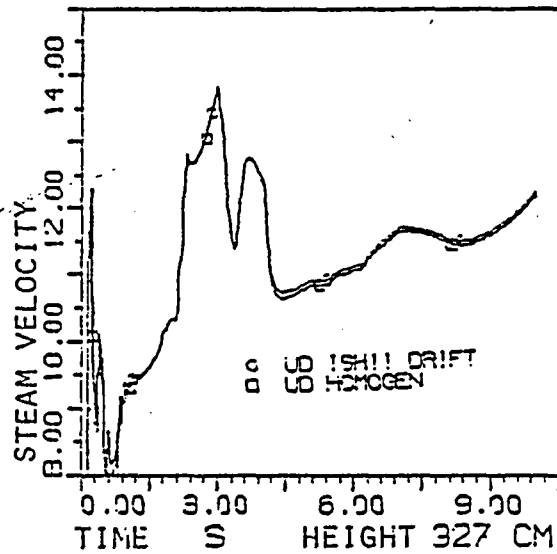


Fig. 41: Comparison of the steam velocities calculated with and without drift

In Figure 42 are shown the calculated courses of the wall temperature and of the heat transfer coefficients. For the calculation of the Reynolds number there was used in this case the steam velocity calculated with the Groeneveld correlation. As shown by the comparison of the results, the influence of the velocity calculated with slippage is not significant upon the course of the wall temperature. Therefore, there was maintained the assumption of homogeneity, as it was also recommended by many authors for this sphere of the steam-droplets cooling.

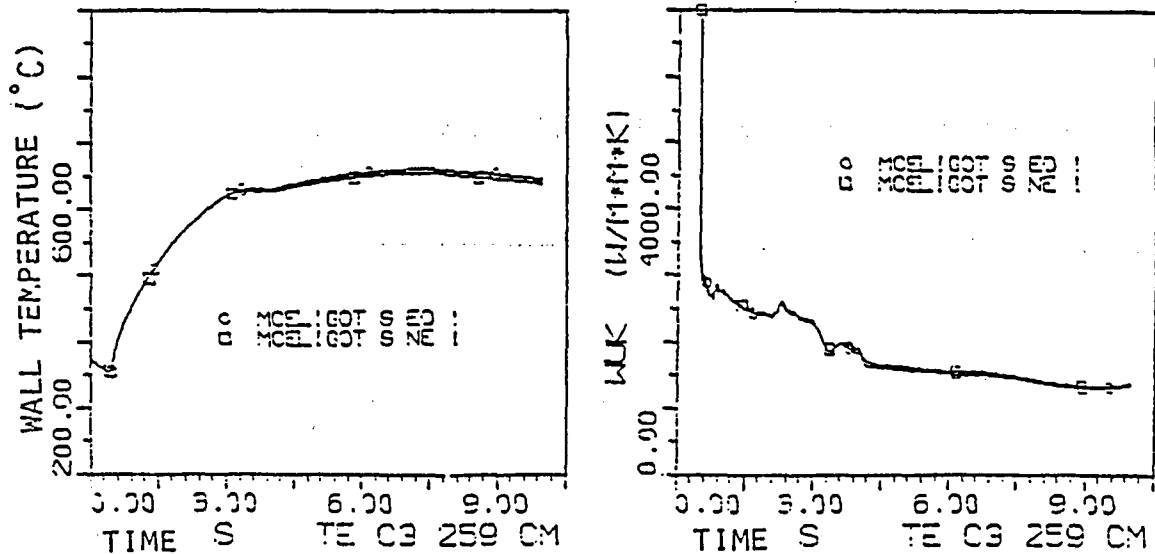


Fig. 42: Comparison of the wall temperatures and the heat transfer coefficients calculated with and without slippage

11.2 Heat transfer between wall and droplets

For the determination of the heat transfer between the heated wall and the individual droplets there was first taken the following assumption:

- The wall temperature lies above the Leyden frost temperature.
- The relative velocity between droplets and wall can be disregarded. (The evaporation time of the droplets lies in the order of 10^{-6} to 10^{-5} s /59/).
- The heat transfer by radiation between wall and droplets can be disregarded /66/.

Under these assumptions, for the calculation of the heat transfer coefficient between wall and droplets there can be used either the correlation for vessel film boiling (equations 60 and 63) or the correlation developed by Baumeister (equation 75).

11.2.1 Determination of the surface inherent to the heat transfer between wall and droplets

For the determination of the surface (area) inherent to the wall-droplets heat transfer there has to be determined the size of the droplet and the number of droplets involved in this process.

11.2.2 Determination of the droplet diameter

The mean droplet diameter was determined in most of the treatises in this sphere from their own experimental investigations /54, 66 and 68/. Since these investigations were normally conducted with low pressure, the values of the droplet diameter determined in these treatises are inadequate for the application in the high pressure region of the steam-droplets cooling. For the determination of the size of droplets in this pressure range, among others, two frequently used empirical correlations were developed:

a) Cumo correlation /69/

$$\delta_T = 123.1 \cdot (1 - P_r)^{0.31} \cdot [\eta_f / (G \cdot x_e)] \quad (102)$$

wherein $P_r = P/P_c$ and $P_c = 22.1$ MPa critical pressure

- b) Determination of the average droplet diameter from the critical Weber number

$$We_{kr} = \text{konst}, We = [\rho_D \cdot (w_d - w_f)^2 \cdot \delta_T] / \sigma$$

therefrom results for the critical droplet diameter

$$\delta_{T,kr} = We_{kr} \cdot \sigma / [\rho_D (w_d - w_f)^2] \quad (103)$$

The average droplet diameter can be then determined by means of various

$$\bar{\delta}_T = f(\delta_{T,kr}) \quad (104)$$

statements.

This method for the determination of the droplet diameter does, however, preclude the knowledge of the phase velocities and of the magnitude of the critical Weber number and is not used in this investigation due to the uncertainties for the determination of the phase velocity (Chapter 11.1). The values of the droplet diameter, calculated with $We = 1$ and slippage according to the Groeneveld equation (equation 98) are shown in Figure 43.

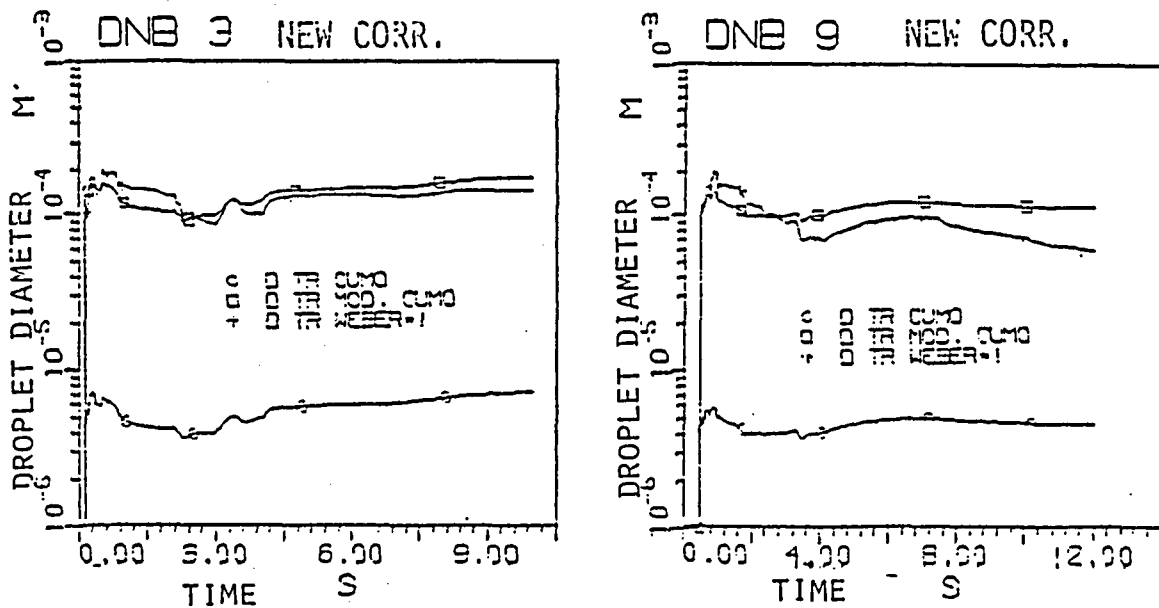


Fig. 43: Comparison of the correlations for the calculation of the droplet diameter

The values of the droplet diameter, determined with the Cumo correlation in the recalculation of the DNB3 and DNB9 tests, are shown in Fig. 43. The average value of the droplet diameter of 6 μ is, however, too low in comparison with the experimentally determined values of 100 to 200 μ . The correlation constant in the Cumo equation was therefore adapted to the experimental values, so that the modified correlation reads:

$$\bar{\delta}_T = 3.0 \cdot 10^3 \cdot (1-P_r)^{0.31} \cdot [\eta_f / (G \cdot x_e)] \quad (105)$$

This correlation will be henceforth used for the calculation of the droplet diameter in the steam-droplets cooling.

11.2.3 Determination of the number of droplets

For the determination of the number of droplets involved in the heat transfer between wall and droplets it is precluded that with the droplets in question it deals with the droplets present in the boundary layer.

The boundary layer thickness is calculated with the Prandtl equation /70/:

$$\delta_{GS} \approx 34.2 / (0.5 \cdot Re)^{0.875} \quad (106)$$

The number of droplets per volume unit of the coolant can be calculated as follows:

$$N_T = 6 \cdot (1-\psi) / [\pi \cdot \delta_T^3] \quad (107)$$

Therefrom results the number of droplets in the boundary layer per surface unit of the wall:

$$N_{T,w} = N_T \cdot \delta_{GS} \quad (108)$$

Forslund and Rohsenow /54/ determined the number of droplets per surface unit of the wall from the equation:

$$N_{T,w} = K \cdot N_T^{2/3} \quad (109)$$

This equation was used for the calculation of the droplets mass flow density.

11.3 Heat transfer between steam and droplets

For the calculation of the heat transfer coefficients between steam and droplets there are generally used the equations for the determination of the heat transfer coefficients for flow-encircled sphere.

Forslund and Rohsenow /54/ used the equation

$$Nu = 2 + f[Re, Pr] \quad (110)$$

$$\text{with } f(Re, Pr) = 0.55 \cdot [(w_D - w_f) \cdot \delta_T / \eta_D \cdot \rho_D]^{0.5} \cdot Pr_D^{1/3} \quad (111)$$

The values of the heat transfer coefficients, calculated with this equation, are shown in Figure 44. The velocity difference required for correlation (111) was determined with the aid of the Groeneveld equation (equation 98) for slippage. The pertinent values of the heat flux density, which were calculated with a temperature difference between steam and water phase of 10 K, are shown in Figure 45 and they are compared with the wall-coolant heat flux density determined from the test.

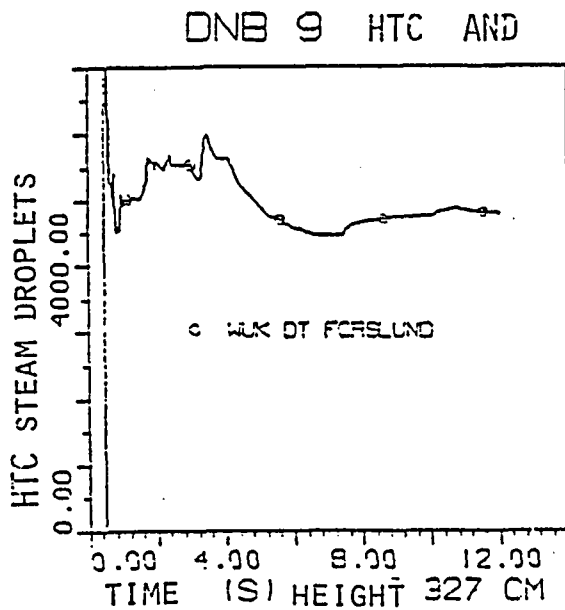


Fig. 44: HTC between steam and droplets

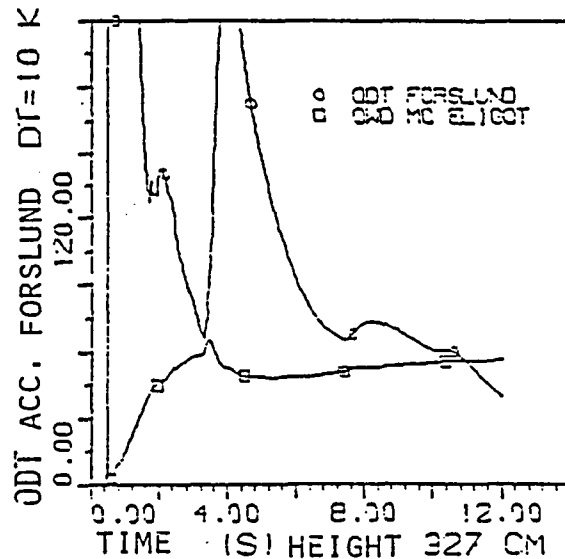


Fig. 45: Heat flux density of steam on droplets

11.4 Calculation of the individual components of the heat flux density between wall and steam-droplets flow

The entire heat flux density between wall and coolant is according to the equation (96):

$$q_{TOT} = \alpha_{w,d} \cdot (1-F_f) \cdot (T_w - T_d) + \alpha_{w,T} \cdot F_f \cdot (T_w - T_{sat}) \quad (112)$$

During the recalculation of the post-DNB tests with low mass flow rate, the correlations for the calculation of the heat transfer coefficients with forced steam convection were compared to each other and with the test results [7]. From the comparison it results, that the best agreement between the measured and the calculated processes of the wall temperature could be obtained with the aid of the McEligot correlation.

The value of the correlation constant in this equation was determined through the adaption to the test results. The modified McEligot equation reads:

$$\alpha_{w,d} = 0.022 \cdot \frac{\lambda_d}{D} \cdot Re_d^{0.8} \cdot Pr_d^{0.4} \cdot \left(\frac{T_d}{T_w}\right)^{0.5} \quad (113)$$

and is used for the calculation of the convective heat transfer between wall and steam.

For the calculation of the heat transfer coefficients between wall and droplets are used the baumeister and Berenson equations (equations 75 and 63). If one postulates a spherical shape of the droplets, the equation for F_f reads:

$$F_f = N_{T,N} \cdot [\pi \cdot \delta_T^2 / 4] \quad (114)$$

The heat per surface unit, which can be eliminated through steam convection (with the assumption, that the steam outside of the boundary layer is not superheated) can be calculated with the following equation:

$$Q_{w,d} = 0.022 \cdot \frac{\lambda_d}{D} \cdot Re_d^{0.8} \cdot Pr_d^{0.4} \cdot \left(\frac{T_{sat}}{T_w}\right)^{0.5} \cdot (T_w - T_{sat}) \cdot (1-F_f) \quad (115)$$

with F_f from equation (114).

The heat transfer between wall and droplets results from the following equation:

$$Q_{w,T} = \alpha_{BAUM} \cdot (T_w - T_{sat}) \cdot F_f \quad (115)$$

or

$$Q_{w,T} = \alpha_{BER} \cdot (T_w - T_{sat}) \cdot F_f \quad (116)$$

The entire heat flux density is then calculated as follows:

$$q_{TOT} = Q_{w,d} + Q_{w,T} \quad (117)$$

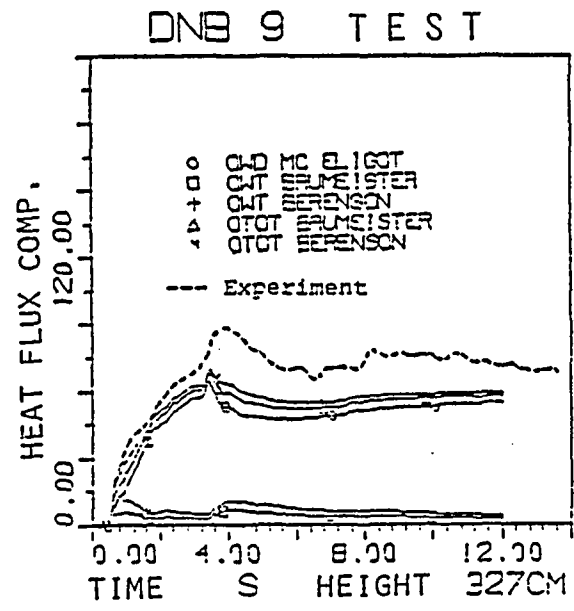
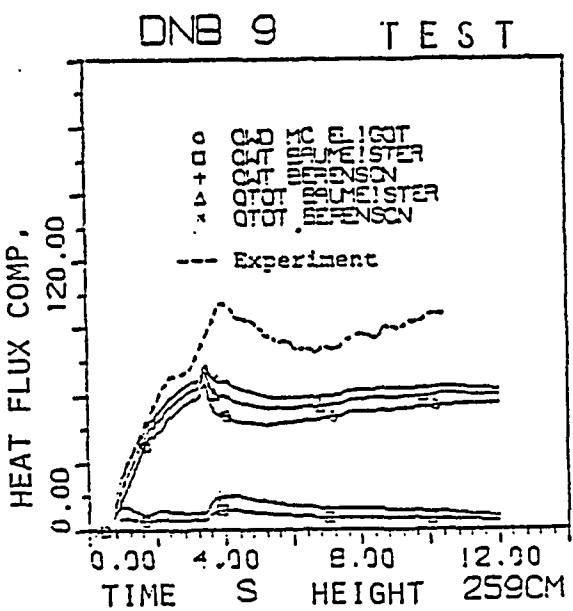
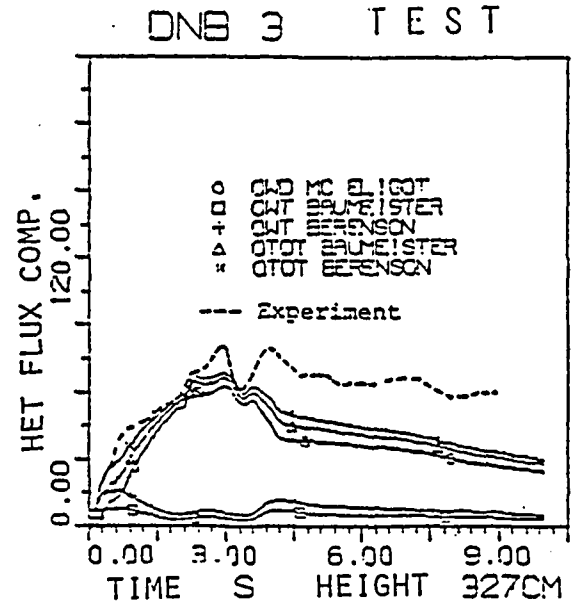
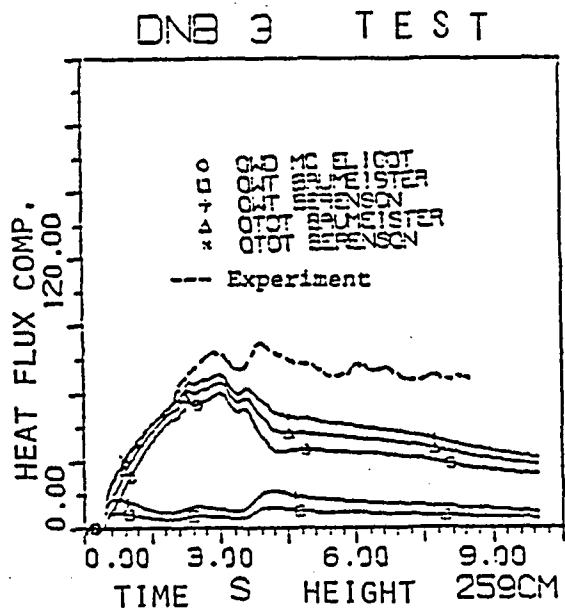
The individual components, as they were determined during the recalculation of the tests DNB1, DNB3 and DNB9, are shown in Fig. 46 and they are compared with the heat flux density calculated from the test. From this comparison it results, that the heat flux density calculated from this model is much too low in comparison with the test. But since the steam convection part was already calculated with the entire temperature difference, the steam-droplets share, to be necessarily too low.

The results in Chapter 11.3 showed, that the heat transfer between superheated steam and the water droplets is very effective. Therefrom, henceforth one starts with the consideration that all droplets present in the boundary layer do immediately evaporate because of the therein reigning great temperature difference. The droplets mass flow density can be defined in the steam-droplets flow as follows:

$$G_T = N_T \cdot [\pi \cdot \delta_T^3 / 6] \cdot w_f \cdot \rho_f \quad (118)$$

With the aid of equation (109) there is effected the correlation of the droplets mass flow density per surface unit of the heated wall as follows:

$$G_{w,T} = N_T^{2/3} \cdot [\pi \cdot \delta_T^3 / 6] \cdot w_f \cdot \rho_f \quad (119)$$



7

Fig. 46: Components of the heat flux in steam-droplets cooling

Another possibility for the determination of the droplets mass flux density results from the consideration for the calculation of the number of droplets in the boundary layer according to equation (108). The mean mass flow density can be calculated by using the mean droplets velocity in the boundary layer as follows:

$$G_{w,T} = N_T \cdot \delta_{GS} \cdot w_{f,GS} \cdot [\pi \cdot \delta_T^3 / 6] \cdot \rho_f \quad (120)$$

The comparison with the droplets mass flow densities per cm² of the wall, calculated with the equations (119) and (120), is shown in Fig. 47.

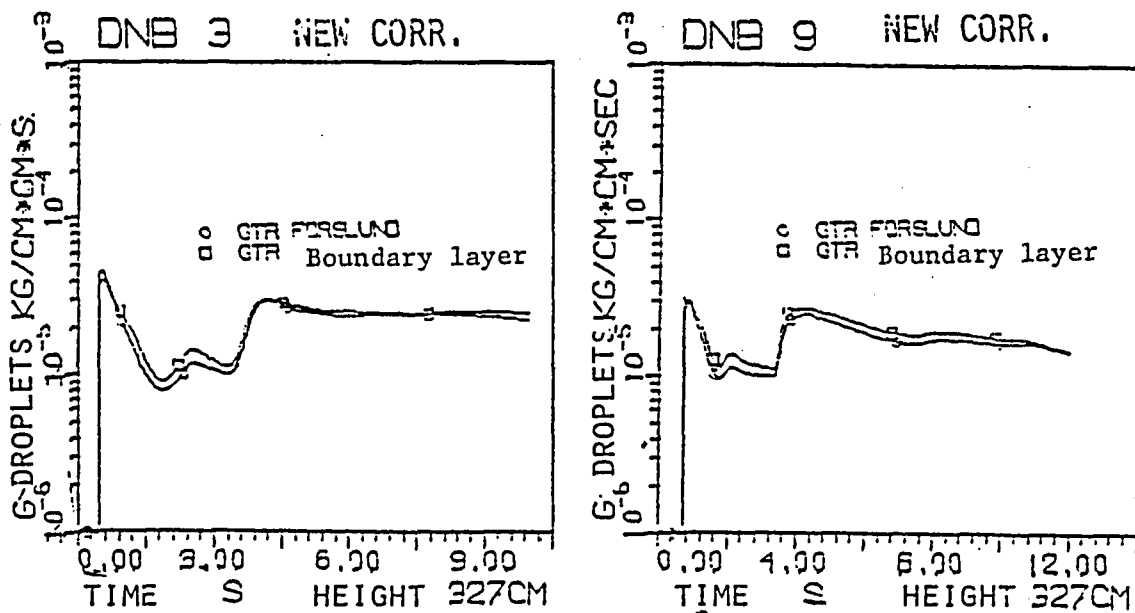


Fig. 47: Comparison of the droplets mass flow densities

The heat per surface unit necessary for the evaporation of the droplets can be calculated from the following equation:

$$Q_{w,T} = \Delta h_e \cdot G_{w,T} \quad (121)$$

The entire heat flux density does then result from the sum of the two components:

$$q_{TOT} = q_{w,d} (1 - F_f) + Q_{w,T} \quad (122)$$

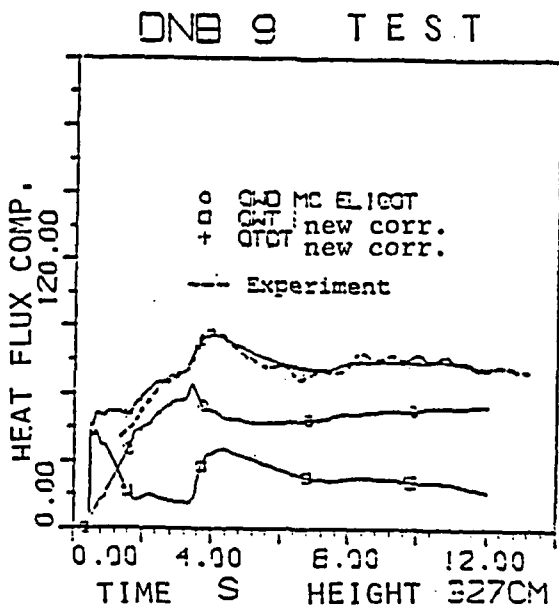
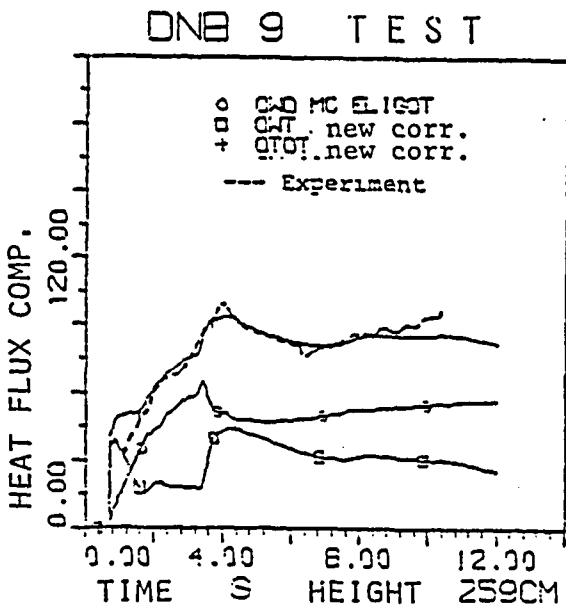
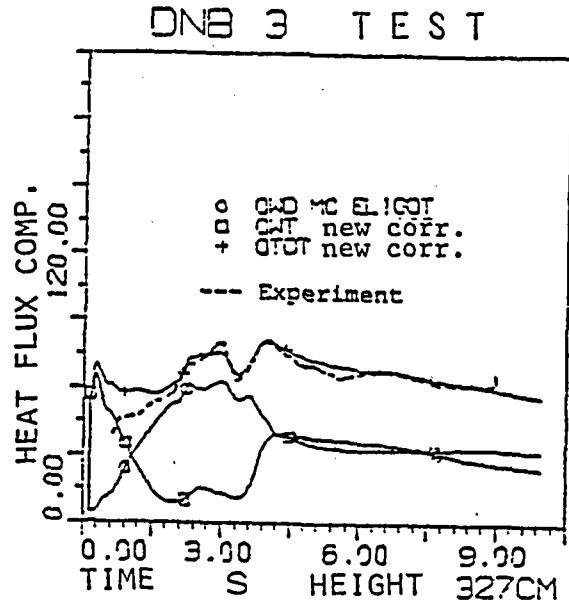
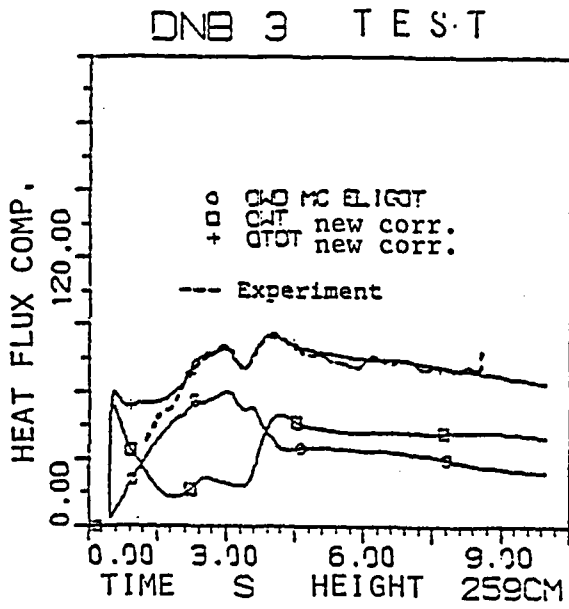


Fig. 48: Components of the hat flux density acc. to the "two-component model"

In Figure 48 are shown the components of the heat flux density, calculated with this model, and compared with the test results. As shown by these results, the agreement of the entire heat flux densities can be considered good.

11.5 Formulation in agreement with the similarity theory of the new model for the calculation of the heat transfer coefficients with steam-droplets cooling

The equation (97) can be expressed as follows:

$$q_{TOT} = \alpha_{w,d} \cdot (1-F_f) \cdot (T_w - T_d) + \alpha_{w,T} \cdot F_f \cdot (T_w - T_{sat}) \quad (123)$$

$$\text{with } \alpha_{w,d} = 0.022 \cdot \frac{\lambda_d}{D} \cdot Re_d^{0.8} \cdot Pr_d^{0.4} \cdot \left(\frac{T_d}{T_w}\right)^{0.5}$$

Hereafter it is postulated that also $\alpha_{w,T}$ can be expressed in a similar manner:

$$\alpha_{w,T} = 0.022 \cdot \frac{\lambda_d}{D} \cdot Re_T^m \cdot Pr_d^{0.4} \cdot \left(\frac{T_{sat}}{T_w}\right)^{0.5} \quad (124)$$

The Reynolds number is formed with the mass flow density of the droplets in the steam-droplets flow.

$$Re_T = [N_D \cdot (\pi \cdot \delta_T^3 / 6) \cdot w_f \cdot \rho_f \cdot D] / \eta_d \quad (125)$$

and with the exponent from the equation (119) there can be established the following equation for $\alpha_{w,T}$:

$$\alpha_{w,T} = 0.022 \cdot \frac{\lambda_d}{D} \cdot Re_T^{2/3} \cdot Pr_d^{0.4} \cdot \left(\frac{T_{sat}}{T_w}\right)^{0.5} \quad (126)$$

The heat flux density share through the heat transfer between wall and droplets per surface unit of the heated wall is then:

$$q_{w,T} = \alpha_{w,T} \cdot (T_w - T_{sat})$$

After the inserting of the equations (123) and (126) into the equation (122), one obtains the expression for the entire heat flux density.

$$q_{TOT} = [0.022 \cdot \frac{\lambda_d}{D} \cdot Re_d^{0.8} \cdot Pr_d^{0.4} \cdot (\frac{T_{sat}}{T})^{0.5} \cdot (1-F_f) \cdot (T_w - T_{sat})] + [0.022 \cdot \frac{\lambda_d}{D} \cdot Re_T^{2/3} \cdot Pr_d^{0.4} \cdot (\frac{T_{sat}}{T_w})^{0.5} \cdot F_f \cdot (T_w - T_{sat})] \quad (127)$$

with Re_T from equation (125).

The equation (127) can be written as follows:

$$q_{TOT} = 0.022 \cdot \frac{\lambda_d}{D} \cdot \{ [Re_d^{0.8} \cdot (1-F_f)] + [Re_T^{2/3} \cdot F_f] \} \cdot Pr_d^{0.4} \cdot (\frac{T_{sat}}{T_w})^{0.5} \cdot (T_w - T_{sat}) \quad (128)$$

and for the entire heat transfer coefficient results:

$$\alpha_{TOT} = 0.022 \cdot \frac{\lambda_d}{D} \cdot \{ [Re_d^{0.8} \cdot (1-F_f)] + [Re_T^{2/3} \cdot F_f] \} \cdot Pr_d^{0.4} \cdot (\frac{T_{sat}}{T_w})^{0.5} \quad (129)$$

In order to eliminate the difficulties that result in the practical application of this correlation for the determination of the surface distribution for the steam and droplets components (droplets diameter, number of droplets, and shape of droplets), it was attempted to determine the abovementioned distribution with the aid of the steam content. The ratio between the variables F_f and x was taken into consideration through the introduction of a corrective factor, which was defined as the proportion of volume and mass steam content. The exponent of this corrective factor was determined through the adaption to the test values.

$$K = (\frac{\psi}{x})^{0.21} \quad (130)$$

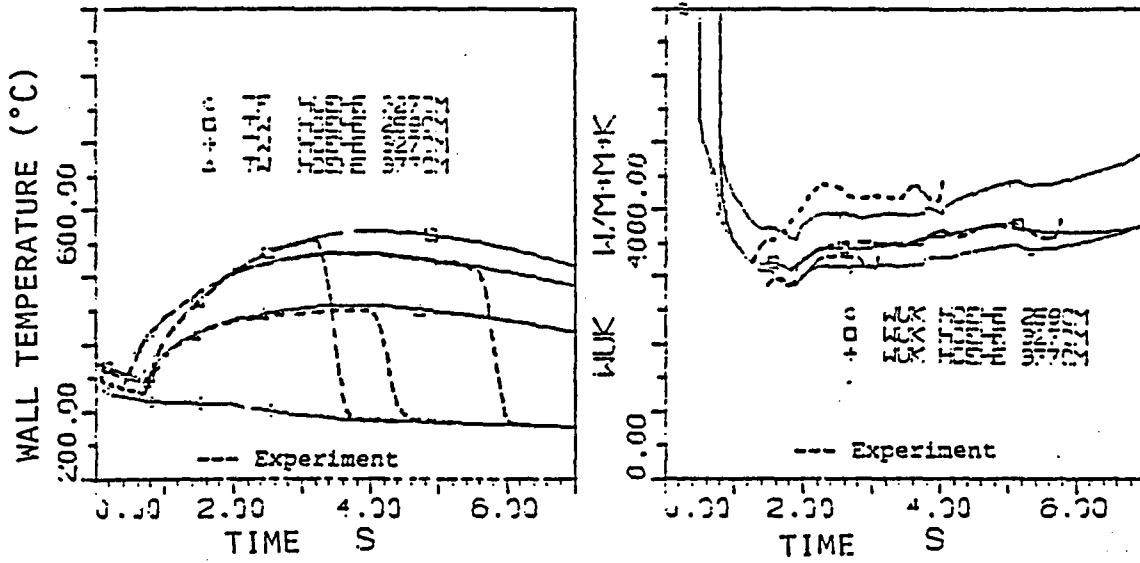
The correlation for the calculation of the heat transfer coefficients in the steam-droplets cooling phase can then be written as follows:

$$\alpha_{TOT} = 0.022 \cdot \frac{\lambda_d}{D} \cdot \{ (Re_d^{0.8} \cdot x) + [Re_T^{2/3} \cdot (1-x)] \} \cdot (\frac{\psi}{x})^{0.21} \cdot Pr_d^{0.4} \cdot (\frac{T_{sat}}{T_w})^{0.5} \quad (131)$$

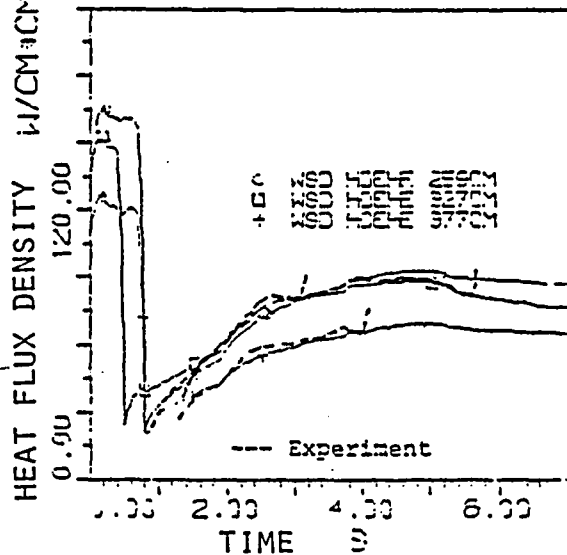
The physical characteristics in this equation were generally calculated with the mean temperature between wall and coolant. The physical characteristics of the Reynolds number are relative to the saturation temperature.

This equation for the calculation of the heat transfer coefficients was used for the recalculation of the tests DNB1, DNB3, DNB9, and PDNB11 in the phase after the exceeding of the critical heat flux (KHB). The results of these computer runs are shown in the Figures 49 to 52 and the calculated time behaviors of the wall temperature, of the heat transfer coefficients, and of the heat flux are compared with the test results. From this comparison it results, that the agreement between the calculated and the test results in the sphere of the test parameters can be described as very good. The comparison of the calculated time behaviors of the wall temperature and of the heat transfer coefficients, calculated with the aid of the new correlation and other equilibrium correlations, is shown in Attachment 11 and compared with the test result.

DNB 1 NEW CORRELATION



DNB 1 NEW CORRELATION



HOEHE: HEIGHT

Fig. 49: Results from the recalculation of the test DNB1 with the application of the new correlation for the calculation of the heat transfer coefficients

DNB 3 NEW CORRELATION

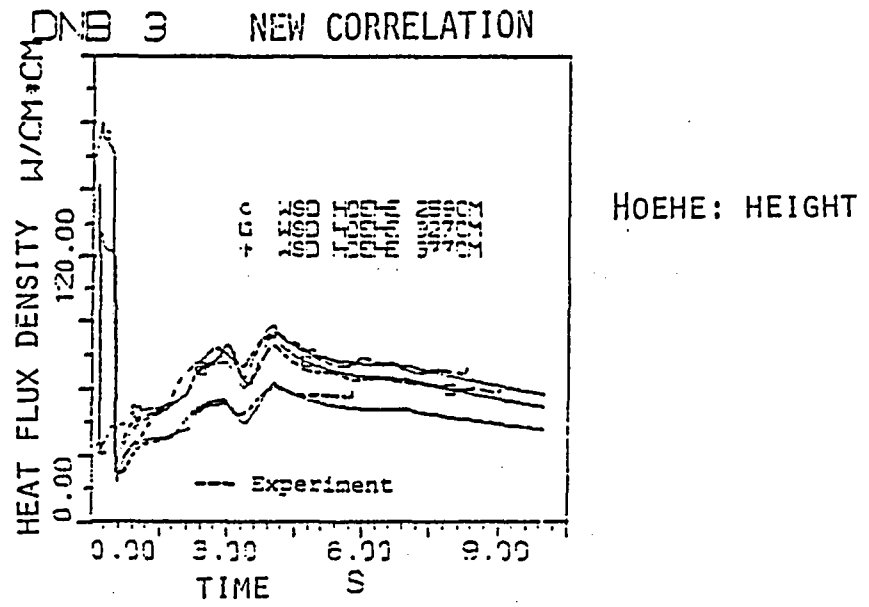
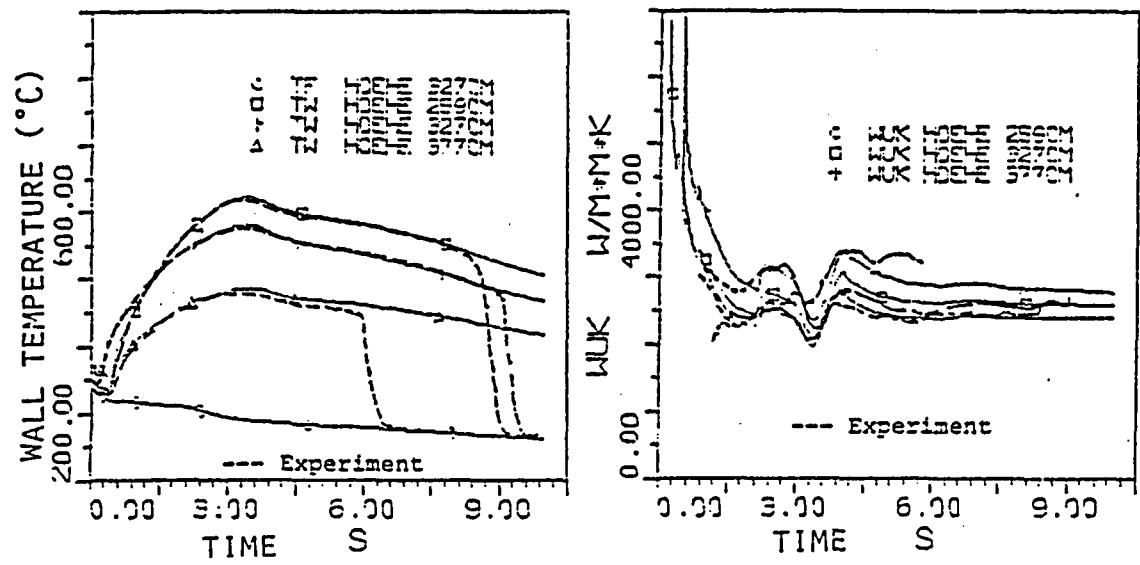
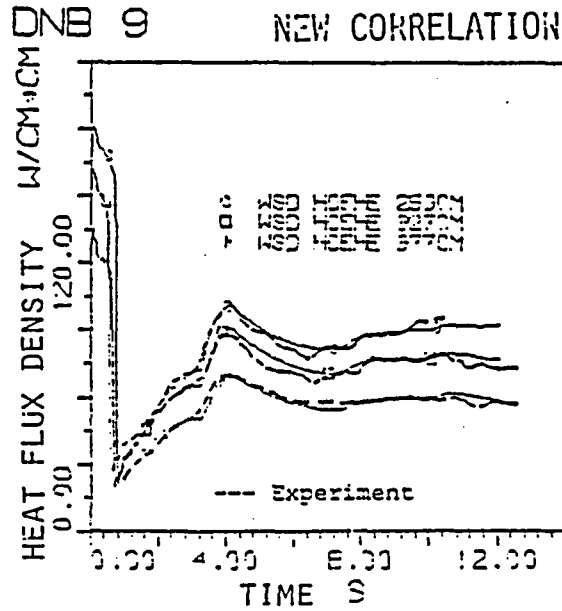
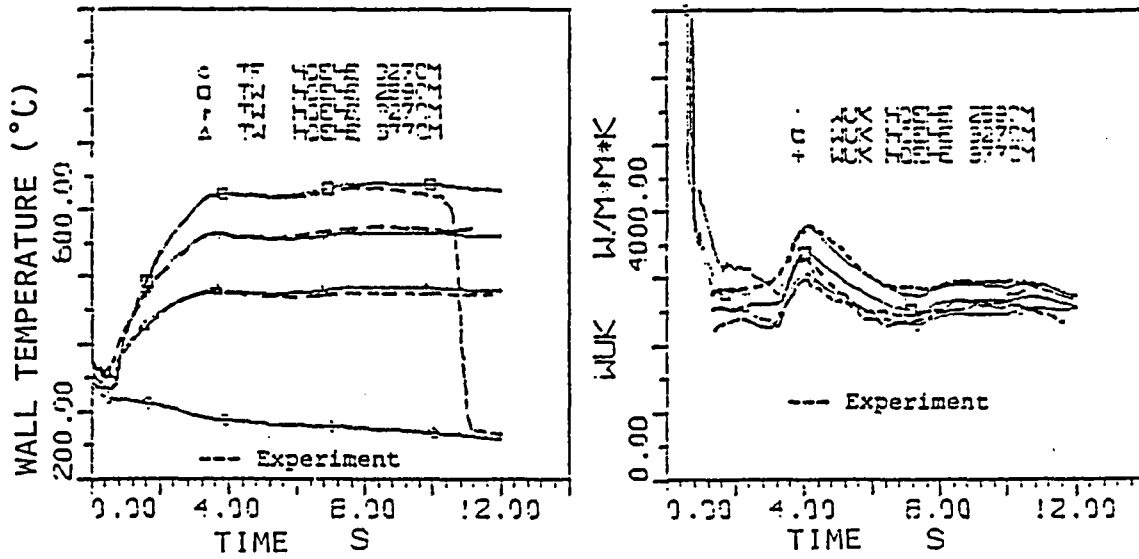


Fig. 50: Results of the recalculation of the test DNB3 with the application of the new correlation for the calculation of the heat transfer coefficients

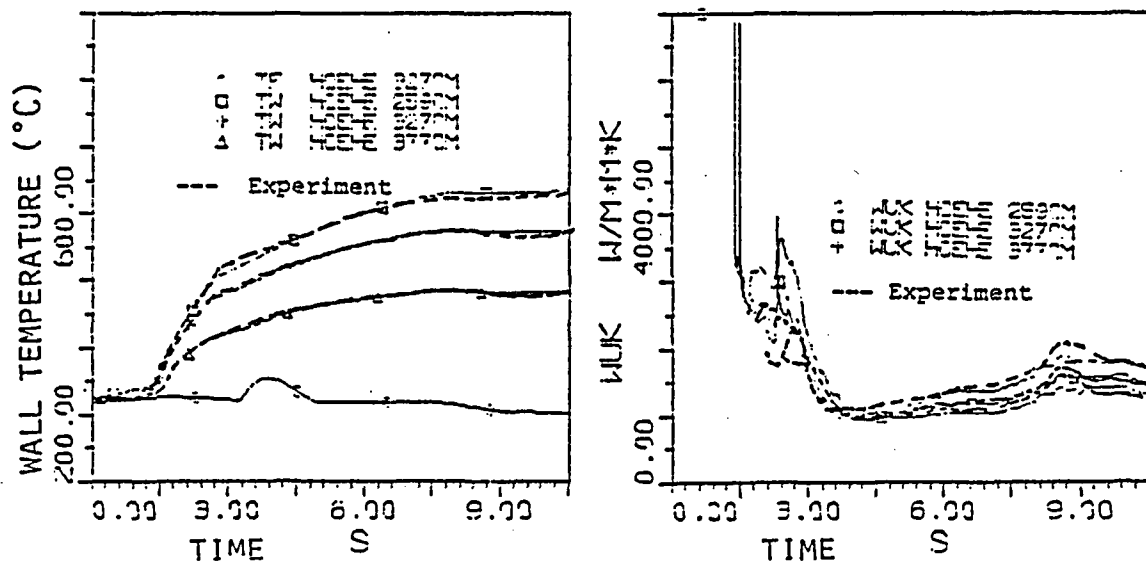
DNB 9 NEW CORRELATION



HOEHE: HEIGHT

Fig. 51: Results from the recalculation of the test DNB9 with the application of the new correlation for the calculation of the heat transfer coefficient

PDNB 11 NEW CORRELATION



PDNB 11 NEW CORRELATION

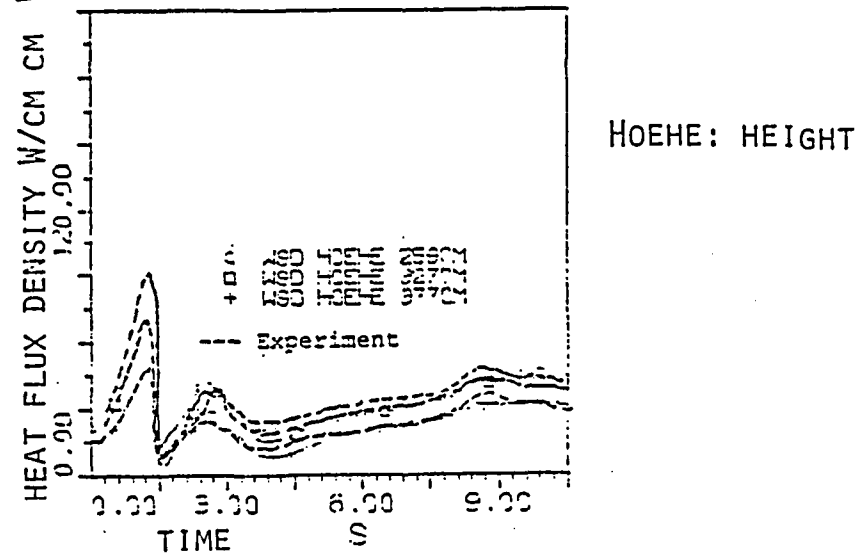


Fig. 52: Results from the recalculation of the test PDNB11 with application of the new correlation for the calculation of the heat transfer coefficients

12. CONCLUSIONS

The 25-rod bundle tests, conducted within the framework of the research project RS 37C, furnished a valuable experimental data-base for the verification of the compiled models and correlations for the calculation of the critical heat flux and of the heat transfer coefficients in the steam-droplets cooling regime.

The verification of the various correlations for the calculation of the maximum critical heat flux illustrated the limitation of the spheres of application of the individual correlations and showed, that none of the equations used in the wide sphere of the important thermal and fluid dynamic test parameters can be recommended for an accurate prediction of the DNB moment and point. A similar result was shown in the verification of the correlations for the calculation of the heat transfer coefficients after the exceeding of the maximum critical heat flux. Even the use of new models, which took into consideration the thermodynamic non-equilibrium between the steam and water phases, did not lead to the expected approximation of the calculated and measured time behaviors of the wall temperatures. It was further established, that the herein verified correlations for the calculation of the minimum temperature difference between wall and coolant, and of the minimum critical heat flux for the conditions with rewetting in the high pressure phase of a pressure drop process cannot be used for a prediction of the rewetting phenomenon at least in the sphere of the parameter combinations, cropped up in the 25-rod bundle tests.

The application of the "two components correlation," developed for the calculation of the heat transfer coefficients in the steam-droplets cooling regime, led to a very good agreement between the test and calculated results during the recalculation of the representative DNB and post-DNB tests. (Test parameter range: pressure 3 to 12 MPa, steam content 0.3 to 1 and mass flow rate 300 to 1400 kg/m² sec).

To prove the general validity of this correlation there is necessary the examination with the aid of further experimental investigations, which is planned within the framework of the evaluation of various experiments.

13. BIBLIOGRAPHY

- / 1/ Agemar, Brand, Emmerling, Flittner, Koehler, Loser
Final Report on the Start-up of the Testing Device for the
controlled bundle testings and on the first tests with a
PWR 25-rod bundle
Technical Report KWU R52-3015

- / 2/ Agemar, Brand, Emmerling
PWR Main Tests with a 25-rod bundle
Part 1: Experimental Implementation and Documentation of
the Test Results
KWU-RE23/012/77

- / 3/ Emmerling
PWR Main Tests with a 25-rod bundle
Part 2: Calculation of the Heat Transfer Coefficients
KWU-RE23/029/77

- / 4/ HD-Heat Transfer in 25-rod bundle tests
Test Evaluation
PSP Ingenieur-Planung No. 8204

- / 5/ H. Karwat, K. Wolfert
BRUCH-D- A Digital Program for PWR Blowdown Investigations
Nucl. Eng. Des. 11, 1970, p. 241-254

- / 6/ K.J. Liesch, F. Steinhoff, I. Vojtek, K. Wolfert
BRUCH-D-02 - A Computer Code for the Analysis of the Fluid and
Thermodynamic Processes in the Primary Loop of PWR with
large LOCAs
MRR-I, Laboratory for Reactor Controls and Plant Safety

- / 7/ I. Vojtek
PWR-25-rod bundle tests
Verification of the conducted DNB and post-DNB Tests
MRR-I, December 1976

- / 8/ I. Vojtek
Evaluation of the 25-rod bundle Tests with the Computer Code
BRUDI-VA
GRS-A-208, September 1978

- / 9/ F.W. Dittus, L.M.K. Boelter
Heat Transfer in Automobile Radiators of the Tubular Type
Uni. of Cal. Publications in Engineering, Vol. 2, No. 13, pp 443-461
October 1980

- /10/ E.N. Sieder, G.E. Tate
Heat Transfer and Pressure Drop of Liquids in Tubes
Industrial and Engineering Chemistry, Vol 28, No. 12, pp 1429-1435

- /11/ D.M. McEligot, L.W. Ormand, M.C. Perkins
Internal Low Reynolds Number Turbulent and Transitional Gas Flow
with Heat Transfer
J. of Heat Transfer, Trans ASME, May 1966
- /12/ H. Hausen
Representation of the Heat Transfer in Tubes through Generalized
Exponential equations
VDI-Zeitschrift, 1943
- /13/ K.J. Liesch, G. Raemhild, K. Hofmann
For the Determination of the Heat Transfer and the Critical Heat Flux
in View of Special Conditions in the Coolant Channels of a PWR with
large LOCAs
MRR 150, 1975
- /14/ W.H. Jens, P.A. Lottes
Analysis of Heat Transfer, Burnout, Pressure Drop and Density
Data for High Pressure Water
USAEC Rep. ANL-4627, 1951
- /15/ I.R.S. Thom et al
Boiling in Subcooled Water During Flow Up Heated Tubes or Annuli
Proc. Instr. Mech. Engrs. 1965-1966, Vol. 180, 3C, 1966
- /16/ J.G. Collier
Convective Boiling and Condensation
McGraw-Hill Book Company, 1972
- /17/ J.C. Chen
Correlation for Boiling Heat Transfer to Saturated Fluids in
Convective Flow
1-EC Process Design and Development, Vol. 5, No. 3, July 1966
- /18/ V.E. Schrock, L.M. Grossmann
Forced Convection Boiling in Tubes
Nucl. Sci. and Eng. 12, pp 474-481, 1962
- /19/ S. Nukiyama
Maximum and Minimum Values of Heat Transmitted from Metal to
Boiling Water under Atmospheric Pressure
J. Soc. Mech. Engrs., Japan 37, 53-54 and 367-374, 1934
- /20/ S.S. Kutateladze
Fundamentals of Heat Transfer
Edward Arnold (Publishers) Ltd., 1963
- /21/ N. Zuber
Hydrodynamic Aspects of Boiling Heat Transfer
Ph. D. Thesis, University of California, Los Angeles, 1959
- /22/ Y.P. Chang, N.W. Snyder
Heat Transfer in Saturated Boiling
Chem. Progr. Symp. Ser. 56, No. 30, 1960

- /23/ S.S. Kutateladze, A.I. Leontev
Some Applications of Asymptotic Theory of the Turbulent Boundary Layer
Proc. 3rd Int. Heat Transfer Conference, 1960
- /24/ L.S. Tong
Boiling Heat Transfer and Two-Phase Flow
John Wiley, Inc., 1966
- /25/ D. Maines
Slip Ratios and Friction Factors in the Bubble Flow Regime in Vertical Tubes
Institut for Atomenergi, Kjeller, Norway, 1966
- /26/ F.G. Thorgerson, D.M. Knoebel, J.H. Gibbons
A Model to Predict Convective Subcooled Critical Heat Flux
Trans ASME Series C, 96, 1976
- /27/ M. Monde, Y. Katto
Burnout in a High Heat Flux Boiling System with an impinging Jet
Int. J. H. M. Transfer 21, 1978
- /28/ Y. Katto, K. Ishii
Burnout in a High Heat Flux Boiling System with a Forced Supply of Liquid through a Plane Jet
6th Int. Heat Transfer Conference, 1978
- /29/ L.S. Tong et al
Influence of Axially Non-Uniform Heat Flux on DNB
8th National Heat Transfer Conference, Los Angeles, 1965
- /30/ L.S. Tong
Boiling Heat Transfer and Two-Phase Flow
John Wiley, Inc., 1966
- /31/ S. Milioti
A Survey of Burnout Correlations as applied to Water Cooled Nuclear Reactors
M. Engng. thesis, Pennsylvania State University, 1964
- /32/ L.S. Tong
Prediction of Departure from Nucleate Boiling for one Axially Non-uniform Heat Flux Distribution
Jour. of Nucl. Energy, Vol. 21, pp 241-243, 1967
- /33/ R.H. Wilson, L.J. Stanek, J.S. Gellerstedt
Critical Heat Flux in a Non-uniformly Heated Rod Bundle
9th Winter Annual Meeting, Los Angeles, Cal., November 16-20, 1969
- /34/ D.C. Leslie, Kirby
Application of Flow Model to Predicting Burnout under Transient Conditions
AEEW R542, 1967

- /35/ W. Belda
Dryout delay with LOCA in Nuclear Reactors
Dissertation TU Hannover, 1975
- /36/ F. Mayinger, W. Belda
Some Deliberations and Measurements Concerning Burnout-Delay
During Blowdown
European Two-Phase Flow Group Mtg., Harwell, 1974
- /37/ Y.Y. Hsu, W.D. Beckner
Correlation for the Onset of Transient CHF
Unpublished report
- /38/ P. Griffith, J.F. Pearson, R.J. Lepkowski
Critical Heat Flux during Loss-of-Coolant Accident
Nuclear Safety 18, 298, 1977
- /39/ B.C. Slifer
Loss-of-Coolant Accident and Emergency Core Cooling Models for
General Electric Boiling Water Reactors
NEDO-10329, 1971
- /40/ V.N. Smolin et al
Teploenergetica No. 4, p. 54-58, 1967
- /41/ L. Biasi et al
Studies on Burnout, Part 3
Energia Nucleare, Vol 14, No. 9, September 1967
- /42/ Bertolotti et al
Heat Transfer Crisis with Steam-Water Mixtures
Energia Nucleare, Vol 12, 1965
- /43/ J.H. Awberry
J. Iron and Steel Inst. 144, 1941
- /44/ A. Bromley, R. Norman
Heat Transfer in Forced Convection Film Boiling
Ind. and Eng. Chemistry, Vol 45, December 1953
- /45/ Y.Y. Hsu, J.W. Westwater
AI ChE Journal, Vol. 15, 1958
- /46/ P.J. Berenson
Film Boiling Heat Transfer from a Horizontal Surface
J. of Heat Transfer, Vol 83, August 1961
- /47/ R.S. Dougall, W.M. Rohsenow
Filmboiling on the Inside of Vertical Tubes with Upward Flow of the
Fluid at Low Qualities
MIT 9079-26, September 1963

- /48/ Z.L. Miropolskij
Heat Transfer in Film Boiling of Steam-Water Mixture in Steam
Generating Tubes
Teptoenergetica Vol. 10, No. 5, pp 49-53, 1963
- /49/ D.C. Groeneveld
An Investigation of Heat Transfer in the Liquid Deficient Regime
AECL-3281, December 1969
- /50/ D.C. Groeneveld
Post Dryout Heat Transfer
Physical Mechanisms and Survey of Prediction Methods
Nuclear Engineering and Design 32, 1975
- /51/ K.G. Condie, S.J. Bengston, S.L. Richlien
Post-CHF Heat Transfer Data, Analysis, Comparison and Correlation
Unpublished Report
- /52/ J.D. Parker, R.J. Grosh
Heat Transfer to a Mist Flow
ANL-6291, 1962
- /53/ W.F. Laverty, W.M. Rohsenow
Film Boiling of Saturated Liquid Nitrogen Flowing in a Vertical Tube
J. of Heat Transfer, Vol 89, pp 90-98, 1967
- /54/ R.P. Forslund, W.M. Rohsenow
Dispersed Flow Film Boiling
ASME Paper No. 68-HT-44, J. of Heat Transfer, 1968
- /55/ K.J. Baumeister, T.D. Hamill, G.J. Schoessow
A Generalized Correlation of Vaporization Times of Drops in Film
Boiling on a Flat Plate
U.S.-AICHE, 3rd International Heat Transfer Conference, August 1966
- /56/ S.J. Hynek, W.M. Rohsenow, A.B. Bergles
Forced Convection Dispersed Flow Boiling
MIT Report No. DSR 70586-63, 1969
- /57/ D.C. Groeneveld, G.G.J. Delorme
Prediction of Thermal Non-Equilibrium in the Post-Dryout Regime
Nuclear Engineering and Design 36, pp 17-26, 1976
- /58/ G. Hadaller, S. Banarjee
Heat Transfer to Superheated Steam in Round Tubes
AECL unpublished Report, 1969
- /59/ J.C. Chen, F.T. Ozkaynak, B.K. Sundaram
Vapor Heat Transfer in Post-CHF Region including the Effect of
Thermodynamic Non-Equilibrium
Nuclear Engineering and Design 51, pp. 143-155, 1979

- /60/ D.H.R. Beattle
Friction Factors and Regime Transition in High Pressure Steam-Water
Flows
Aus. Atomic Energy Com. Sutherland 2232, NSW, Australia
- /61/ P.J. Berenson
Trans. ASME J. Heat Transfer, 83, 351, 1961
- /62/ R.E. Henry
A Correlation for the Minimum Film Boiling Temperature
AIChE Sym. Series No. 138, Vol. 70, pp. 81-90, 1974
- /63/ O.C. Iloeje, D.N. Plummer, W.M. Rohsenow, P. Griffith
An Investigation of the Collapse and Surface Rewet in Film Boiling
in Forced Vertical Flow
Trans. of the ASME, J. of Heat Transfer, May 1975
- /64/ S.Y. Ahmad
Axial Distribution of Bulk Temperature and Void Fraction in a
Heated Channel with Inlet Subcooling
ASME J. of Heat Transfer, 92, pp. 595-509, 1970
- /65/ D.C. Groeneveld
The Thermal Behaviour of a Heated Surface at and beyond Dryout
Ph.D. Thesis University of Western Ontario, 1972
- /66/ D. Hein
Model Representations for Rewetting through Flooding
Dissertation, Techn. Universitaet, Hannover, 1980
- /67/ M. Ishii
One Dimensional Drift-Flux Model and Constitutive Equations for
Relative Motion between Phases in Various Two-Phase Flow Regimes
ANL-77-47, Argonne National Laboratory, 1977
- /68/ A. Ghazanfari
Experimental Investigation of the Heat Transfer in a Droplet Flow
after Exceeding of the Rewetting Temperature
Dissertation, Techn. Universitaet, Bochum, 1977
- /69/ M. Cumo, G.E. Farello, G. Ferrari, G. Palazzi
On Two-Phase Highly Dispersed Flows
ASME paper 73-HT-18, 13th National Heat Transfer Conference,
Atlanta, 1973
- /70/ W. Bohl
Technical Fluid Dynamics
Vogel Verlag, 1971

ATTACHMENT 1

Compilation of the important parameters at DNB moment (extract)

NR.	MOENE (M)	STAD	TONO (S)	GH (W/CH/CH)	JEL	F (BAR)	XONE	CODE (KCS)
1505	2.59	B4	0.5	160.	144.	107.	0.163771	7.812400
1505	2.59	D2	0.5	136.	136.	102.	0.163771	7.812400
1505	2.59	B3	0.5	136.	136.	103.	0.163771	7.812400
1505	3.18	B2	0.5	120.	120.	102.	0.117633	10.433400
1505	3.18	D3	0.5	120.	120.	104.	0.117633	10.433400
1505	3.18	D4	0.5	122.	122.	103.	0.117633	10.433400
1506	2.59	D4	1.0	136.	136.	103.	0.131152	8.271670
1506	2.59	D2	1.0	134.	134.	104.	0.131152	8.271670
1506	2.59	D3	1.0	130.	130.	103.	0.131152	8.271670
1506	2.59	B3	1.0	139.	139.	105.	0.131152	8.271670
1506	2.59	B4	0.5	142.	142.	107.	0.131152	8.271670
1506	2.59	D2	0.5	137.	137.	106.	0.131152	8.271670
1506	3.18	D3	0.5	122.	122.	109.	0.103813	10.434600
1506	3.18	D4	0.5	124.	124.	110.	0.103813	10.434600
1506	3.18	B2	0.5	121.	121.	110.	0.103813	10.434600
1507	2.59	B2	0.5	168.	149.	118.	0.094189	8.728200
1507	2.59	D3	0.5	164.	142.	112.	0.094189	8.728200
1507	2.59	D4	0.5	173.	148.	109.	0.094189	8.728200
1507	2.59	B4	0.5	170.	146.	112.	0.094189	8.728200
1507	2.59	D2	0.5	167.	144.	115.	0.094189	8.728200
1507	2.59	D3	0.5	169.	143.	109.	0.094189	8.728200
1507	3.18	D4	0.5	149.	128.	117.	0.102855	12.626200
1507	3.18	D3	0.5	150.	126.	115.	0.102855	12.626200
1507	3.18	B2	0.5	152.	126.	116.	0.102855	12.626200
1509	2.59	D4	0.5	169.	150.	117.	0.124289	8.393250
1509	2.59	D3	0.5	161.	143.	114.	0.124289	8.393250
1509	2.59	B2	0.5	165.	148.	109.	0.124289	8.393250
1509	2.59	D2	0.5	160.	140.	112.	0.124289	8.393250
1509	2.59	B3	0.5	162.	141.	112.	0.124289	8.393250
1509	2.59	B4	0.5	166.	144.	112.	0.124289	8.393250
1509	3.18	B2	0.5	144.	125.	114.	0.132872	8.938990
1509	3.18	D3	0.5	146.	125.	112.	0.132872	8.938990
1509	3.18	D4	0.5	148.	125.	113.	0.132872	8.938990
1510	2.59	B4	0.5	166.	146.	111.	0.162266	7.326900
1510	2.59	B3	0.0	166.	145.	114.	0.162266	7.326900
1510	3.18	D2	0.5	147.	125.	109.	0.140996	9.062100
1510	3.18	D3	0.5	148.	125.	109.	0.140996	9.062100
1510	3.18	D4	0.5	149.	126.	111.	0.140996	9.062100
1513	2.59	D4	0.5	169.	157.	115.	0.180299	6.444350
1513	2.59	D3	0.5	162.	144.	119.	0.180299	6.444350
1513	2.59	D2	0.5	164.	141.	111.	0.180299	6.444350
1513	2.59	B3	0.5	179.	142.	114.	0.180299	6.444350
1514	2.59	D4	1.0	121.	121.	108.		
1514	2.59	D3	0.5	160.	140.	120.		
1514	2.59	D2	1.0	130.	130.	112.		
1514	2.59	B3	1.0	130.	130.	112.		
1514	2.59	B4	1.0	133.	133.	112.		
1514	3.18	B2	0.5	140.	124.	120.		
1514	3.18	D3	0.5	141.	125.	114.		
1514	3.18	D4	0.5	141.	126.	120.		
1515	2.59	D4	1.0	133.	130.	114.	0.144118	6.543820
1515	2.59	D3	1.0	122.	122.	114.	0.144118	6.543820
1515	2.59	D2	1.0	128.	120.	116.	0.144118	6.543820
1515	2.59	B4	1.0	130.	130.	116.	0.144118	6.543820
1515	3.18	B2	1.0	114.	114.	116.	0.118276	7.034580
1515	3.18	D3	1.0	114.	114.	116.	0.118276	7.034580
1515	3.18	D4	1.0	114.	114.	116.	0.118276	7.034580
1516	2.59	B3	0.5	170.	148.	111.		
1516	3.18	D3	0.5	154.	126.	105.		
1516	3.18	D4	0.5	154.	120.	110.		

ATTACHMENT 2

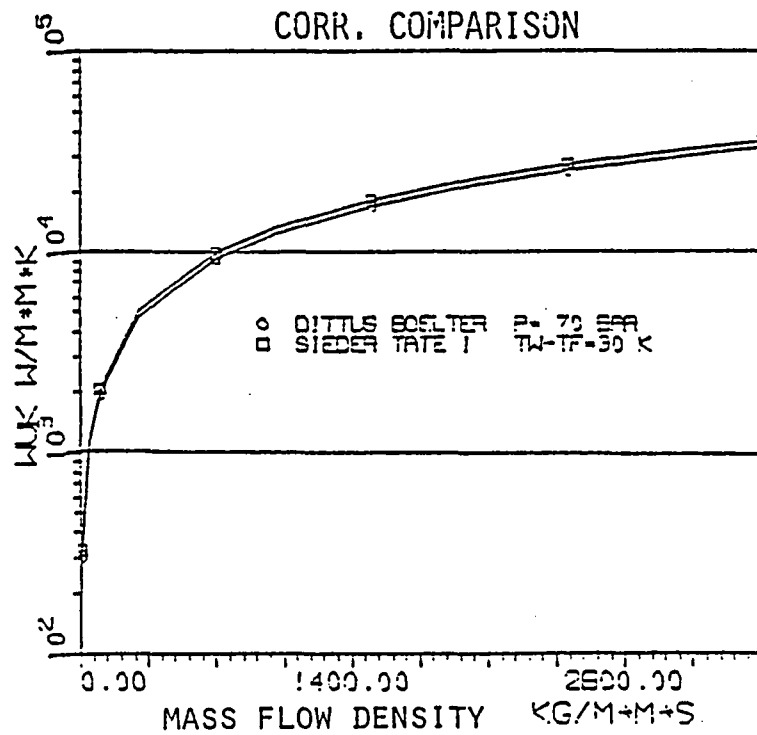
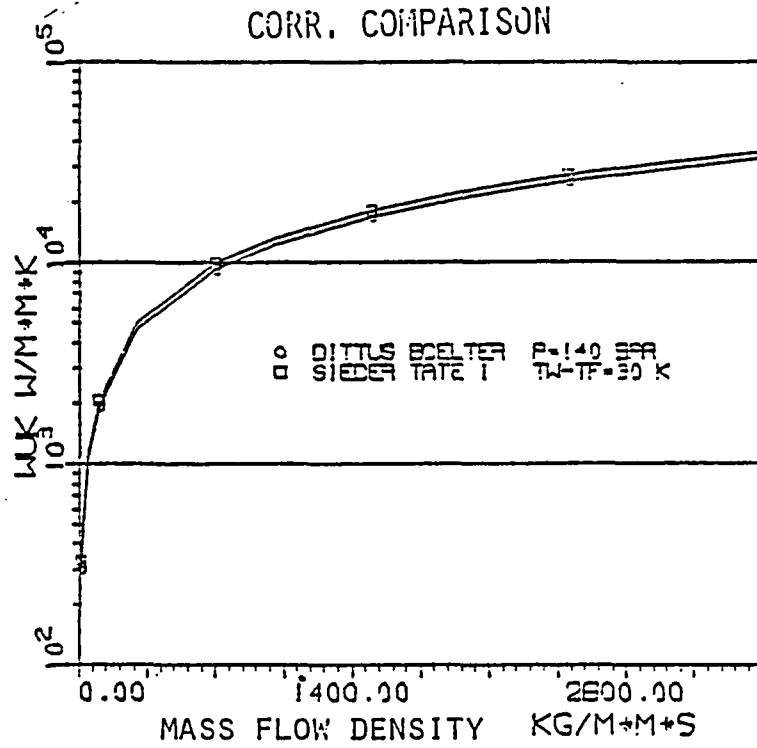
Compilation of the important parameters at RNB moment (extract)

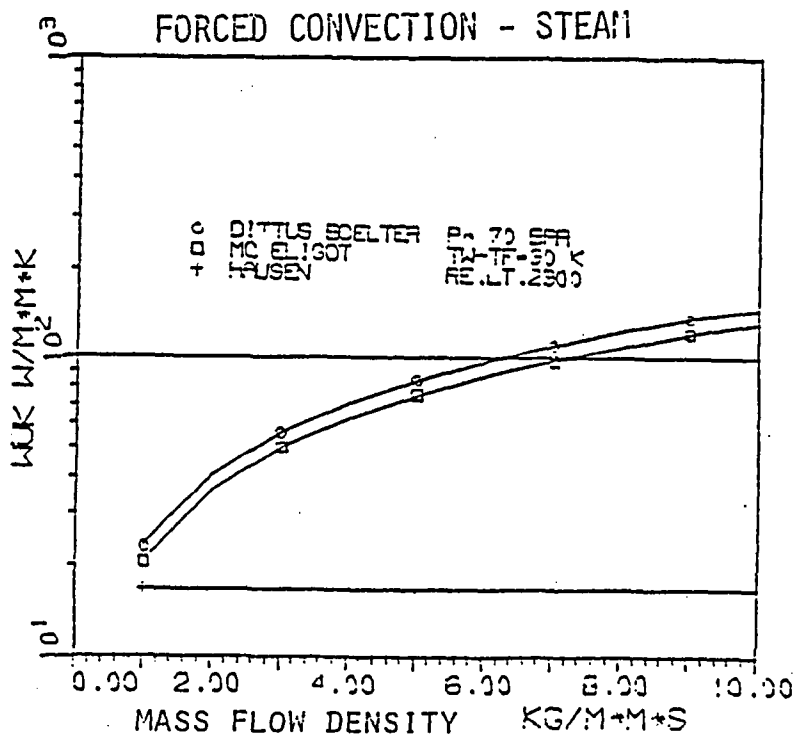
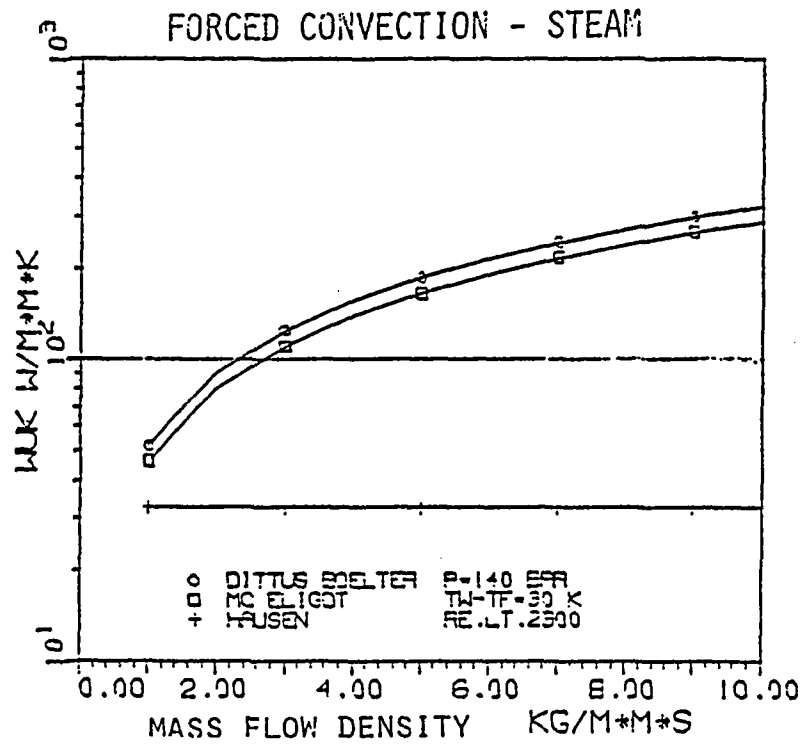
1507	3.68	C4	5.	64.	46.	66.	17.			0.339192	3.999770
1507	3.68	C3	4.5	54.	46.	66.	170.	450.	280.	0.339192	3.999770
1507	3.68	04	4.5	46.	46.	66.	160.	450.	250.	0.339192	3.999770
1507	3.68	B2	5.5	54.	44.	64.	17.	450.	280.	0.339192	3.999770
1507	3.77	C3	6.0	56.	42.	62.	170.			0.339192	3.999770
1507	3.77	04	6.0	45.	45.	62.	170.	450.	280.	0.339192	3.999770
1507	3.77	03	6.0	45.	45.	62.	170.	450.	280.	0.339192	3.999770
1509	2.50	C4	3.0	76.	110.	76.	24.			0.243691	4.635250
1509	2.50	C4	2.5	115.	115.	83.	21.	510.	350.	0.243691	4.635250
1509	2.50	C3	3.0	135.	135.	73.	240.	530.	250.	0.243691	4.635250
1509	2.50	C2	2.0	120.	120.	59.	13.	440.	310.	0.243691	4.635250
1509	2.50	C3	6.0	94.	68.	62.	28.			0.243691	4.635250
1509	2.50	C2	5.0	94.	74.	66.	270.	450.	280.	0.243691	4.635250
1509	2.50	P3	6.0	01.	81.	64.	28.	560.	280.	0.243691	4.635250
1509	2.50	P4	6.0	94.	71.	61.	29.	570.	280.	0.243691	4.635250
1509	3.10	C4	6.0	82.	66.	63.	24.			0.289825	4.294560
1509	3.10	02	6.0	70.	64.	65.	230.	510.	240.	0.289825	4.294560
1509	3.10	03	6.0	67.	61.	62.	230.	510.	280.	0.289825	4.294560
1509	3.10	04	6.0	70.	65.	63.	240.	520.	280.	0.289825	4.294560
1509	3.27	C3	7.0	74.	51.	59.	23.			0.289825	4.294560
1509	3.27	C2	7.5	65.	54.	59.	24.	520.	280.	0.289825	4.294560
1509	3.27	P3	7.0	50.	53.	56.	23.	500.	270.	0.289825	4.294560
1509	3.27	P4	7.5	65.	52.	58.	230.	500.	270.	0.289825	4.294560
1509	3.68	C4	4.0	68.	69.	72.	16.			0.299935	6.029970
1509	3.68	C4	6.5	51.	68.	73.	160.	450.	250.	0.299935	6.029970
1509	3.68	C3	3.5	61.	69.	72.	160.	450.	250.	0.299935	6.029970
1509	3.68	02	4.0	56.	66.	71.	160.	450.	290.	0.299935	6.029970
1509	3.77	C3	5.0	74.	58.	66.	17.			0.299935	6.029970
1509	3.77	P3	5.0	61.	61.	66.	180.	460.	200.	0.299935	6.029970
1509	3.77	P4	5.0	67.	63.	66.	170.	450.	280.	0.299935	6.029970
1510	2.50	C3	3.0	90.	102.	74.	27.			0.285558	5.135980
1510	2.50	P4	3.0	120.	120.	76.	26.	550.	290.	0.285558	5.135980
1510	2.50	P3	3.0	103.	103.	75.	270.	560.	290.	0.285558	5.135980
1510	3.10	C4	4.0	90.	84.	69.	22.			0.267914	6.543770
1510	3.10	02	3.5	87.	87.	71.	210.	500.	290.	0.267914	6.543770
1510	3.10	C3	3.5	91.	91.	74.	210.	500.	250.	0.267914	6.543770
1510	3.10	C4	3.5	85.	85.	71.	220.	510.	290.	0.267914	6.543770
1510	3.27	C3	6.0	91.	82.	61.	24.			0.267914	6.543770
1510	3.27	P3	6.0	82.	82.	59.	230.	510.	280.	0.267914	6.543770
1510	3.27	C2	4.5	85.	85.	65.	24.	530.	290.	0.267914	6.543770
1510	3.27	P4	5.0	83.	83.	61.	220.	500.	280.	0.267914	6.543770
1510	3.77	C3	4.0	72.	64.	67.	160.			0.262275	7.975080
1510	3.77	P4	4.0	67.	67.	71.	160.	450.	290.	0.262275	7.975080
1510	3.77	02	3.5	62.	68.	72.	160.	450.	290.	0.262275	7.975080
1510	3.77	03	4.0	67.	67.	69.	160.	450.	290.	0.262275	7.975080
1515	3.68	C4	6.0	64.	61.	58.	13.			0.349084	4.887450
1515	3.68	02	5.0	54.	59.	58.	180.	450.	270.	0.349084	4.887450
1515	3.68	C3	5.5	62.	62.	58.	190.	460.	270.	0.349084	4.887450
1515	3.68	04	6.0	54.	59.	58.	100.	460.	280.	0.349084	4.887450
1515	3.77	02	7.0	60.	67.	56.	190.	460.	270.	0.349084	4.887450
1515	3.77	03	7.0	61.	61.	54.	190.	460.	270.	0.349084	4.887450
1515	3.77	P4	7.0	64.	58.	55.	180.	450.	270.	0.349084	4.887450

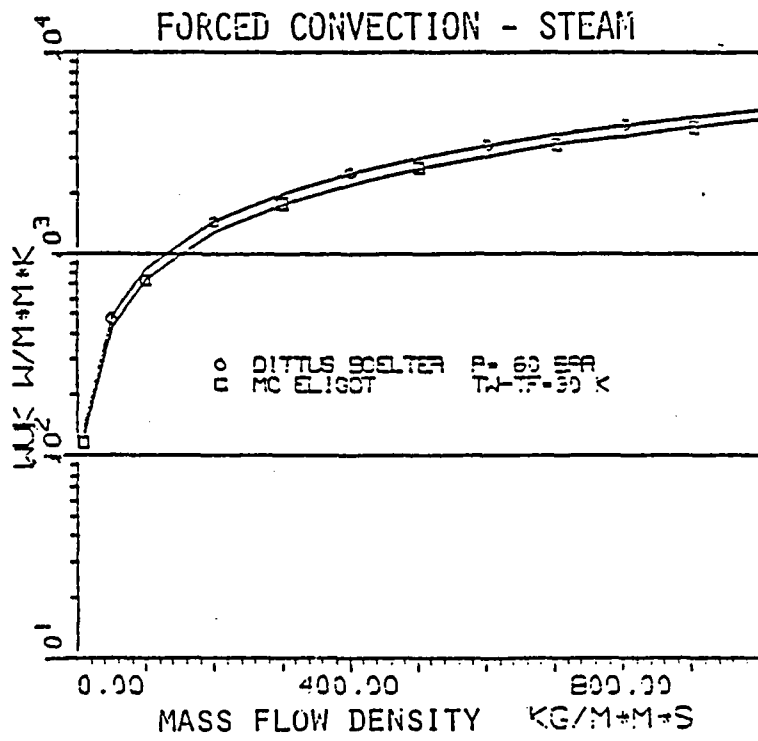
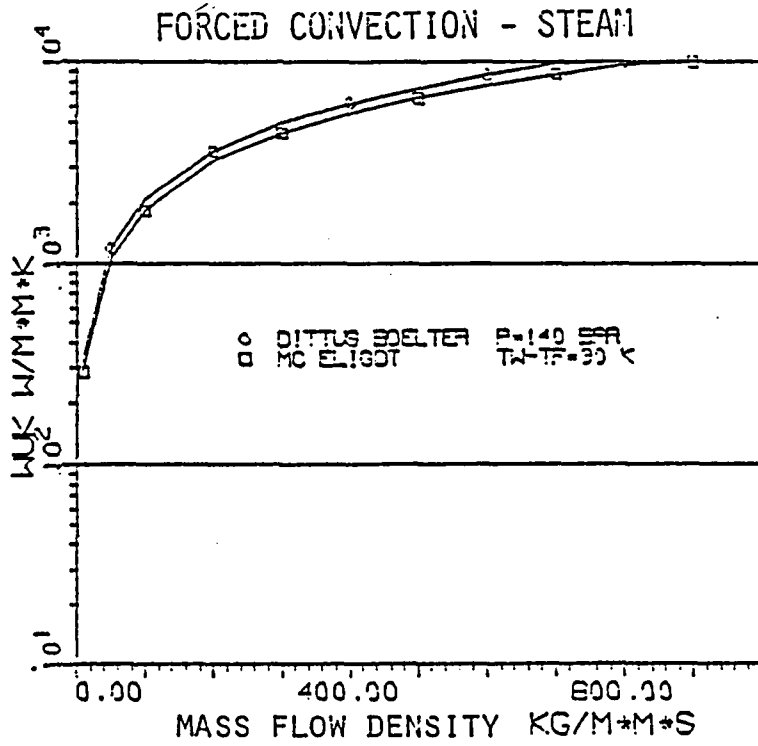
NR.	MOENE (M)	STAD	TRIM I (S)	GH (W/CMBCH)	ZEL	I (EAR)	II (K)	TRANK (C)	TRASSER (C)	XPAD	CPMP (KC/S)
1505	2.59	C3	3.0	9.	111.	74.	26.			0.226699	6.387850
1505	2.59	C4	3.0	134.	108.	74.	27.	560.	250.	0.226699	6.387850
1505	2.59	D2	2.0	118.	118.	91.	19.	490.	300.	0.226699	6.387850
1505	2.59	P3	3.0	136.	106.	74.	27.	560.	250.	0.226699	6.387850
1505	3.18	C4	4.0	92.	88.	69.	22.			0.242861	6.467770
1505	3.18	P2	3.5	80.	88.	77.	22.	510.	290.	0.242861	6.467770
1505	3.18	C3	3.5	87.	87.	69.	22.	510.	290.	0.242861	6.467770
1505	3.18	D4	3.5	88.	88.	77.	21.	500.	290.	0.242861	6.467770
1505	3.27	C3	5.5	86.	73.	64.	23.			0.242861	6.467770
1505	3.27	C2	4.5	80.	81.	65.	25.	530.	280.	0.242861	6.467770
1505	3.27	B4	5.0	77.	72.	63.	23.	510.	280.	0.242861	6.467770
1505	3.27	B3	6.0	67.	67.	62.	23.	510.	280.	0.242861	6.467770
1505	3.68	C4	3.0	65.	74.	74.	16.			0.373814	5.398120
1505	3.68	P2	2.0	81.	81.	77.	12.	420.	300.	0.373814	5.398120
1505	3.68	C3	2.5	77.	79.	82.	12.	420.	300.	0.373814	5.398120
1505	3.68	D4	2.0	80.	80.	88.	12.	420.	300.	0.373814	5.398120
1505	3.77	C3	4.0	71.	67.	68.	16.			0.373814	5.398120
1505	3.77	B3	4.0	69.	69.	68.	16.	450.	290.	0.373814	5.398120
1505	3.77	D2	3.5	70.	70.	71.	15.	450.	290.	0.373814	5.398120
1505	3.77	B4	3.0	68.	68.	68.	16.	450.	290.	0.373814	5.398120
1506	2.50	C4	3.0	84.	112.	80.	25.			0.236465	4.887870
1506	2.50	D4	2.0	120.	120.	89.	21.	510.	300.	0.236465	4.887870
1506	2.50	P2	2.0	122.	122.	84.	17.	480.	310.	0.236465	4.887870
1506	2.50	C3	3.0	100.	106.	74.	25.	540.	290.	0.236465	4.887870
1506	2.59	C3	6.0	96.	67.	58.	28.			0.236465	4.887870
1506	2.59	B3	6.0	86.	77.	61.	29.	570.	280.	0.236465	4.887870
1506	2.59	D4	6.0	100.	71.	59.	29.	570.	280.	0.236465	4.887870
1506	2.59	D2	5.5	88.	79.	62.	27.	550.	280.	0.236465	4.887870
1506	3.18	C4	6.0	84.	67.	62.	24.			0.301011	4.312060
1506	3.18	C3	6.0	74.	64.	60.	23.	510.	280.	0.301011	4.312060
1506	3.18	D4	6.0	73.	66.	61.	23.	510.	280.	0.301011	4.312060
1506	3.18	D2	6.0	75.	66.	62.	23.	510.	280.	0.301011	4.312060
1506	3.27	C3	8.0	74.	53.	55.	23.			0.301011	4.312060
1506	3.27	B3	9.0	63.	52.	53.	23.	500.	270.	0.301011	4.312060
1506	3.27	D2	7.5	65.	54.	56.	24.	510.	270.	0.301011	4.312060
1506	3.27	P4	7.0	64.	55.	58.	22.	500.	280.	0.301011	4.312060
1506	3.68	C4	4.0	63.	66.	70.	16.			0.296851	6.419020
1506	3.68	C3	4.0	62.	67.	77.	16.	450.	290.	0.296851	6.419020
1506	3.68	D4	4.0	55.	67.	70.	16.	450.	290.	0.296851	6.419020
1506	3.68	F2	4.0	60.	66.	70.	18.	470.	290.	0.296851	6.419020
1506	3.77	C3	5.0	74.	61.	64.	17.			0.296851	6.419020
1506	3.77	D3	4.5	61.	61.	112.	18.	460.	280.	0.296851	6.419020
1506	3.77	D4	5.0	64.	59.	113.	17.	450.	280.	0.296851	6.419020
1507	2.50	C4	5.0	79.	64.	64.	27.			0.261308	3.243120
1507	2.50	P2	4.5	70.	70.	66.	29.	580.	290.	0.261308	3.243120
1507	2.50	C3	5.5	69.	64.	64.	27.	550.	280.	0.261308	3.243120
1507	2.5	D4	5.0	66.	69.	64.	28.	560.	280.	0.261308	3.243120
1507	2.59	C3	8.0	70.	44.	52.	26.			0.261308	3.243120
1507	2.59	D4	8.5	61.	46.	52.	26.	530.	270.	0.261308	3.243120
1507	2.59	C2	7.5	66.	54.	56.	26.	530.	270.	0.261308	3.243120
1507	2.59	P3	8.0	53.	48.	54.	27.	540.	270.	0.261308	3.243120
1507	3.18	C4	7.0	64.	51.	50.	22.			0.324343	3.086220
1507	3.18	D4	7.5	54.	47.	55.	22.	490.	270.	0.324343	3.086220
1507	3.18	C3	7.5	55.	46.	56.	23.	500.	270.	0.324343	3.086220
1507	3.18	D2	7.5	57.	47.	56.	22.	490.	270.	0.324343	3.086220
1507	3.27	C3	9.0	60.	40.	51.	22.			0.324343	3.086220
1507	3.27	B4	8.0	50.	41.	53.	21.	480.	270.	0.324343	3.086220
1507	3.27	P2	8.0	57.	44.	55.	24.	510.	270.	0.324343	3.086220
1507	3.27	F3	9.5	38.	30.	49.	22.	480.	260.	0.324343	3.086220

ATTACHMENT 3

Comparison of the correlations for the calculation of the heat transfer coefficients with forced convection

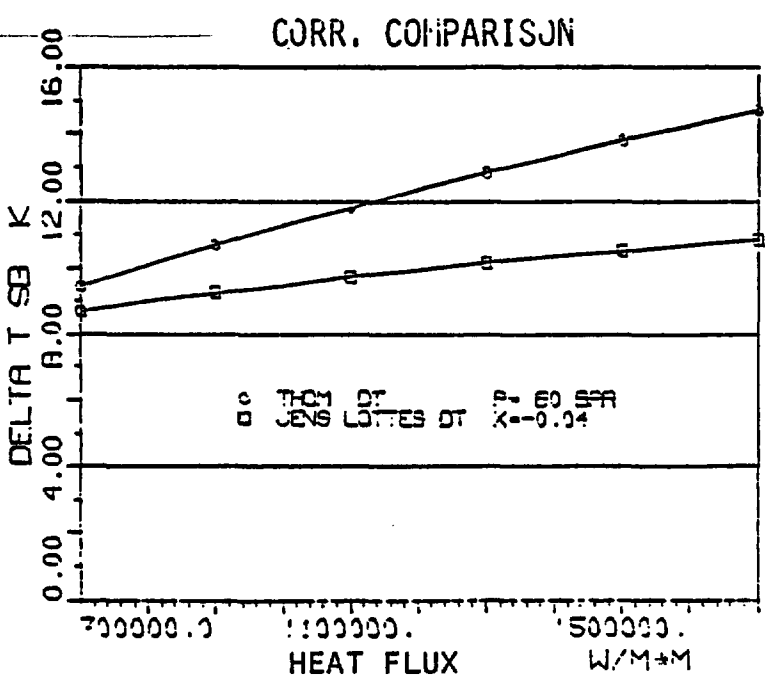
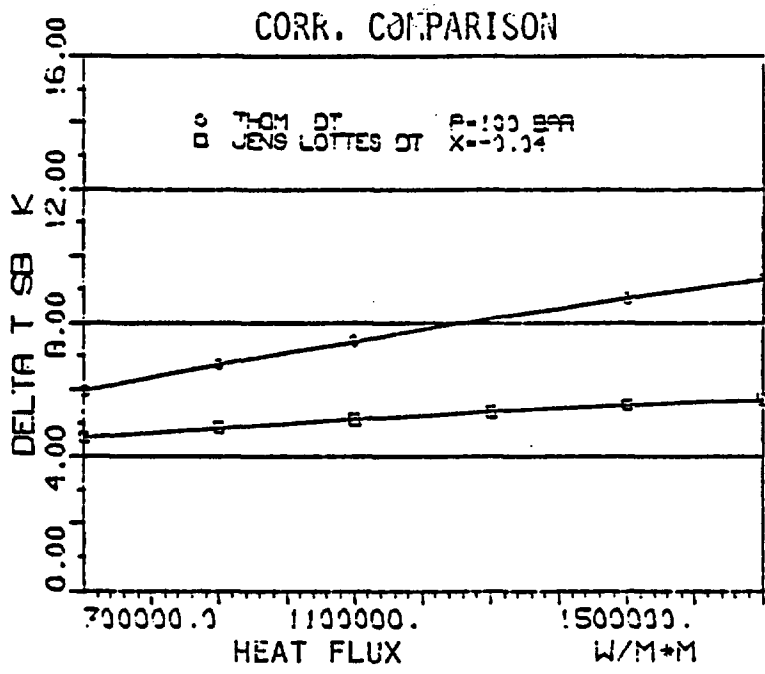


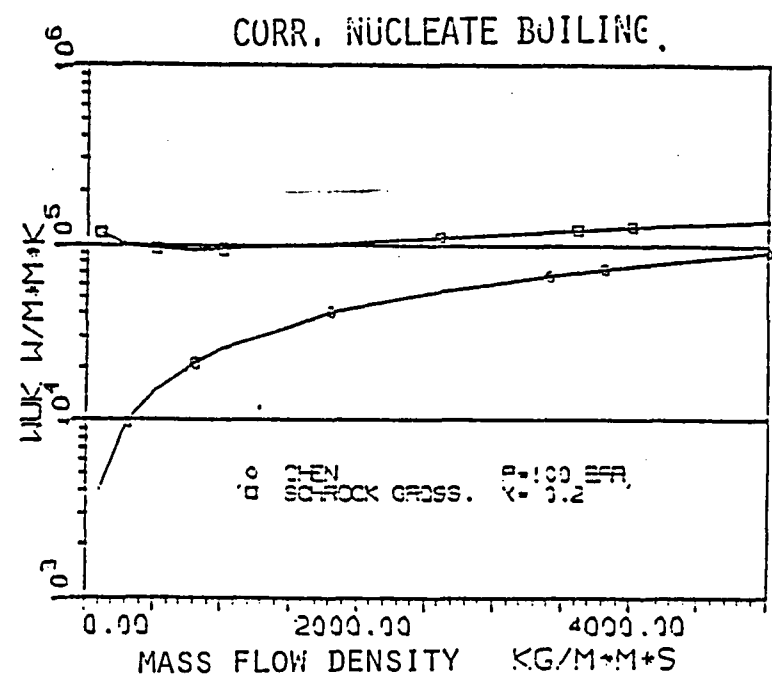
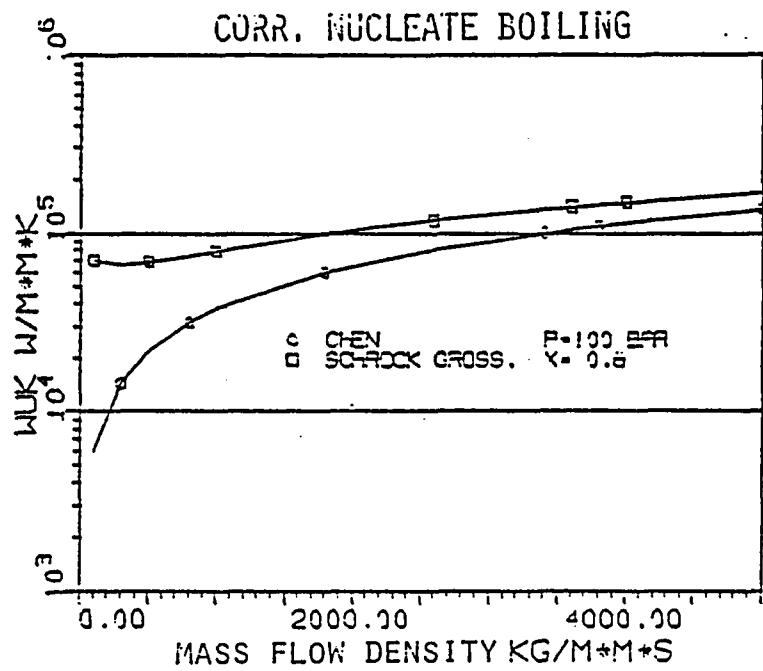




ATTACHMENT 4

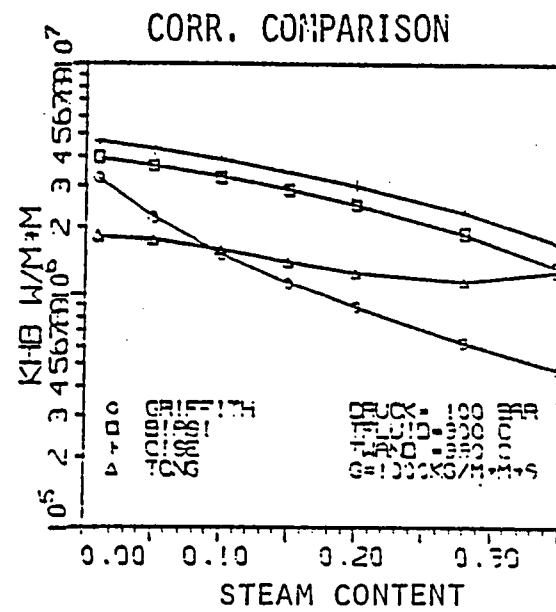
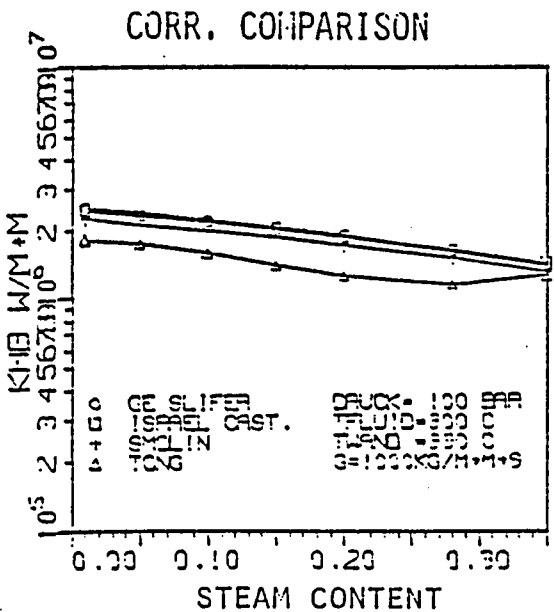
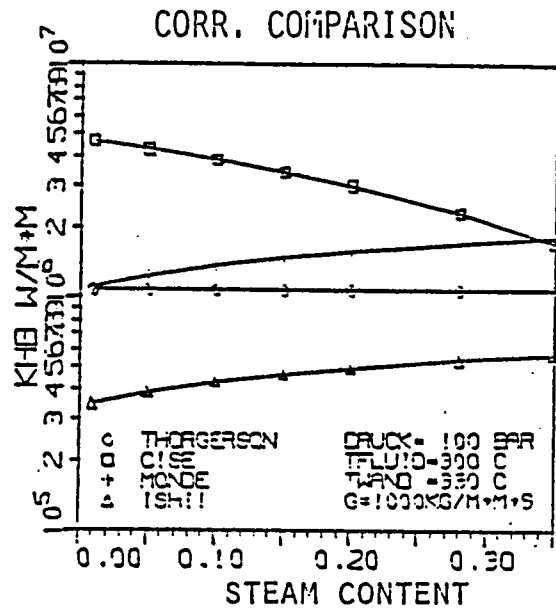
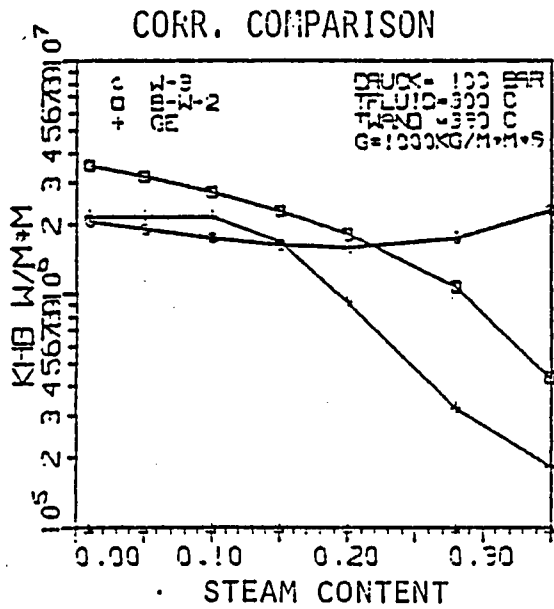
Comparison of the correlations for the calculation of the heat transfer coefficients and of the temperature difference in nucleate boiling



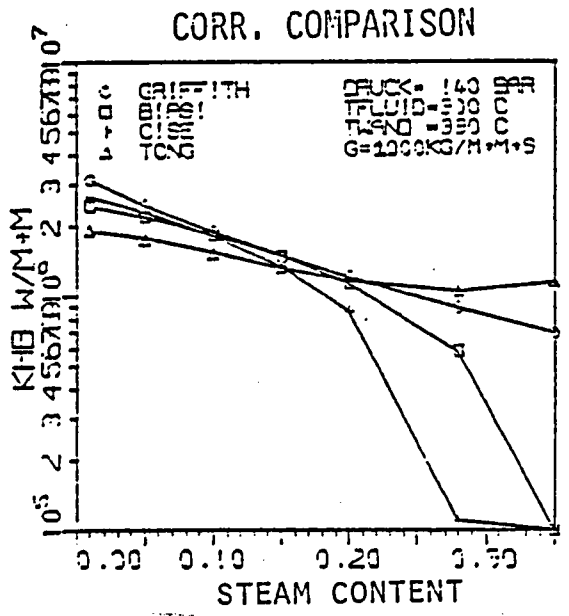
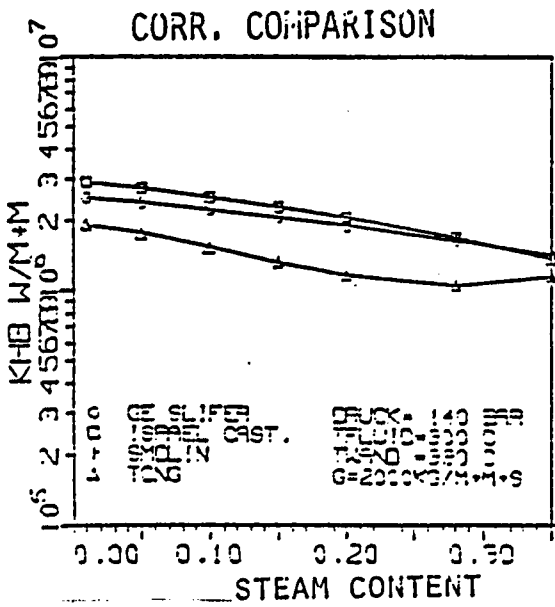
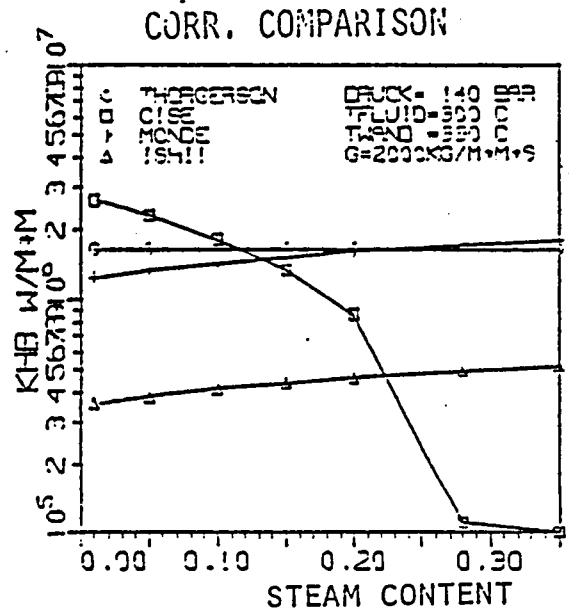
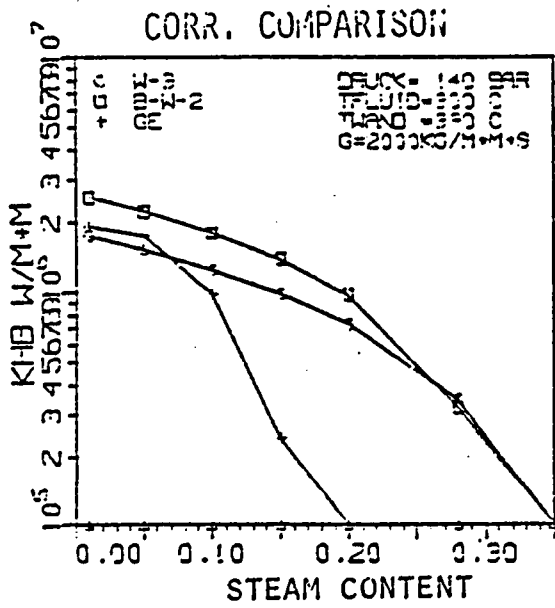


ATTACHMENT 5

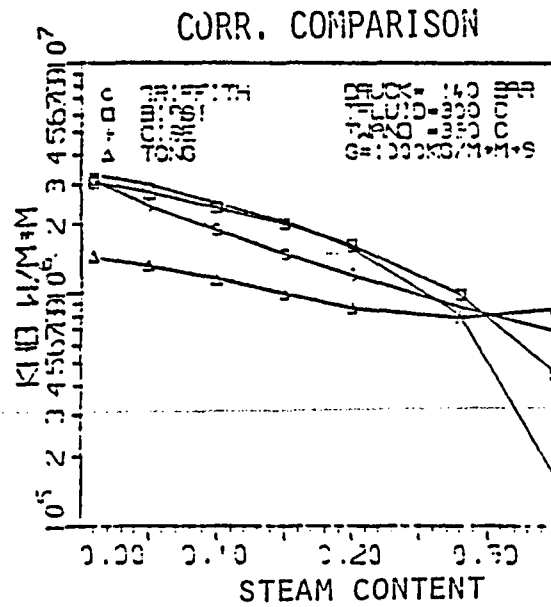
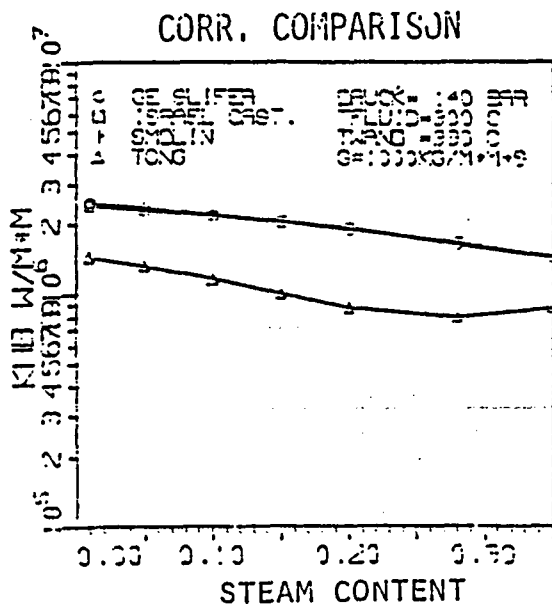
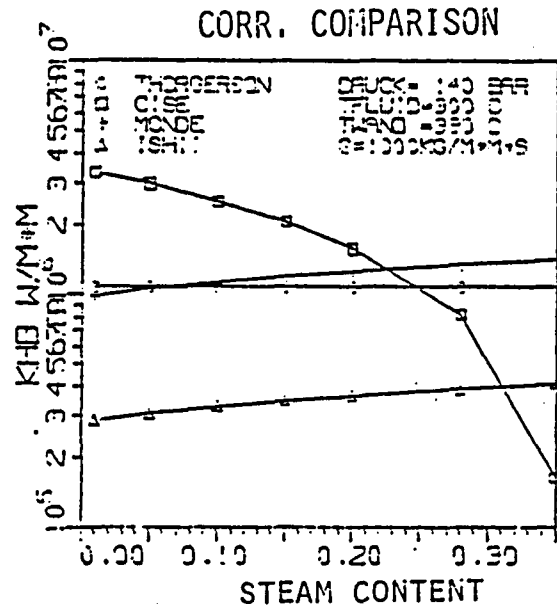
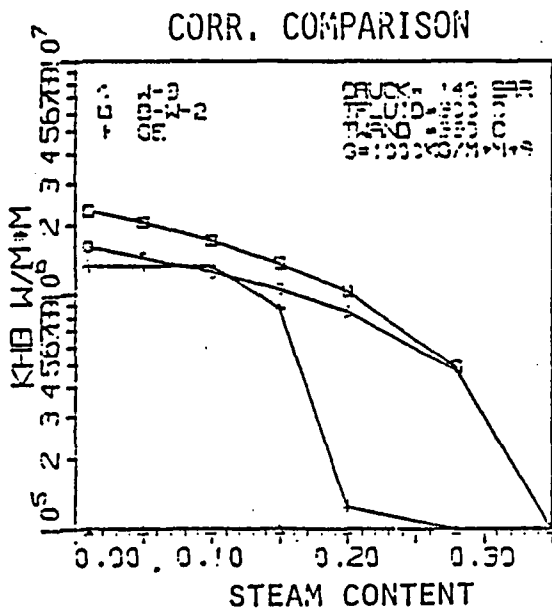
Comparison of the correlations for the calculation of the maximum critical heat flux



Inside legends: Druck = pressure
 Wand = wall



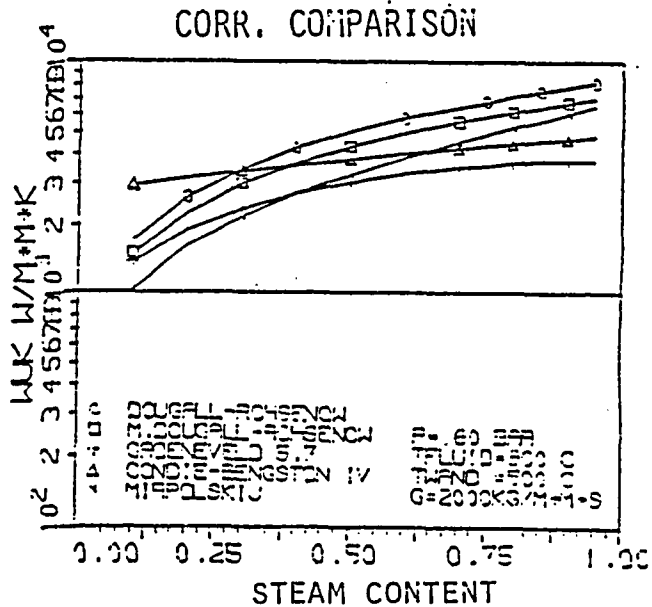
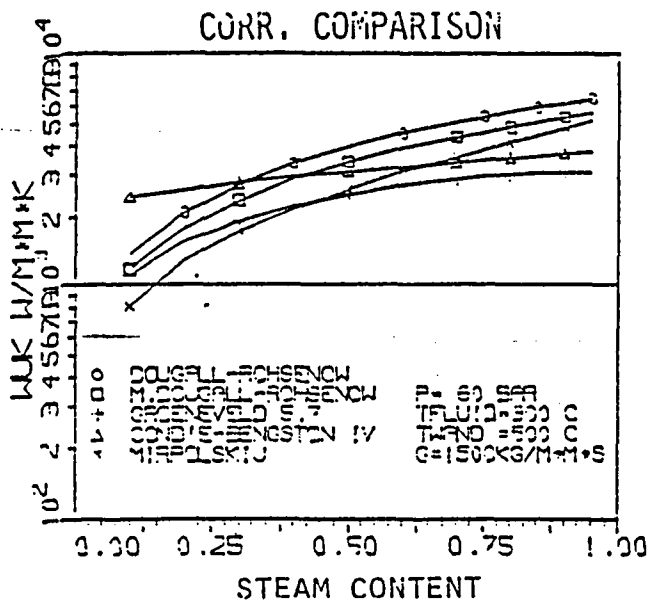
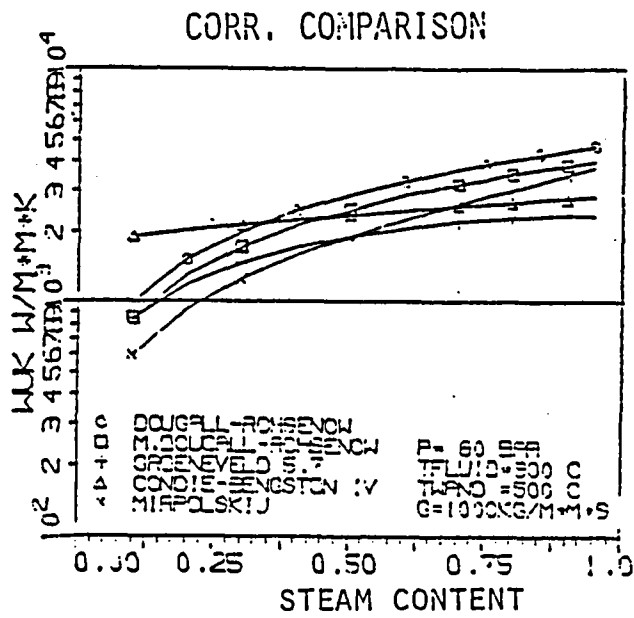
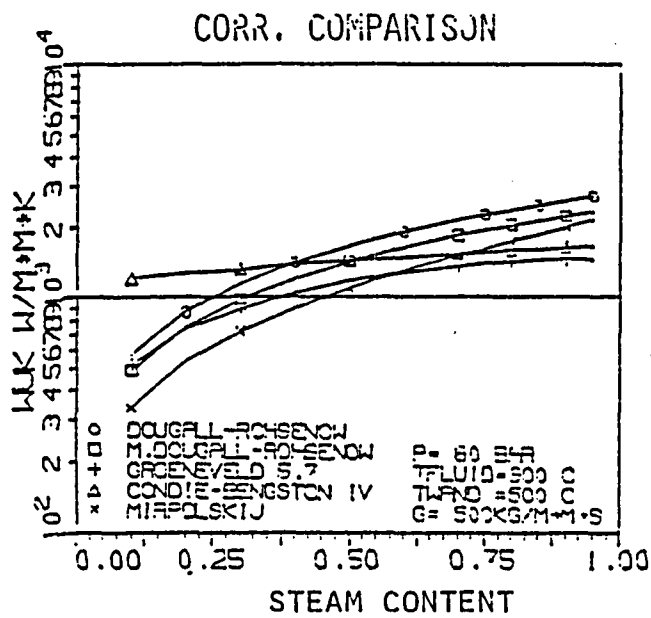
Inside legends: Druck = pressure
Wand = wall

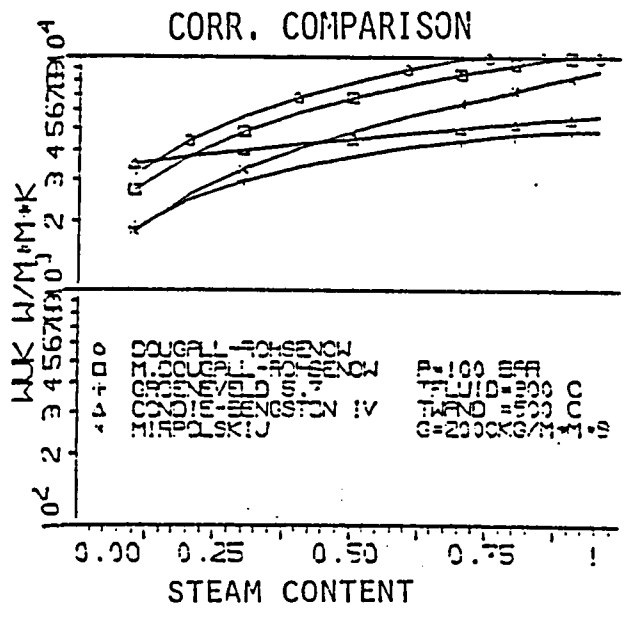
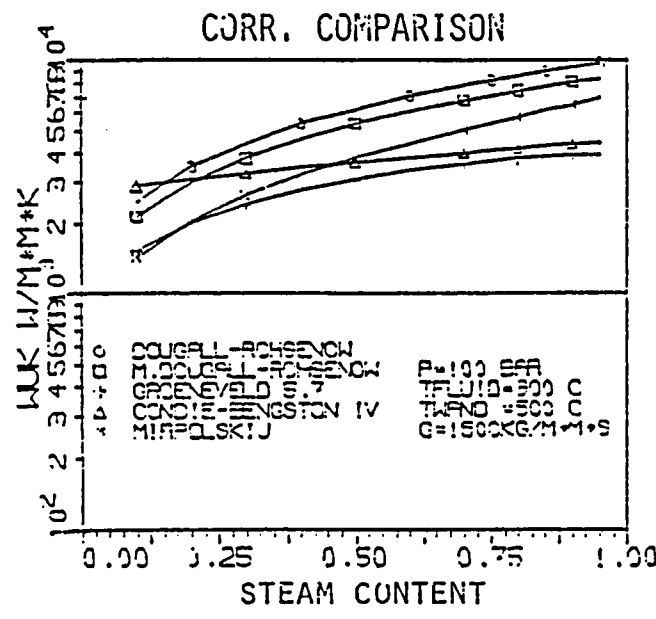
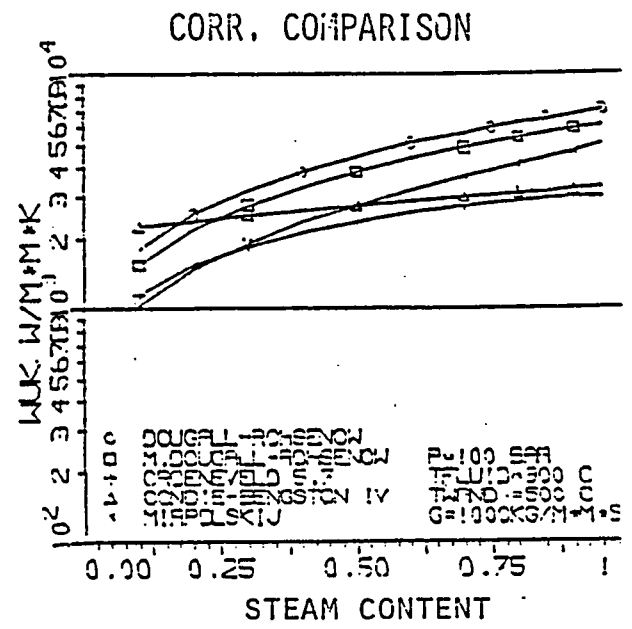
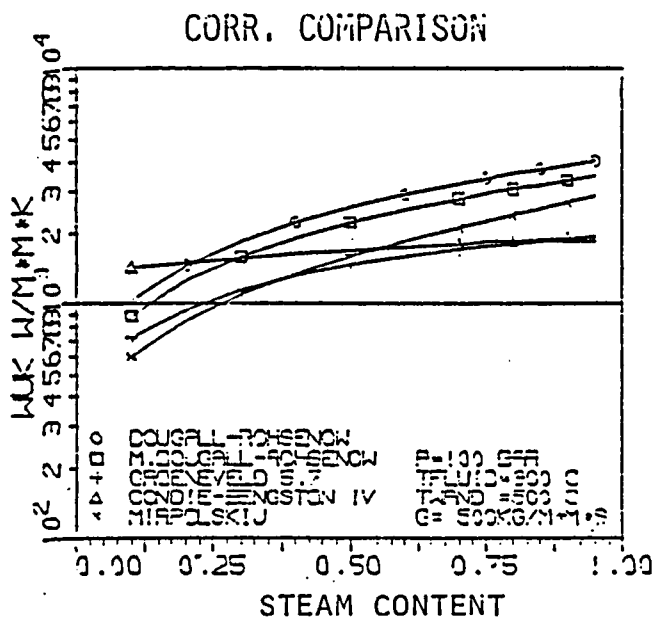


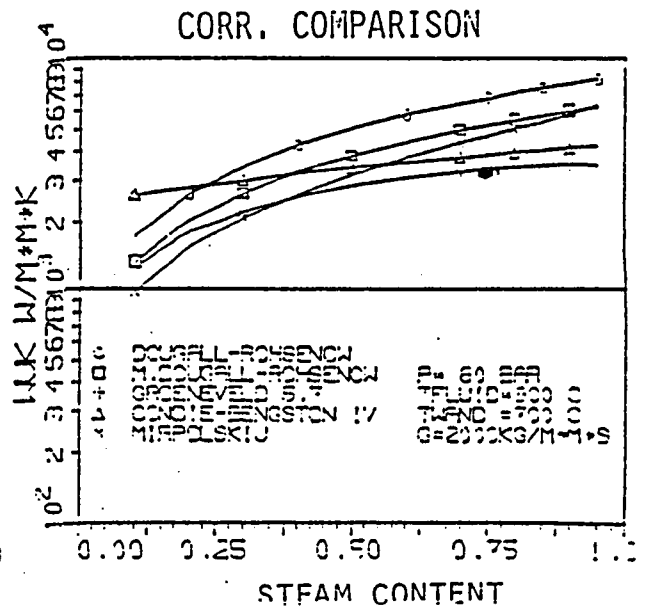
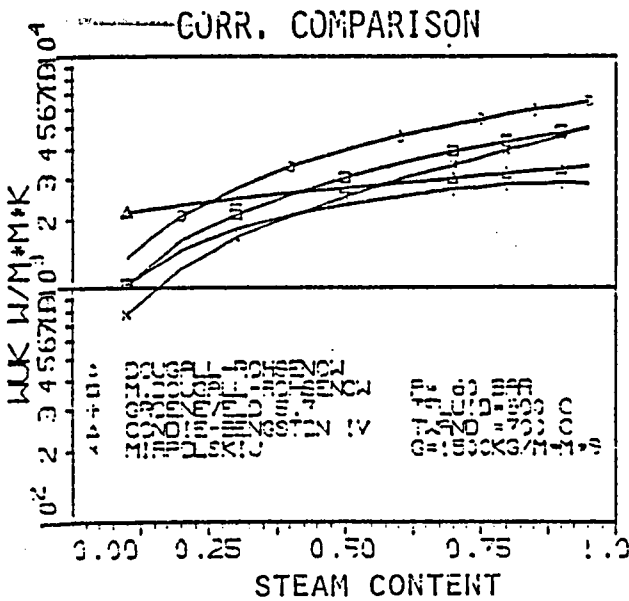
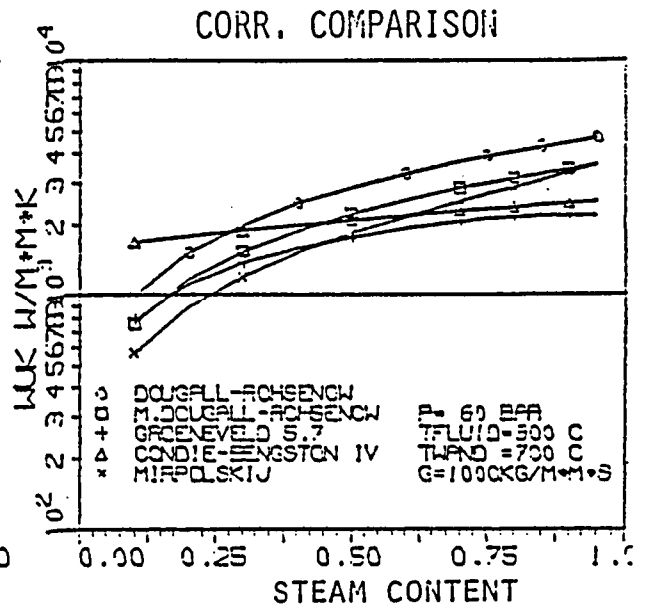
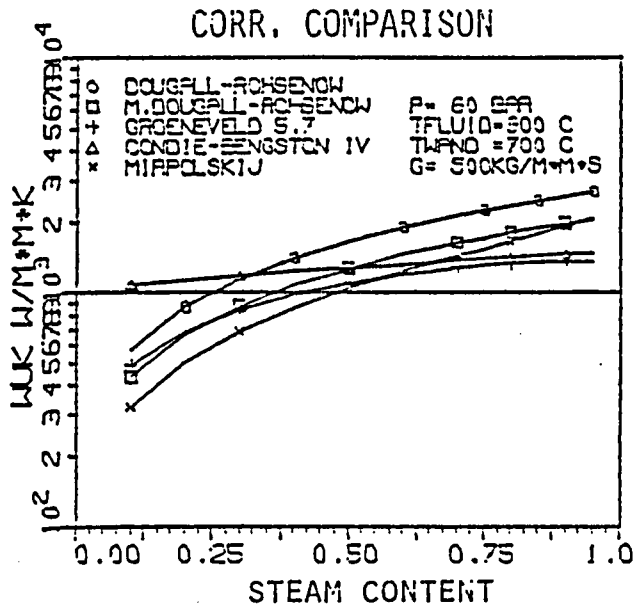
Inside legends: Druck = pressure
Wand = wall

ATTACHMENT 6

Comparison of the correlations for the calculation of the heat transfer coefficients in the steam-droplets cooling regime



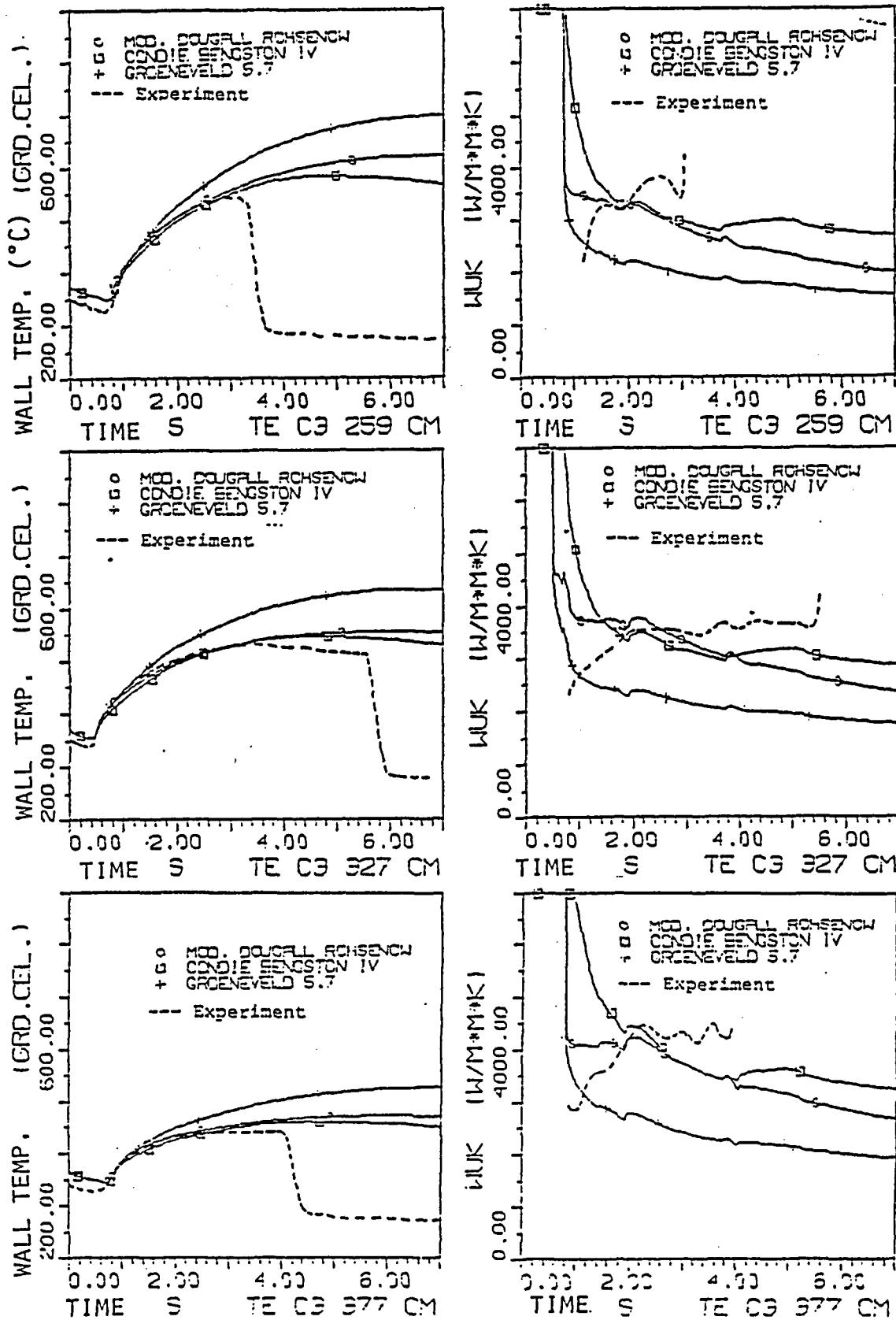




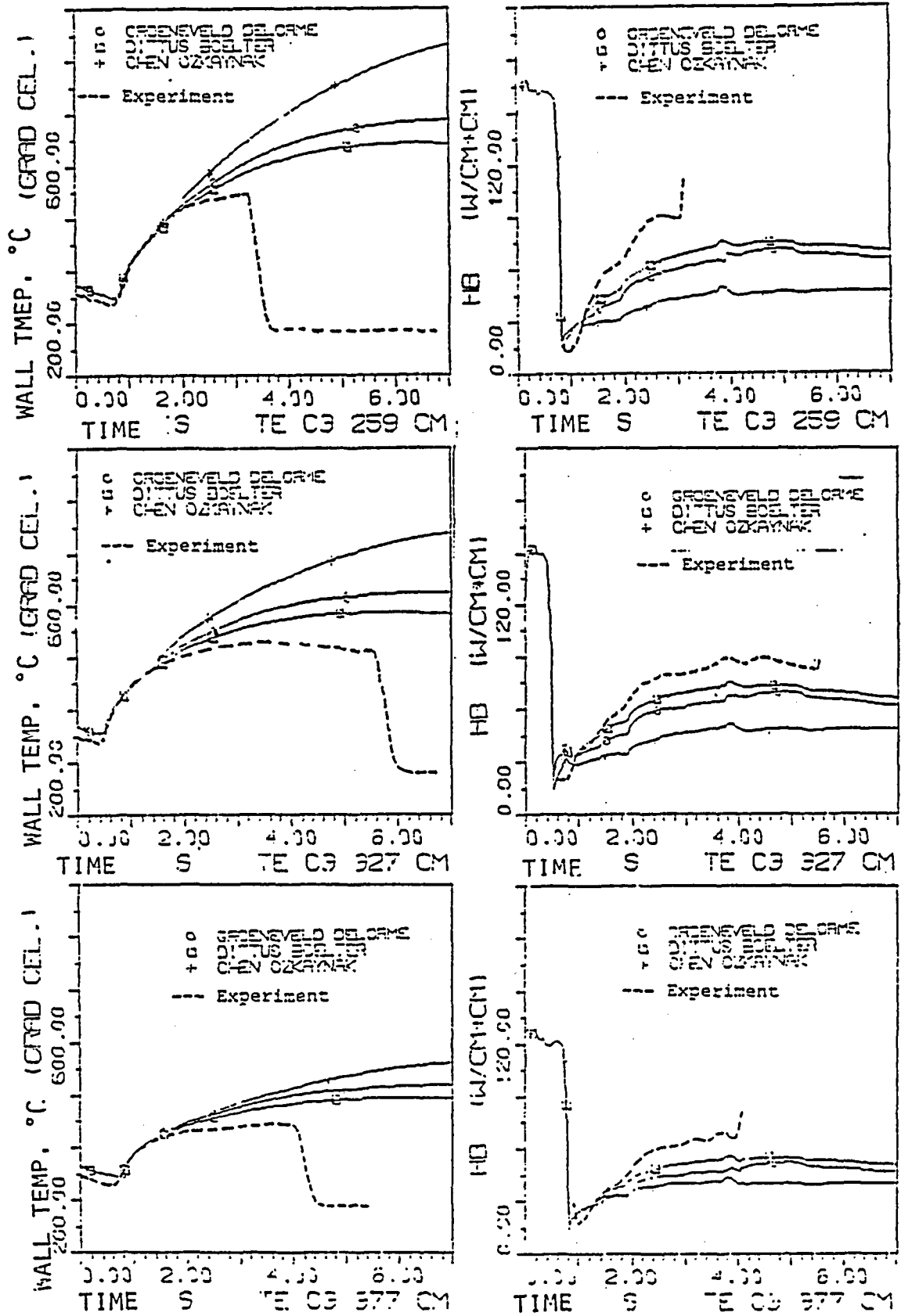
ATTACHMENT 7

Test parameters and results from the recalculation - Test DNB1 -

Comparison of the equilibrium correlations



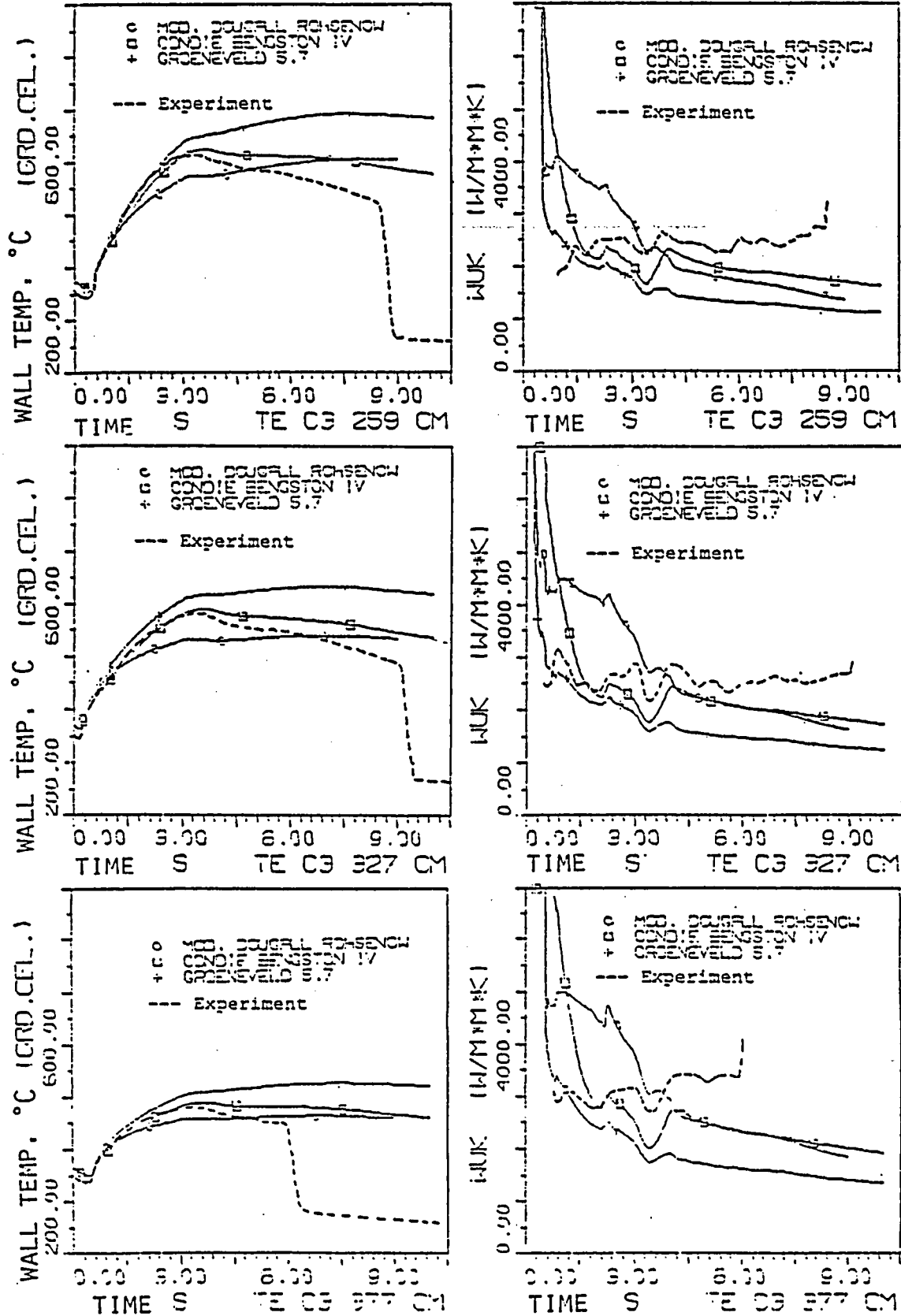
Comparison of the non-equilibrium correlations



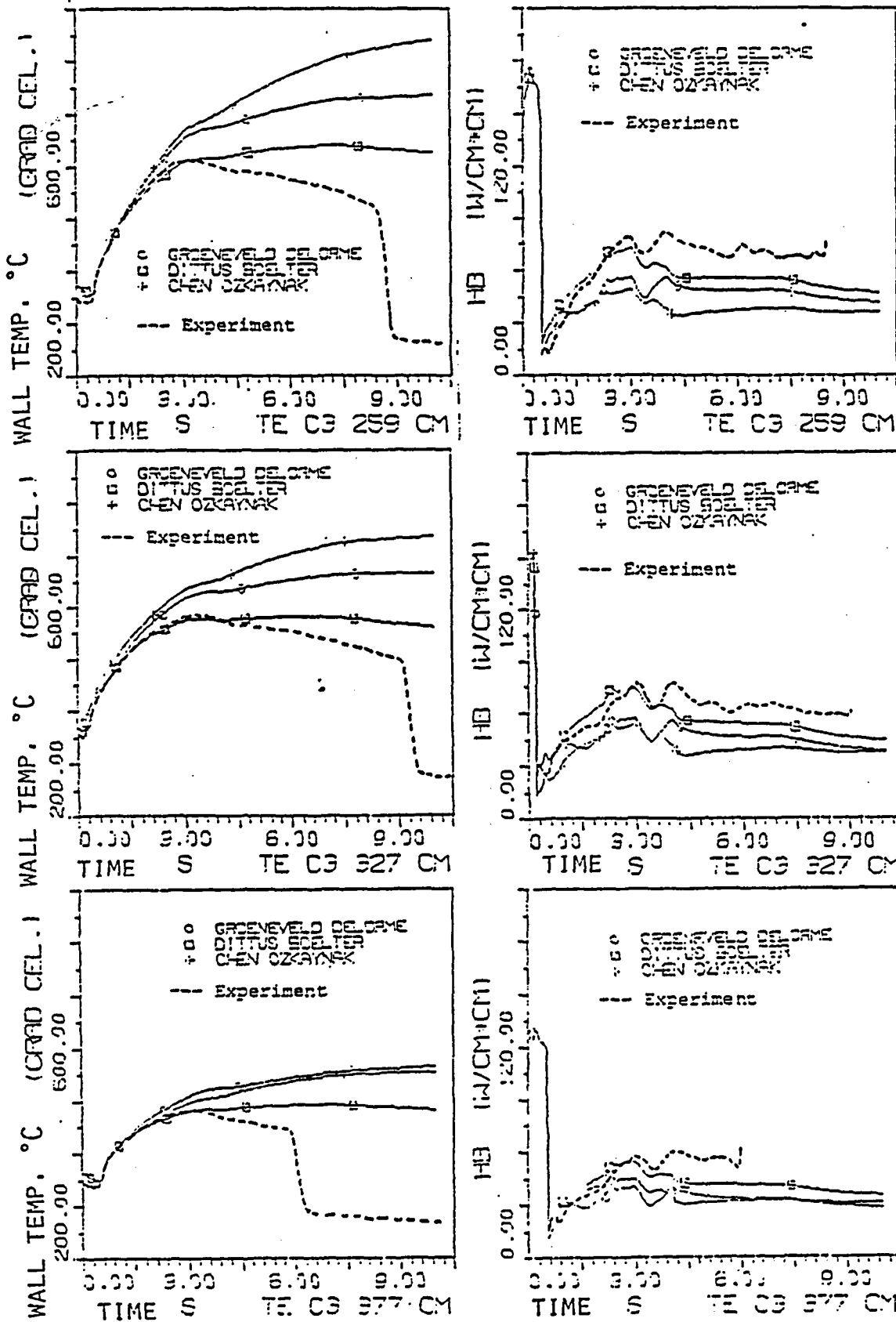
ATTACHMENT 8

Test parameters and results from the recalculation - Test DNB3 -

Comparison of the equilibrium correlations



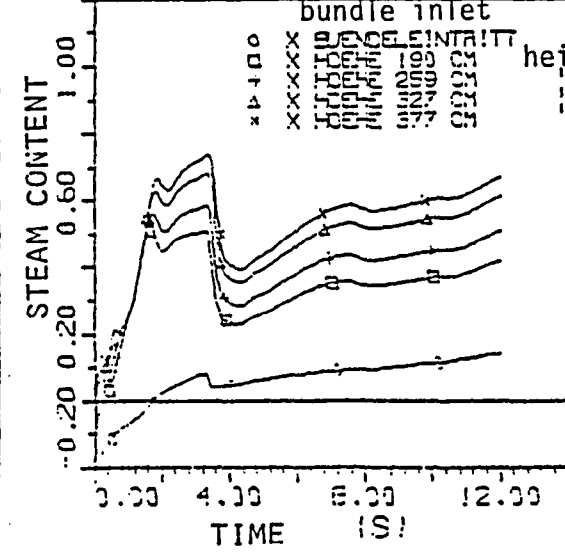
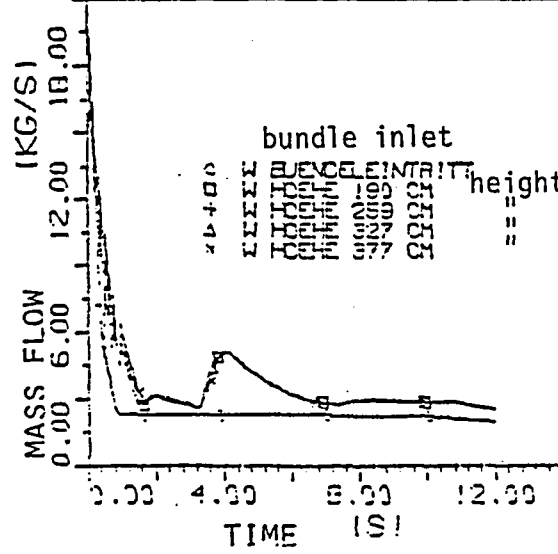
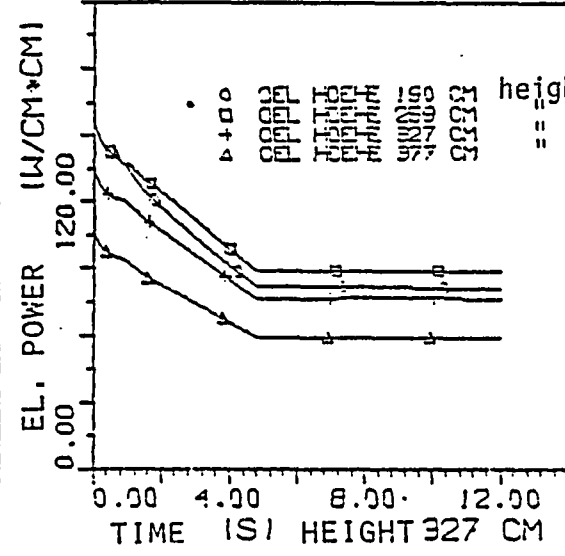
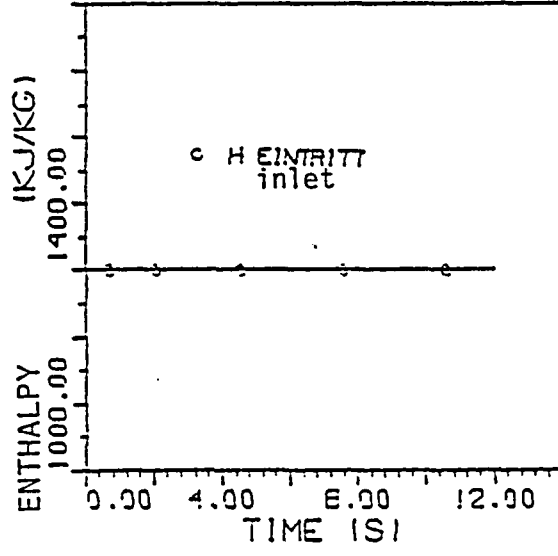
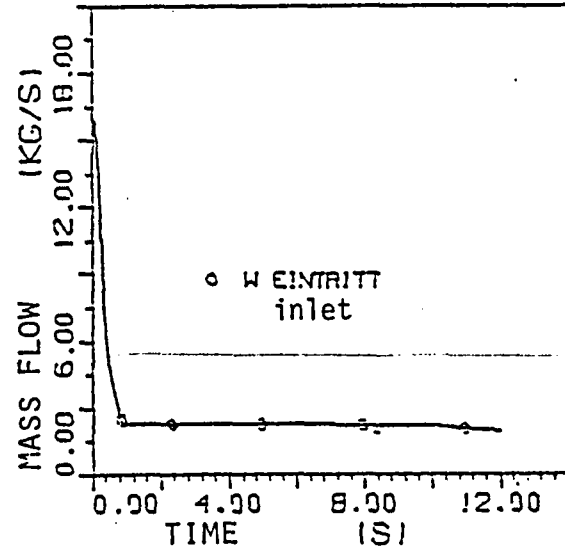
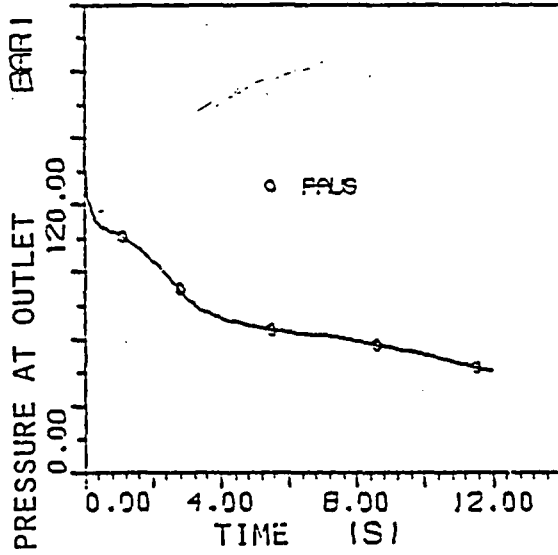
Comparison of the non-equilibrium correlations



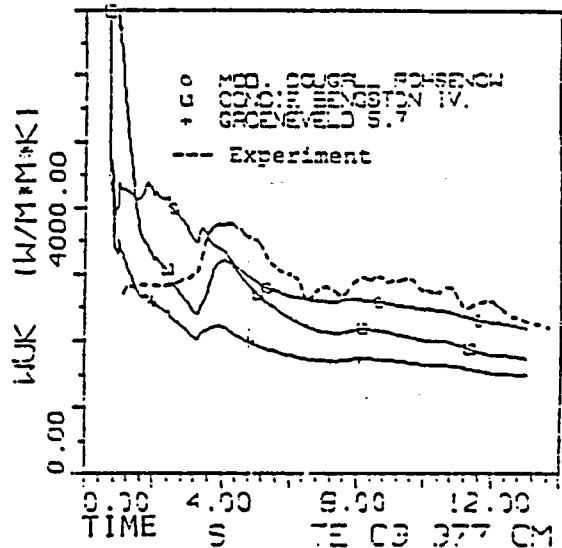
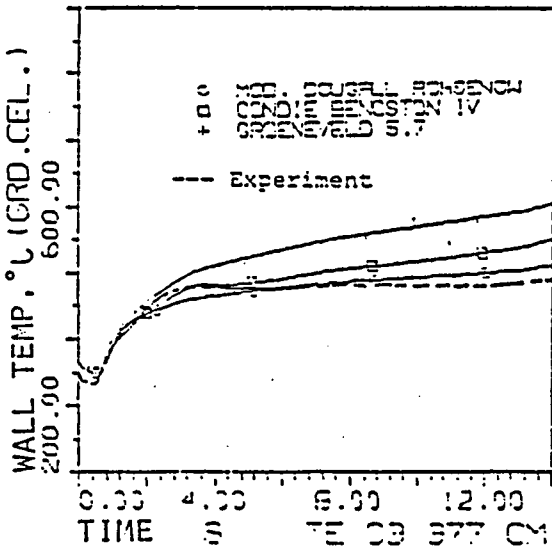
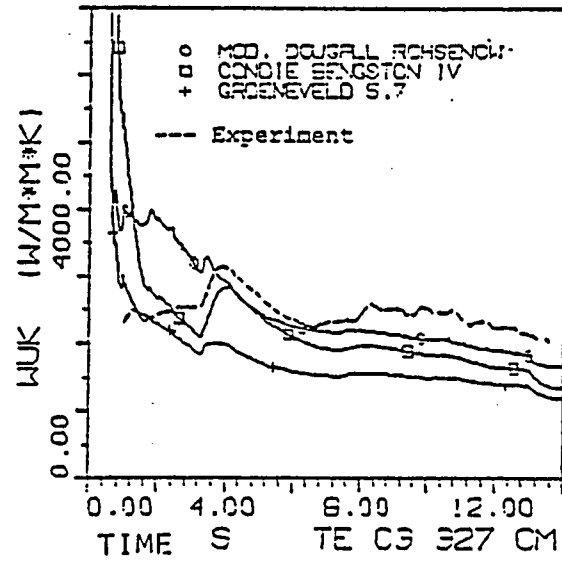
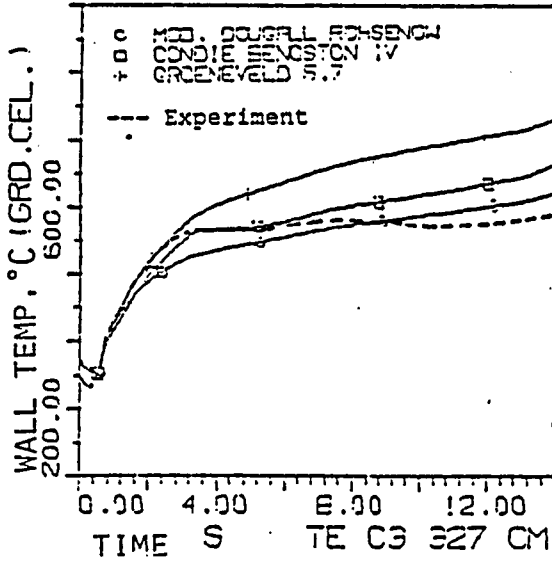
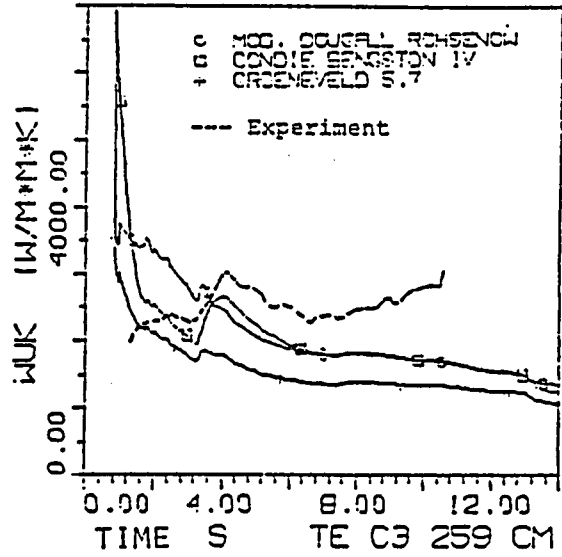
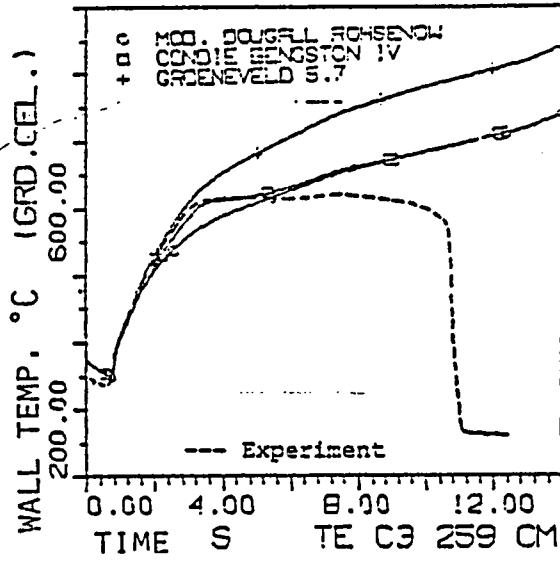
ATTACHMENT 9

Test parameters and results from the recalculation - test DNB9 -

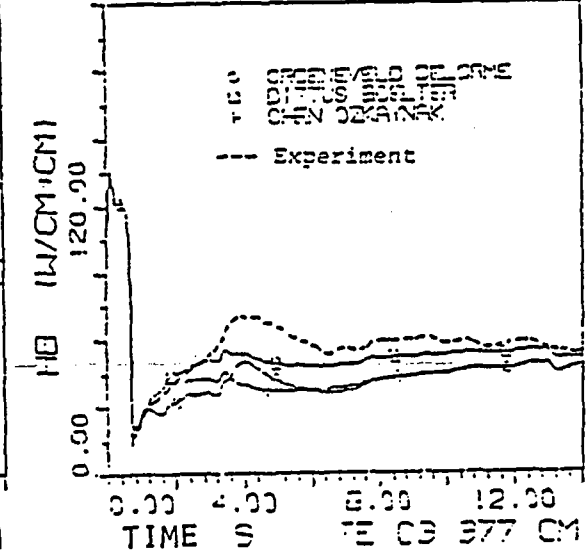
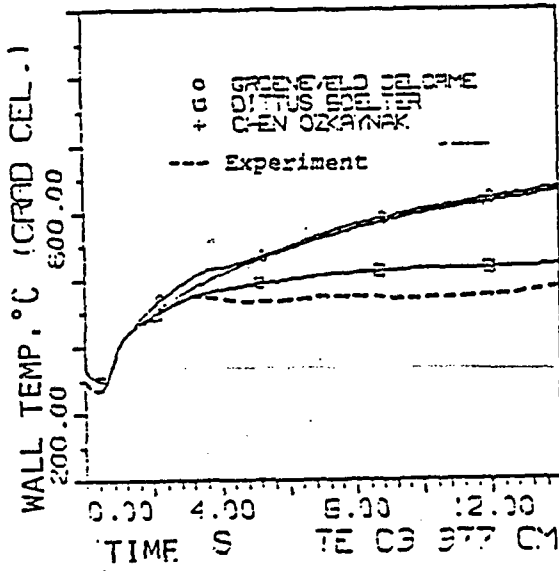
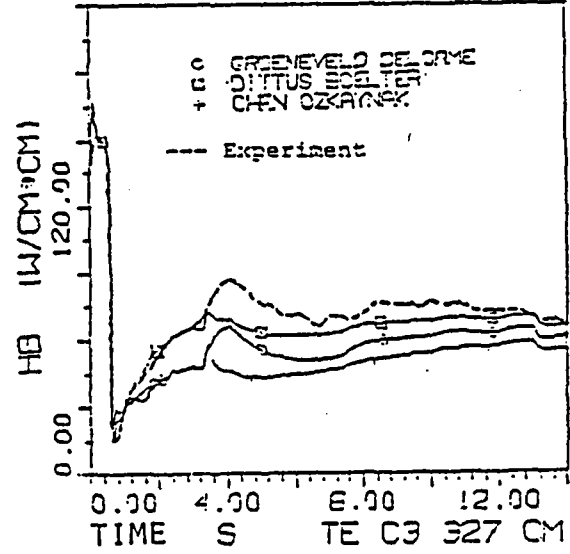
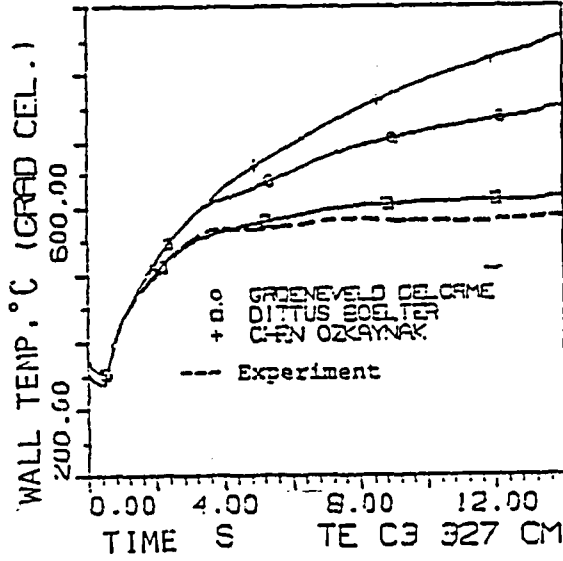
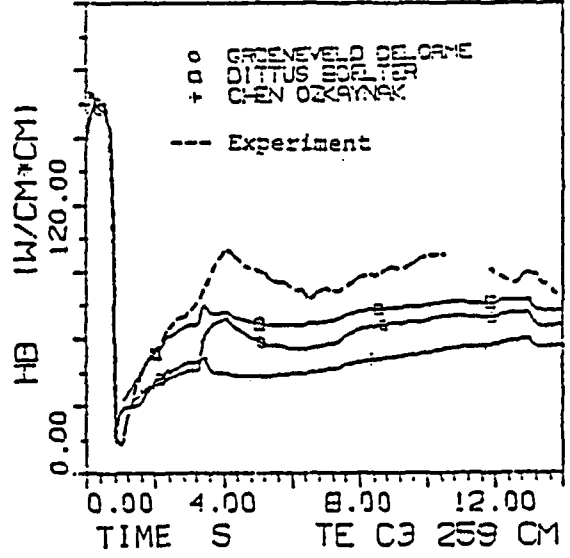
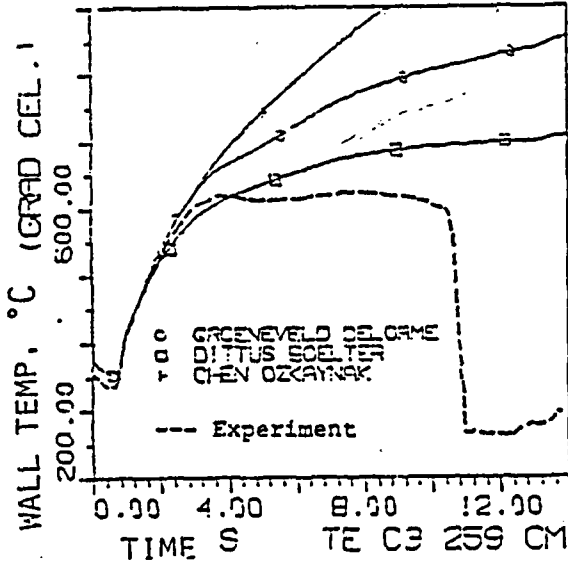
Test parameters and local values of the mass flow and steam content



Comparison of the equilibrium correlations



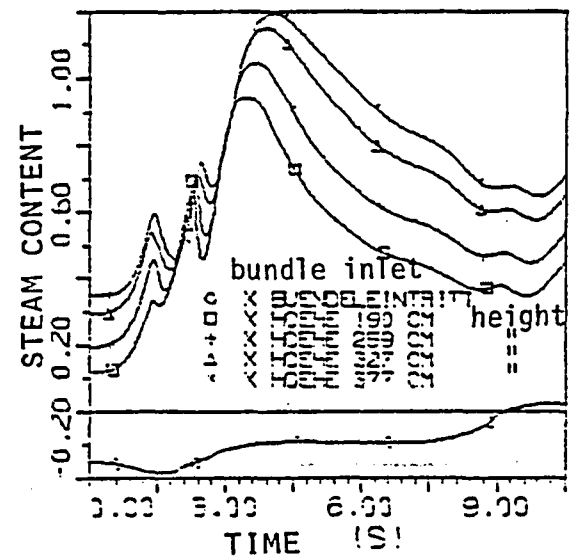
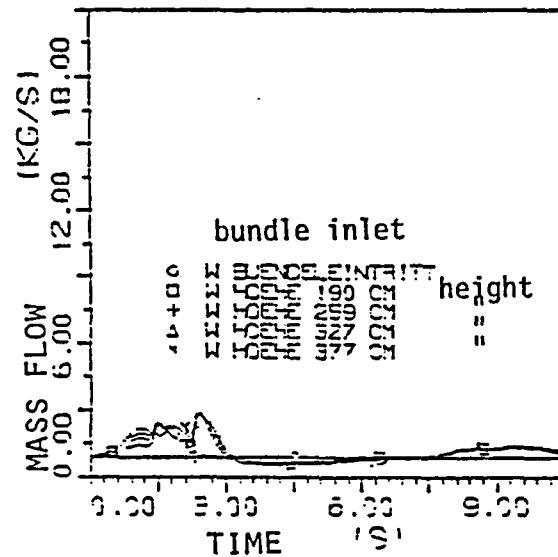
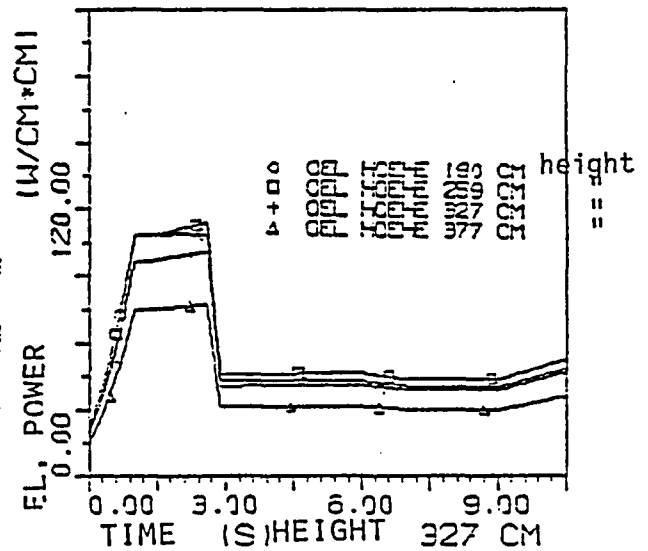
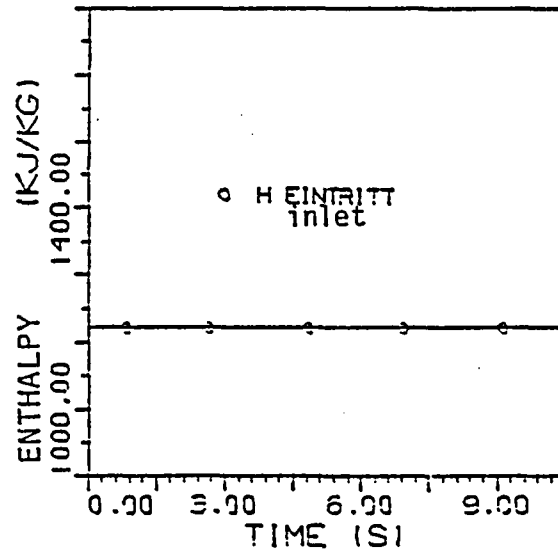
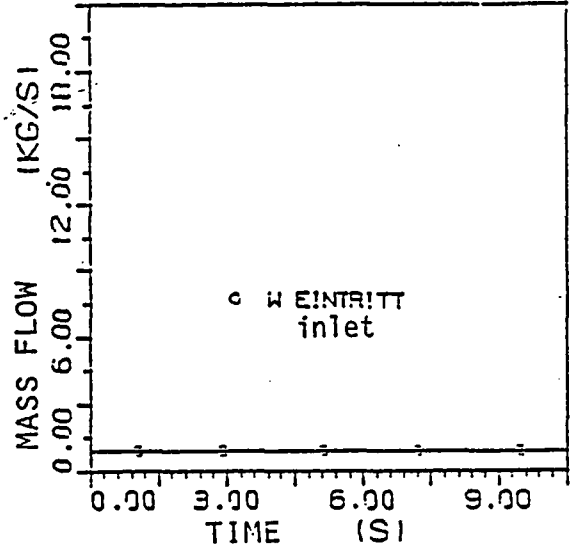
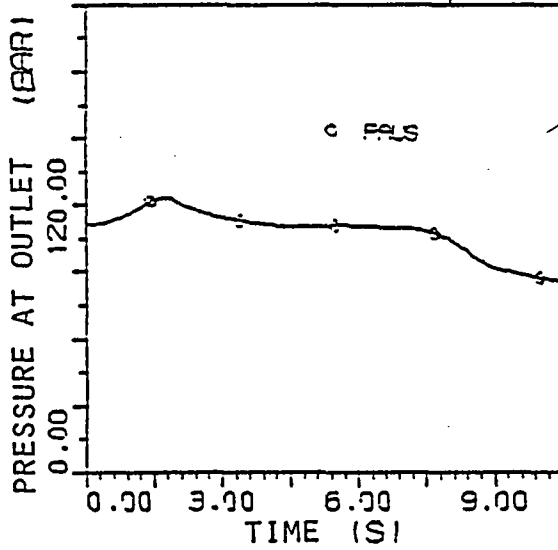
Comparison of the non-equilibrium correlations



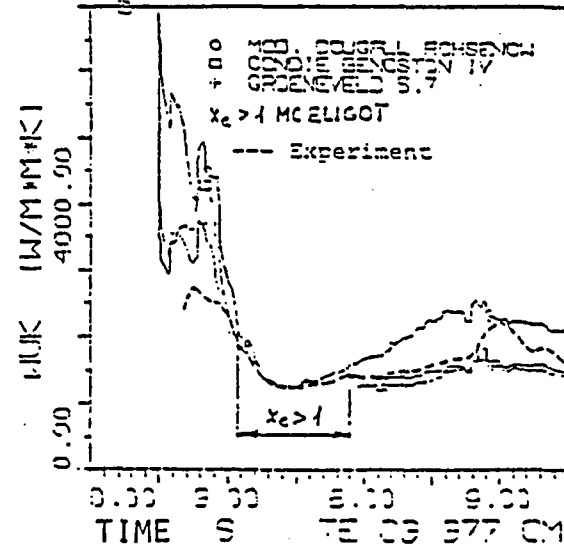
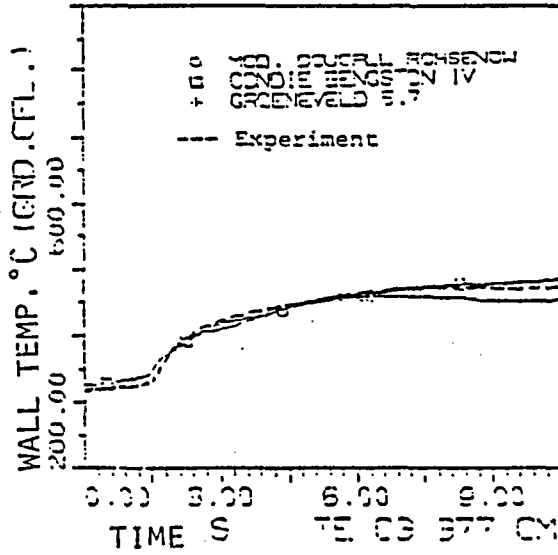
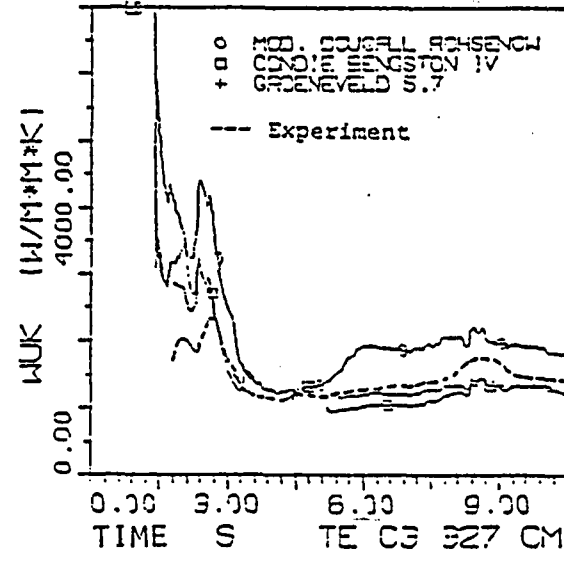
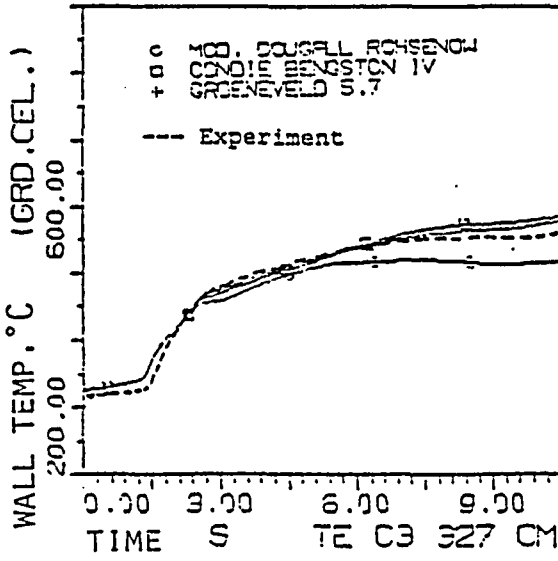
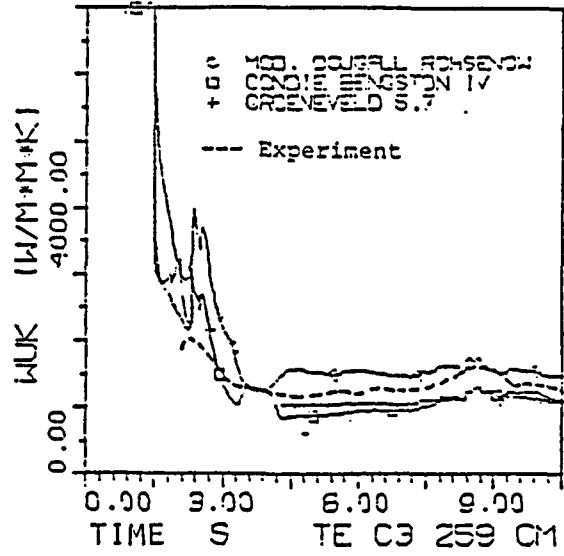
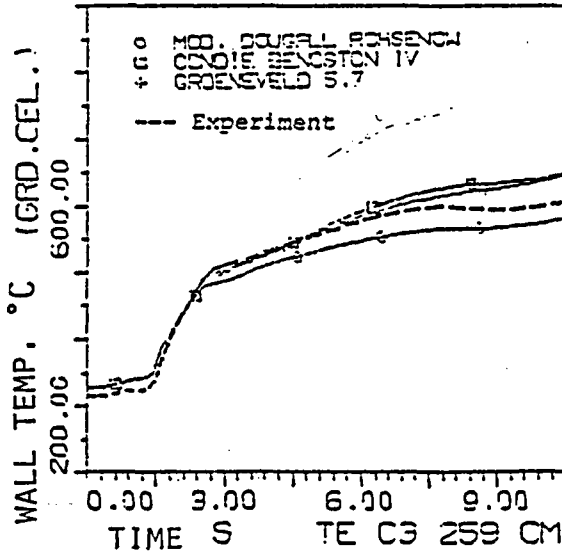
ATTACHMENT 10

Test parameters and results from the recalculation - Test PDNB11 -

Test parameters and local values of the mass flow and steam content



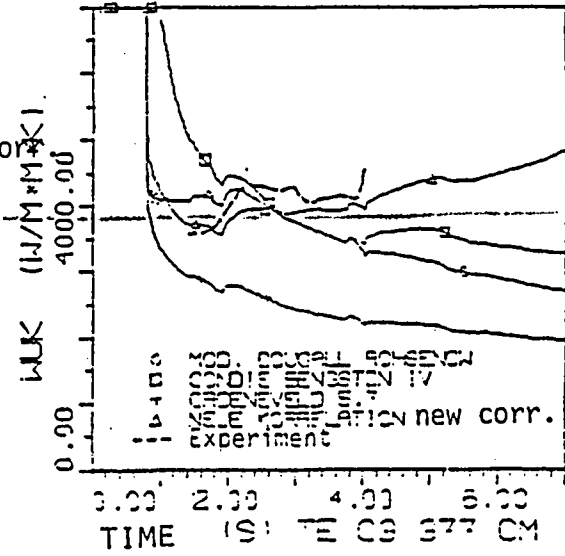
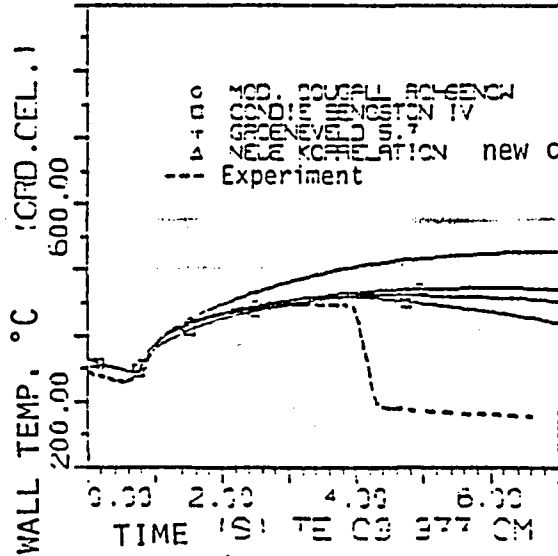
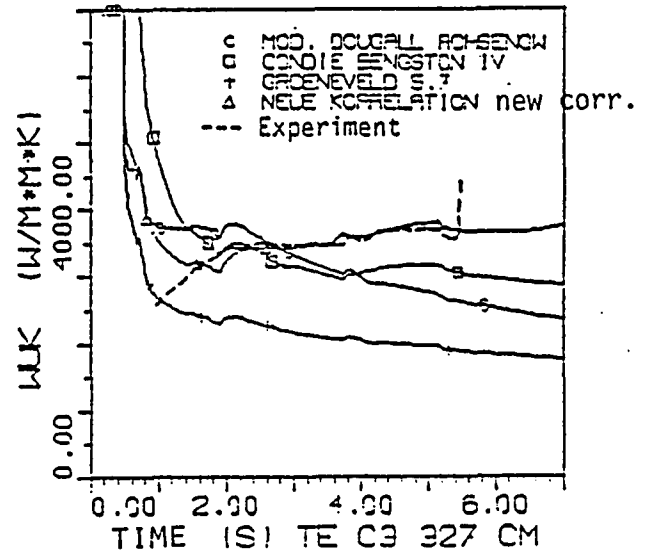
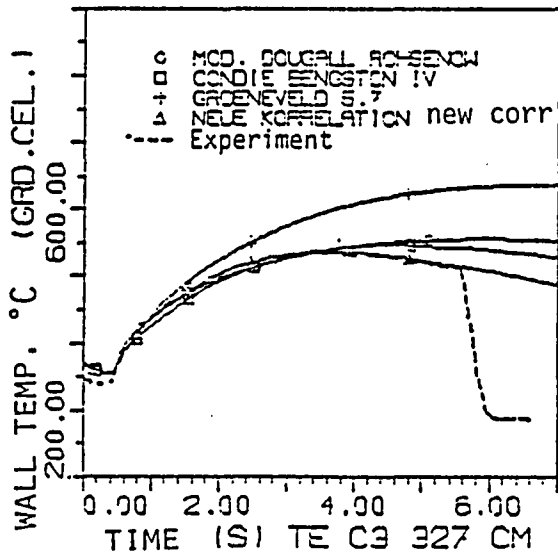
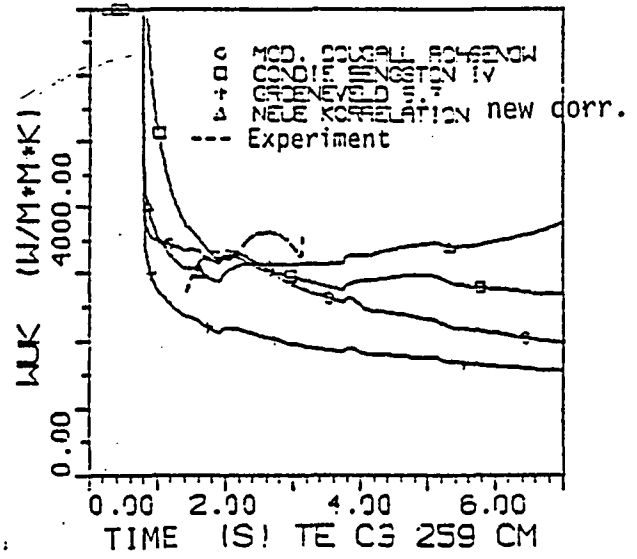
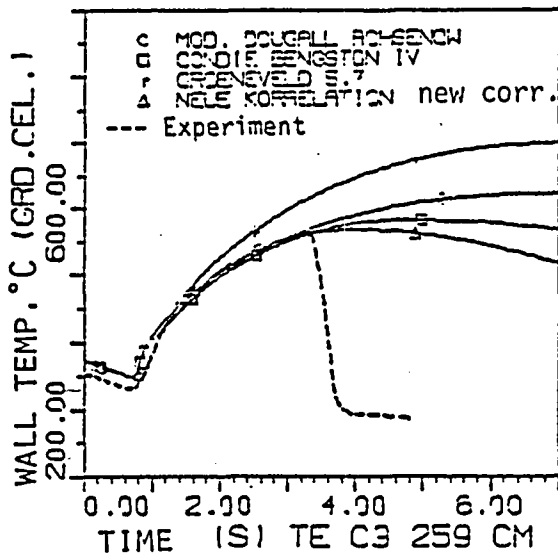
Comparison of the equilibrium correlaticns



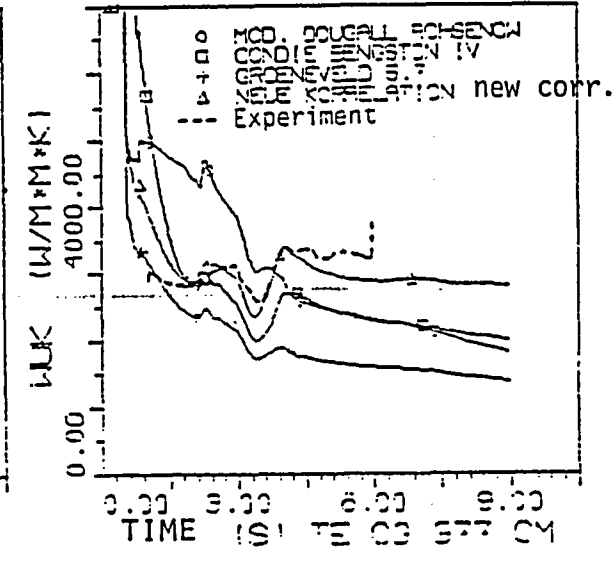
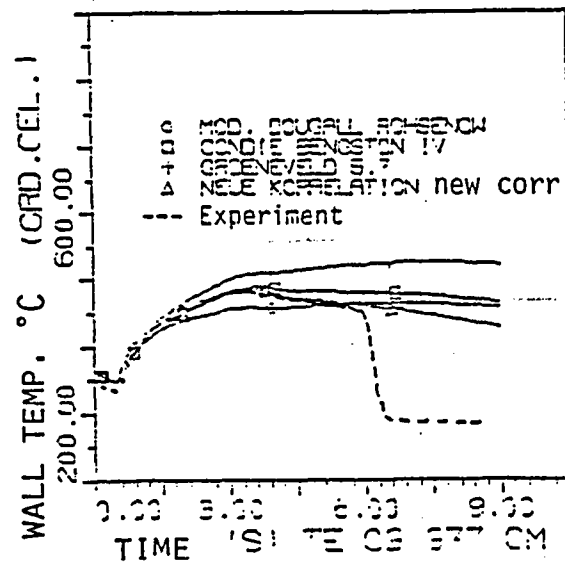
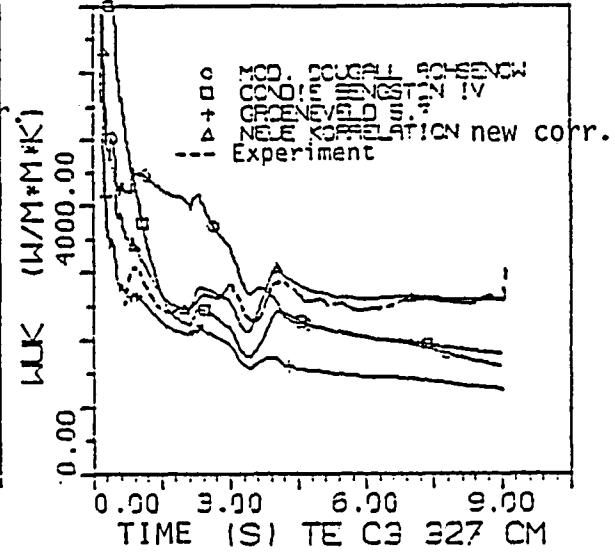
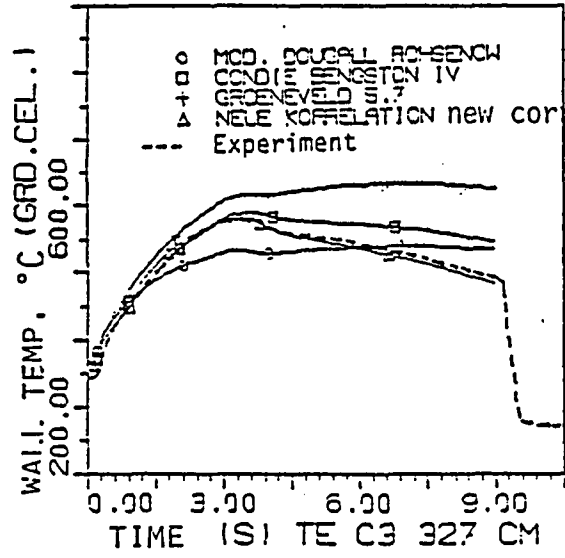
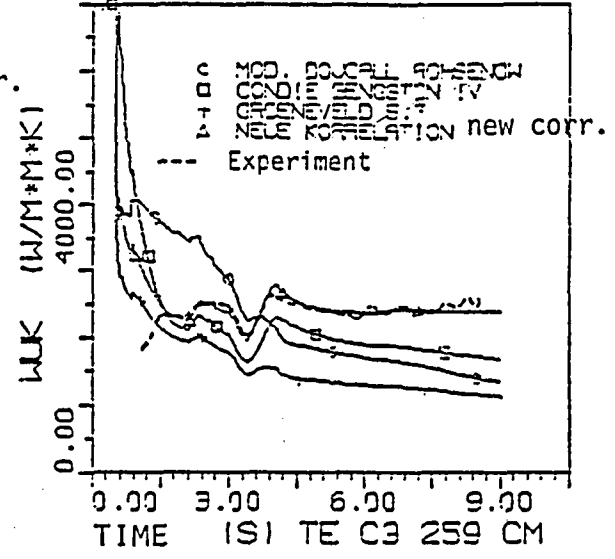
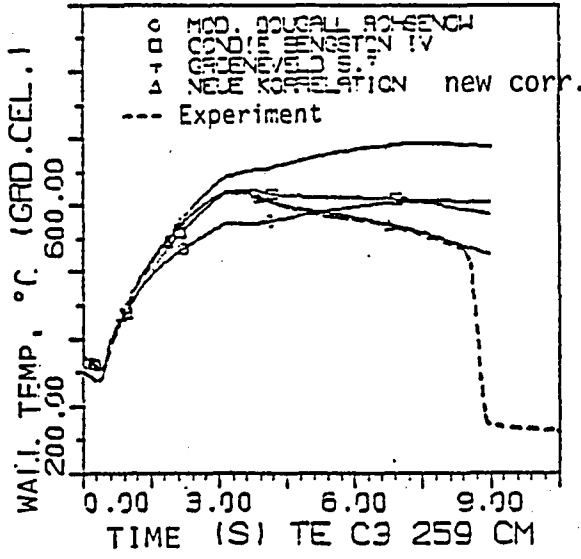
ATTACHMENT 11

Comparison of the new correlations with the equilibrium correlations and with the measured values

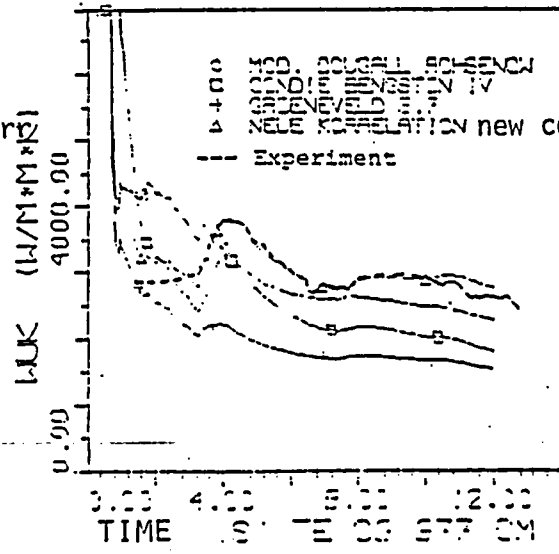
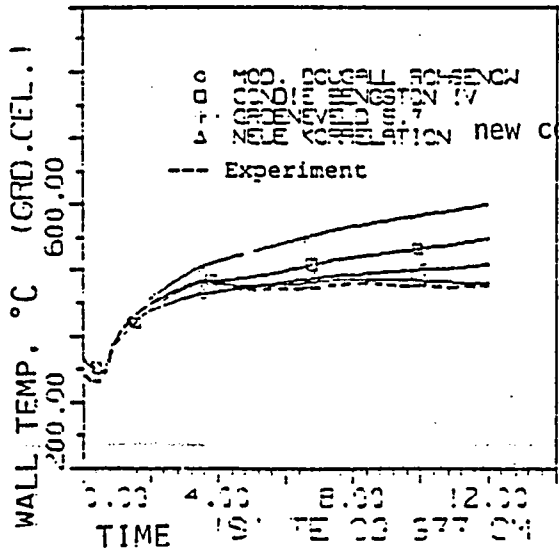
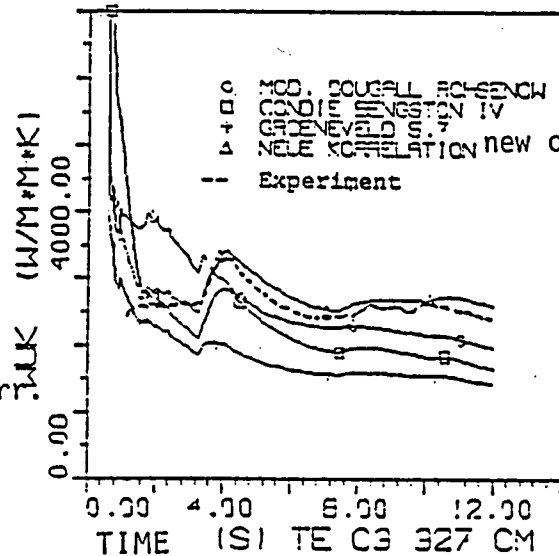
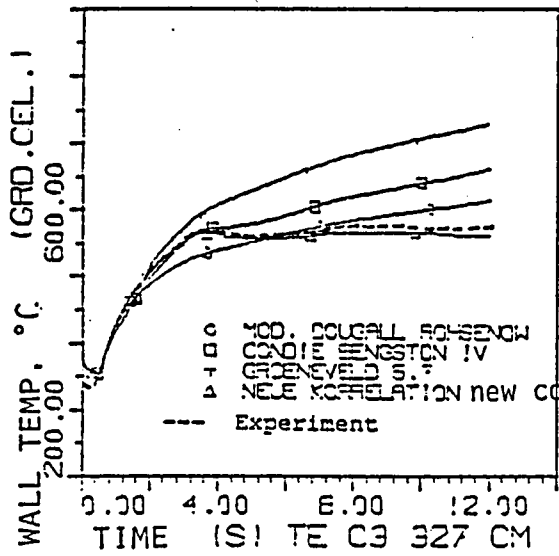
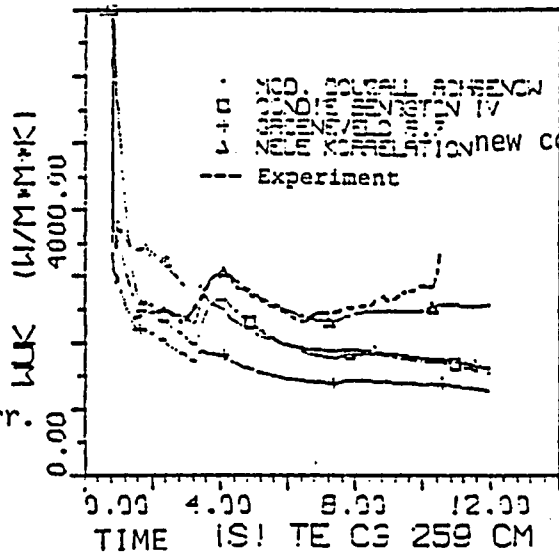
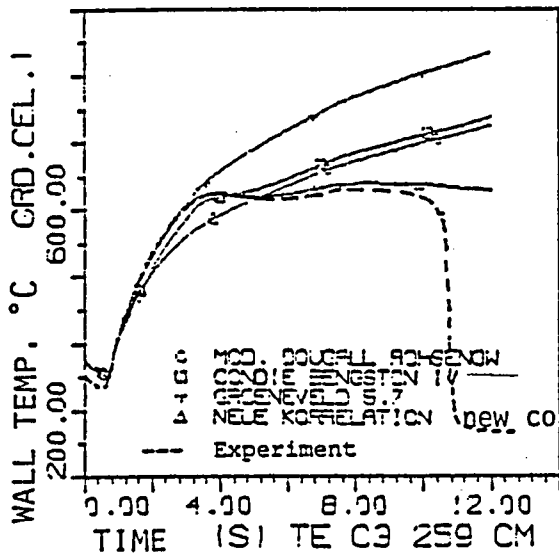
Test DNB1



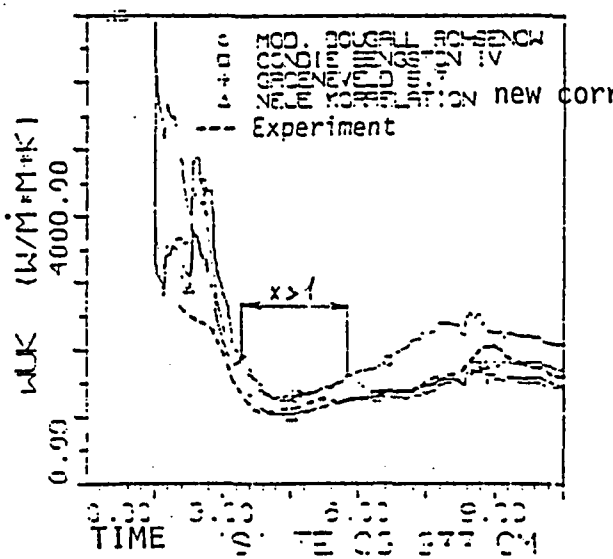
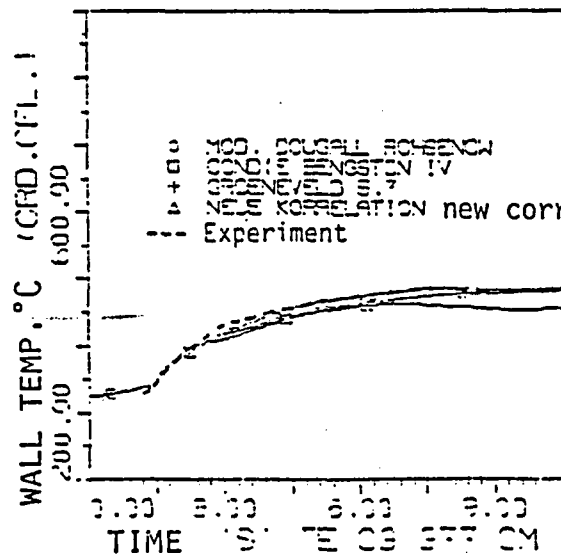
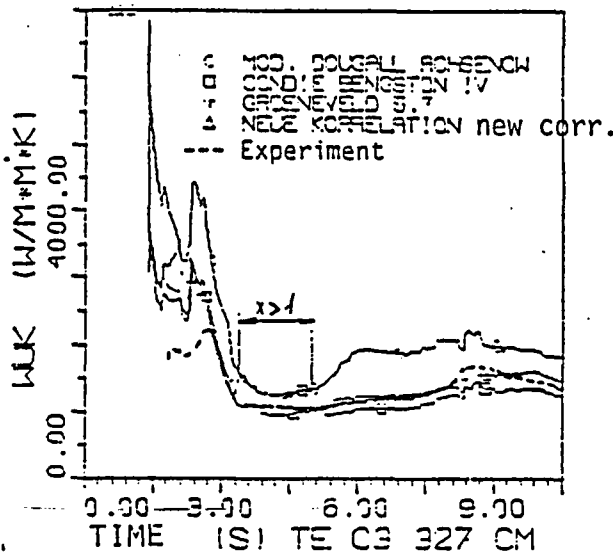
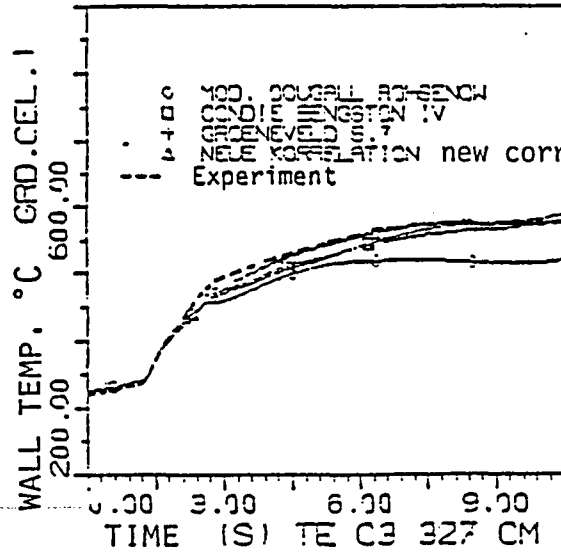
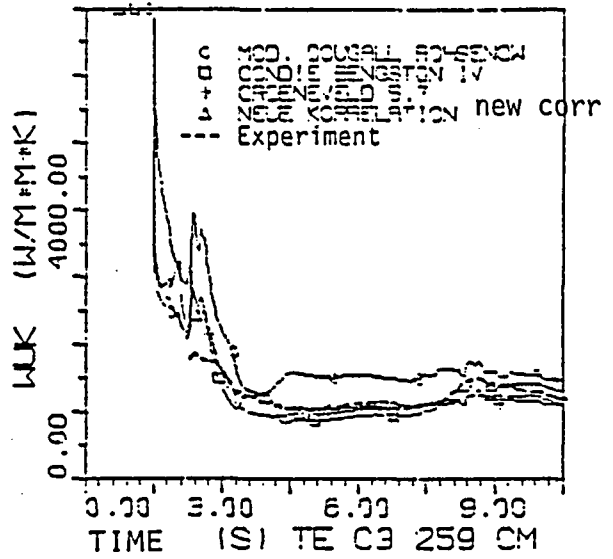
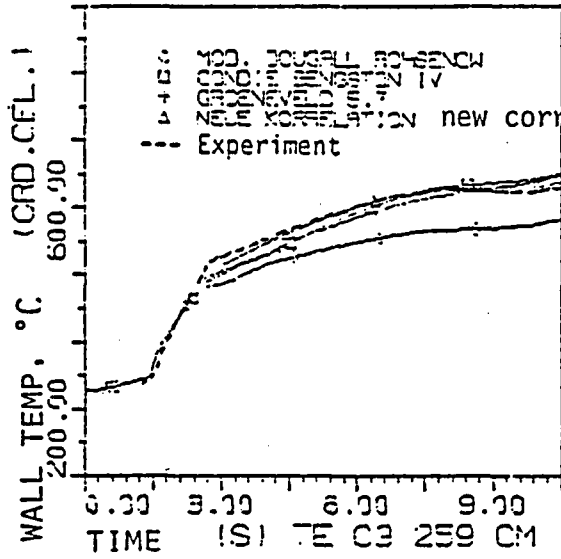
Test DNB3



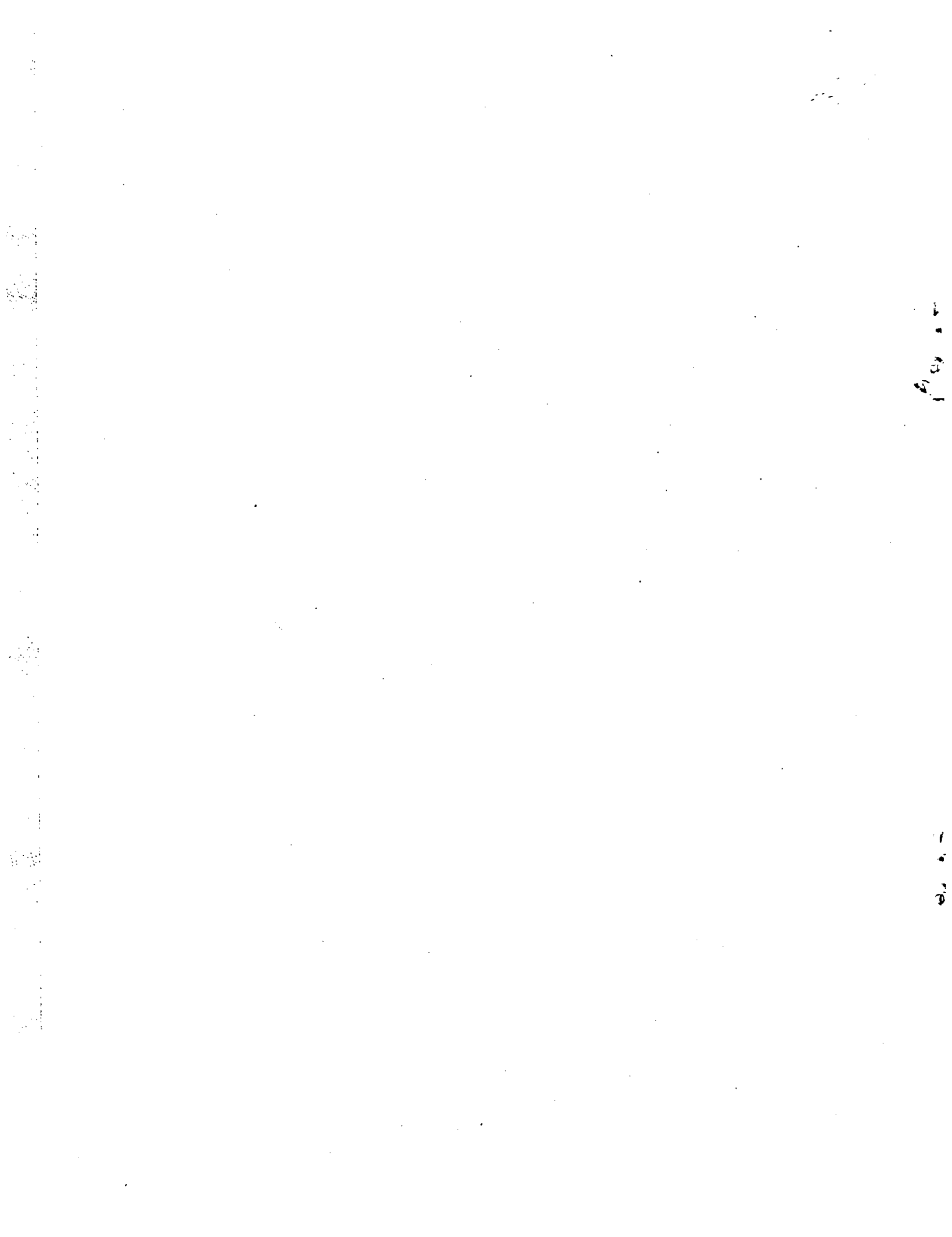
Test DNB9



Test PDNB11



NRC FORM 335 (2-84) NRCM 1102, 3201, 3202		U.S. NUCLEAR REGULATORY COMMISSION		1. REPORT NUMBER (Assigned by TIDC, add Vol. No., if any)	
BIBLIOGRAPHIC DATA SHEET				NUREG/IA-0002	
SEE INSTRUCTIONS ON THE REVERSE.				3. LEAVE BLANK	
2. TITLE AND SUBTITLE				4. DATE REPORT COMPLETED	
Heat Transfer Processes During Intermediate and Large Break LOCAs.				MONTH YEAR	
				March 1982	
5. AUTHOR(S)				6. DATE REPORT ISSUED	
I. Voitek				MONTH YEAR	
				September 1986	
7. PERFORMING ORGANIZATION NAME AND MAILING ADDRESS (Include Zip Code)				8. PROJECT/TASK/WORK UNIT NUMBER	
Reactor Safety Corporation Gesellschaft Fuer Reaktorsicherheit Forschungsgelaende, 8046 Garching West Germany				9. FIN OR GRANT NUMBER	
10. SPONSORING ORGANIZATION NAME AND MAILING ADDRESS (Include Zip Code)				11a. TYPE OF REPORT	
Division of Reactor System Safety Office of Nuclear Regulatory Research U.S. Nuclear Regulatory Commission Washington, D.C. 20555				Technical Report	
				b. PERIOD COVERED (Inclusive dates)	
12. SUPPLEMENTARY NOTES					
13. ABSTRACT (200 words or less)					
<p>The general purpose of this project was the investigation of the heat transfer regimes during the high pressure portion of blowdown. The main attention has been focussed on the evaluation of those phenomena which are most important in reactor safety, such as maximum and minimum critical heat flux and forced convection film boiling heat transfer. The experimental results of the 25-rod bundle blowdown heat transfer tests, which were performed at the KWU heat transfer test facility in Karlstein, were used as a database for the verification of different correlations which are used or were developed for the analysis of reactor safety problems. The computer code BRUDI-VA was used for the calculation of local values of important thermohydraulic parameters in the bundle.</p>					
14. DOCUMENT ANALYSIS - a. KEYWORDS/DESCRIPTORS				15. AVAILABILITY STATEMENT	
Critical Heat Flux (CHF) rewet Minimum film boiling temperature Film Boiling				Unlimited	
				16. SECURITY CLASSIFICATION	
b. IDENTIFIERS/OPEN-ENDED TERMS				(This page)	
				Unclassified	
				(This report)	
				Unclassified	
				17. NUMBER OF PAGES	
				18. PRICE	



10
A

21



UNITED STATES
NUCLEAR REGULATORY COMMISSION
WASHINGTON, D.C. 20555

OFFICIAL BUSINESS
PENALTY FOR PRIVATE USE, \$300

SPECIAL FOURTH-CLASS RATE
POSTAGE & FEES PAID
USNRC
WASH. D.C.
PERMIT No. G-67

NUREG/IA-0002

HEAT TRANSFER PROCESSES DURING INTERMEDIATE AND LARGE BREAK
LOSS-OF-COOLANT ACCIDENTS (LOCAs)

SEPTEMBER 1986